Crystallization Behavior of Long Chain Compounds on Polyolefin Thin Films(Dissertation_全文)

AUTHOR(S):

Okihara, Takumi

Crystallization Behavior of Long Chain Compounds on Polyolefin Thin Films

Takumi Okihara

1991

Crystallization Behavior of Long Chain Compounds on Polyolefin Thin Films

Takumi Okihara

1991

contents

General Introduction

Epitaxial growth means the phenomenon that a crystal grows on a crystalline substrate with a particular orientation determined by the substrate. This phenomenon was known in natural minerals for a long time. Royer defined the word 'epitaxy' originally in 1928[1]. Epitaxial growth occurs from a liquid phase and a vapor phase. The epitaxial growth from the liquid phase has been studied for a long time. The first example of epitaxy from the vapor phase was reported by Bruck in 1936[2]. There are several kinds of epitaxial modes; for example, homoepitaxy means an oriented overgrowth between crystals of the same kind, in which crystals the crystallographic coincidence of different axes is performed in their contact plane, and

heteroepitaxy means overgrowth on different kinds of compound crystals. In the normal crystallization from melt and solution, crystals grow through the formation of secondary nuclei on the surface of a mother crystal. The nuclei are formed and oriented so as to adjust their lattices to the substrate lattice at the interface. They grow by adsorption of atoms or molecules with the same lattice fitting. Thus, we may say all kinds of crystal growth are based on epitaxial growth. There are many studies on epitaxial growth of metals or inorganic compounds[3-6]. Particularly, in the field of semiconductor, a lot of techniques utilizing epitaxial growth are developed for manufacturing electronic devices; for example, thin crystalline films on a substrate are necessary for integrated circuits. Theoretical studies on the epitaxial growth of inorganic compounds are proceeding. In the epitaxy, the orientation of growing crystals is determined at the stage of nucleation. Frank and Van der Merwe theoretically studied the mechanism of epitaxy at an early stage by expressing approximately the interface potential by a simple periodical function[7]. Their study was concerned with a strain, which was produced at the interface when a crystallite grows epitaxially on a substrate. The strain was relaxed by introduction of misfit dislocation. If a different kind of crystal grew on the substrate crystal, there was a misfit between inherent lattices (interatomic spacing) of the overgrown crystal and of the substrate. The misfit is represented by $m=(b-a)/a$, where a is the lattice dimension of the inherent lattice of the

substrate crystal and b is that of the overgrown crystallite. The misfit gives an important criterion on the epitaxial orientation and stability of the nuclei formed on the substrate. This misfit, however, does not always play a decisive role on epitaxial growth because there are many examples of epitaxy with large m; for example in case of Au/NaCl, m=-28%[12]. There are some other factors affecting epitaxial growth. They are the kind of substrate, the substrate temperature, the depositing rate and cleanness of the substrate surface. The substrate temperature is very important for epitaxial growth. Epitaxial growth does not occur if the substrate temperature is below a certain lower limit. This limit is called the epitaxial temperature. The vapor-deposition rate is also an important factor. The higher the rate is, the less oriented the crystallites are. These two factors have an influence on the mobility of atoms on the substrate. When atoms come to a substrate surface, they release a part of their kinetic energy to the substrate by collision. Since the atoms still have much energy, however, they move around on the substrate surface losing their energy and eventually fall in and stop at a site. They are stable if the site is one of the lowest potential minima favorable to epitaxial growth, and nucleation starts there. Otherwise, clusters which are smaller in size than the critical nuclei are formed by collision between moving atoms. Since they further move around on the surface, they collide to form a nucleus. If the substrate temperature is below the epitaxial temperature, atoms reaching the substrate lose too

much kinetic energy to move to the stable site, and they crystallize without taking an epitaxial orientation. If the deposition rate is higher, the moving atoms on the substrate collide very often with one another, and hence clusters are easily formed and coalesce into nuclei without taking the favorable orientation for epitaxial growth. So the higher substrate temperature and the lower deposition rate are favorable for epitaxial growth. Sloope and Tiller proved the fact through the observation of the epitaxy of Ge on the (111) plane of CaF_2[8,9]. Contamination of surface affects the epitaxial growth[10,11]. In epitaxy of gold on the air-cleaved (100) surface of NaCl, the epitaxial temperature (300℃) is higher by 200℃ than that (100℃) on the vacuum-cleaved (100) surface of NaCl[13]. Thus, the epitaxial growth is affected by many factors.

Organic compounds also show epitaxial growth. A metal atom is taken as a sphere, but the shape of an organic molecule is more complex. So epitaxy of organic molecules does not occur so easily as that of metals, and theoretical treatment becomes more complicated. Organic compounds crystallized epitaxially are classified into two groups; one group comprises linear molecules such as n-paraffins and the other group the planar molecules such as phthalocyanine. Long-chain compounds such as n-paraffins crystallize epitaxially on the substrate of alkali halides. For example, n-hexatriacontane crystallizes epitaxially on the (001) plane of KCl[14]. The orientational relation of this epitaxy is $(110)_{\text{n-paraffin}} /\!/ (001)_{KCl}$ and $[001]_{\text{n-paraffin}} /\!/ [110]_{KCl}$. Metallic

salts of fatty acid also crystallize epitaxially on the KCl (001) plane in the same way[15].

Many examples were reported for epitaxial growth of polymer crystals on inorganic substrates [16-26]. Crystalline polymers such as polyethylene (PE) and polyoxymethylene crystallized on the substrates of alkali halides such as NaCl. The epitaxial phenomenon of PE/NaCl was first observed by Willems [16,17] and subsequently by Fisher[18,19]. In this system, molecular chains of PE were oriented in the <110> directions on the NaCl (001) plane, and the (110) plane of PE is in contact with the (001) plane of NaCl. Wittmann et al. epitaxially crystallized polymers onto organic compounds; benzoic acid, trioxane and aromatic hydrocarbons[20,21]. Mauritz et al. examined theoretically the epitaxial orientation by calculating interaction energy between PE and NaCl[27]. Their result agreed with the experimental data. Similar calculations for the epitaxial systems of polyoxymethylene on alkali halides and of PE on graphite were carried out[28,29].

Richards reported the oriented overgrowth of n-paraffins on cold-drawn PE. In the paper, n-paraffin crystals were grown from the solution in white spirit by cooling from about 50℃ to room temperature. His study indicated that lamellar crystals of n-paraffins grew with their c-axes parallel to the c-axis of PE but the interfacial structure of n-paraffin/PE was not refered to. Examples of epitaxy of polymer crystals grown on the substrate of different kinds of polymers were reported by

Takahashi et al[31]. They examined in detail the possibility of epitaxy between different crystalline polymers. PE crystallized epitaxially from the melt on the uniaxially drawn film of isotactic polypropylene (iPP) [32,33]. Figure 1 shows the morphology of this epitaxy and the corresponding diffraction pattern. The diffraction pattern indicates that molecular chains of PE are oriented at an angle of 46° from the c-axis of iPP. In the reference [33], it is shown that the epitaxy may be utilized as an adhesive between two uniaxially drawn films of iPP, the c-axes of which are perpendicular to each other. One of the subjects of this study is to clarify the interfacial structure in epitaxy between polyolefins and between long-chain compounds and polyolefins. It is very difficult to get polyolefin samples with a crystallographically well-defined surface, because large single crystals of polymers as those in metals and inorganic compounds are not formed since flexible-chain polymers crystallize with chain folding[34]. Drawn polymer films are polycrystalline and contain a non-crystalline phase[35]. In them, crystallites are oriented with their molecular axes parallel to the drawn direction, but their orientation is random around the drawn axis. Thus, even when a uniaxially drawn film is used as the substrate for epitaxy, its surface structure is not clearly defined in a crystallographical sense. This study describes the method to prepare polyolefin substrates with a certain crystallographically defined surface and also how to utilize them for epitaxy. To study polymer/polymer epitaxy, we examined as

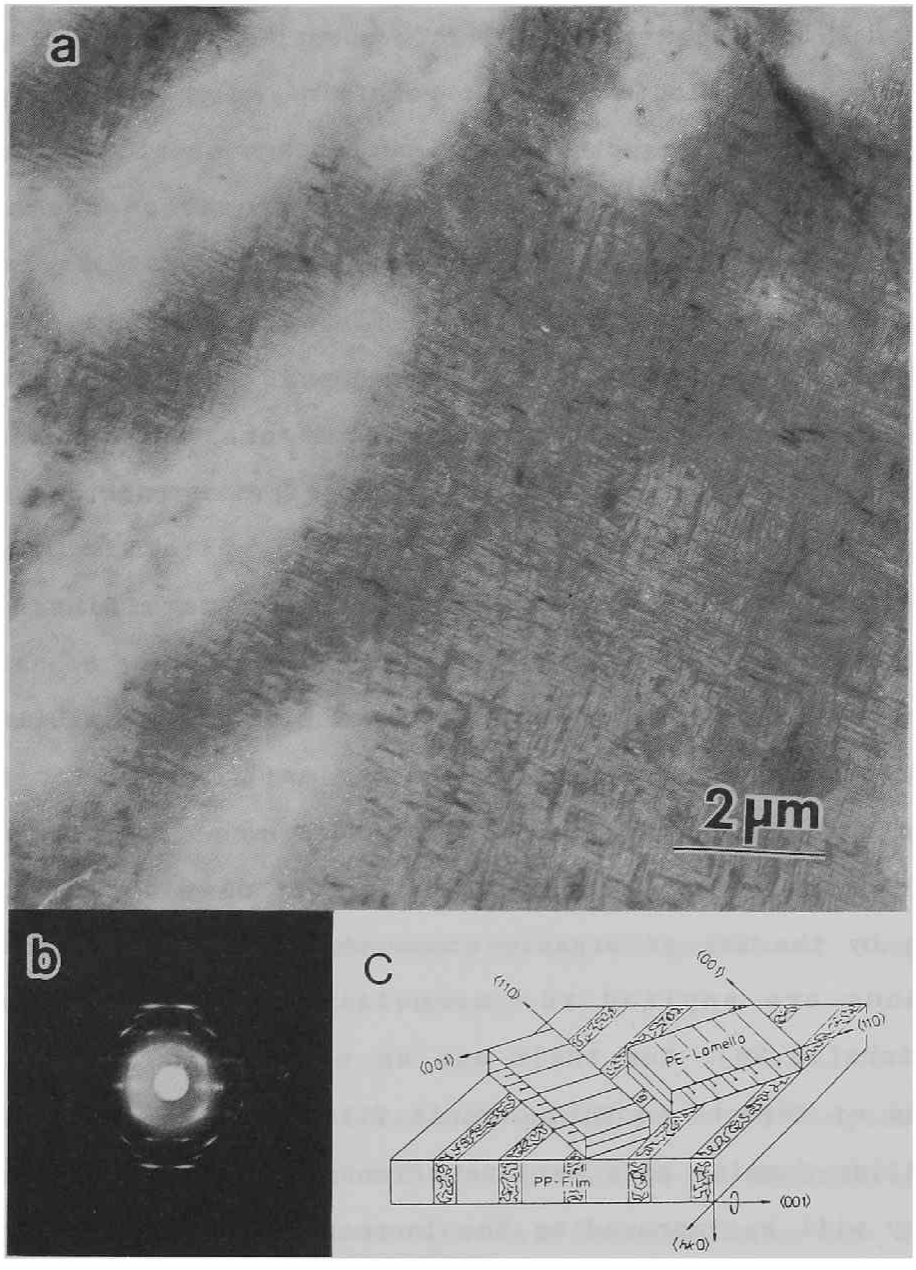

Fig. 1 (a) Transmission electron micrograph of PE crystallized epitaxially on the uniaxially drawn iPP, (b) the corresponding ED pattern and (c) the illustration which shows a model of this epitaxy.

model cases the epitaxial growth of normal long-chain compounds on the drawn polyolefin films; n-paraffins which are oligomers of PE, and normal long-chain compounds such as n-alcohols and n-carboxylic acids with a normal long hydrocarbon chain. In crystallography, the subcell structure of n-paraffins is very similar to the crystal structure of PE[36], and in the chemical structure n-paraffins are the same as PE except methyl end groups. The normal long-chain compounds are the same in the chemical structure as n-paraffins except for a functional group at one end instead of a methyl group of n-paraffin, and are crystallographically almost identical to n-paraffins in the subcell structure.

Another aim of this study is to examine the feasibility of the utilization of the present epitaxy as a method for making organic thin films with molecular chains are arrayed in high order. Recently, many studies proceed to develop electronic devices by the use of organic compounds. Thin films of organic compounds are applied to microlithography[37], used as insulators[38,39]. For their use as electronic devices, the presence of defects in thin organic films and the small size of crystalline domains have serious effects on their property. The property will be improved by the increase in order of molecular arrangement in the thin films. There are many methods to prepare thin organic films. The Langmuir-Blodgett technique is the most popular. The method is as follows[40-42]. First, a solution of a compound which has a hydrophilic group at one end and a

hydrophobic group such as a normal long hydrocarbon chain at the other end is spread onto the surface of water, and a monomolecular layer of the compound is formed. Such molecular layers are piled up on a glass slide. Faults in layered films lead to a weakness of their mechanical property, and the presence of grain boundaries in a monomolecular layer deteriorates their distinctive property such as electric conductivity. The vapor-deposition method is also widely used to prepare thin films. In the metal engineering, this method is utilized to make thin films for many applications. When this method is applied to organic compounds, some difficulties in making thin films are experienced. For example, there are difficulties in controlling the rate of vapor-deposition and the thickness of films of organic compounds and in preventing their thermal decomposition. These difficulties in the method will be overcome in future. In particular, there is much room for improvement in preparing thin organic films, and the present epitaxial growth of long-chain compounds may be one alternative for it.

An outline of this thesis is as follows. In chapter 1, we examined the epitaxial growth of n-paraffins on uniaxially drawn polyolefins. This study was started to elucidate the epitaxy between PE and iPP. n-Paraffins are low molecular weight oligomers of PE, and their crystal structure and chemical structure are well established. We discussed the crystallization behavior of n-paraffins on the substrates of PE, iPP, poly-1-

butene and poly(4-methyl-1-pentene). In all cases, flat-on lamellae of an n-paraffin were observed. They have a particular orientational relation with respect to the substrate. Resultingly, this study gave the key point to solve the PE/iPP epitaxy.

Since the uniaxially drawn polyolefins whose surfaces are not clearly defined crystallographically are used in Chapter 1, the molecular mechanisms of epitaxy and atomic arrangement at the interface are not made clear experimentally. Next two chapters, therefore, are devoted to studying the epitaxy of normal long-chain compounds on PE, the surface of which is crystallographically defined well. There are two crystallographic planes exposed as the surface of PE crystal: (110) and (100) planes. In Chapter 2, the (110) plane of PE was used as the substrate of epitaxy. By the use of the epitaxial growth of PE on the (001) plane of NaCl, the PE thin films whose surface was bounded by the (110) plane of PE crystal were prepared. Crystallization behaviors of long-chain compounds such as n-paraffins, n-alcohols and n-carboxylic acids by vapor deposition or from solution were discussed. The change of orientational mode in epitaxy occurred in case of the (110) plane of PE, depending on the temperature.

In Chapter 3, crystallization behavior of long chain compounds on the (100) surface of PE was discussed. Ultra-drawn, ultra-high molecular weight PE films have the (100) plane as their surface and thus they were used as the substrate. The

epitaxial behavior of long-chain compounds on the (100) plane is different from that on the (110) plane. Edge-on lamellae of long-chain compounds grew on the substrate from the melt. The morphology of epitaxially grown crystals of long-chain compounds and their growing mechanism were compared with those on the (110) plane and discussed in this chapter.

In Chapter 4, the crystallization behavior of long-chain compounds on uniaxially drawn iPP films was examined. The normal long-chain compounds are analogous to n-paraffins and PE in that they have a normal long hydrocarbon chain. Really, they crystallize with a subcell which is quite similar to the unit cell of PE. Epitaxy of these compounds on iPP corresponds to that between PE and iPP. This study gave much information about the PE/iPP epitaxy.

References

[1] M.L.Royer Bull. Soc. Franc. Mineral, 51(1928)7.

[2] L. Bruck, Ann. Phys., 26(1936)233.

[3] D.W.Pashley, Advances in Physics, 5(1956)173.

[4] D.W.Pashley, Advances in Physics, 14(1965)327.

[5] E.Bauer and H.Hoppa, Thin Solid Films 12(1972)167

[6] M.J.Stowell, Thin Solid Films 12(1972)361.

[7] F.C.Frank and J.H.van der Merwe, Proc. Roy. Soc. A198 (1949)205, ibid., A198(1949)216.

[8] B.W.Sloope and C.O.Tiller, J. Appl. Phys., 33(1962)3458.

[9] B.W.Sloope and C.O.Tiller, J. Appl. Phys., 36(1965)3174.

[10] B.A.Joyce and R.R.Bradley, Phil. Mag. 14(1966)289.

[11] G.R.Booker and B.A.Joyce, Phil. Mag. 14(1966)301.

[12] G.W.Jhonson, J. Appl. Phys., 21(1959)449.

[13] S.Ino, D.Watanabe and S.Ogawa, J. Phys. Soc. Japan 17(1962)1074.

[14] Y.Ueda and M.Ashida, J. Electron Microsc., 29(1984)38.

[15] T.Miki, K.Inaoka, K.Sato and M.Okada, Japan J. Appl. Phys. 24(1985)L672.

[16] J.Willems and I.Willems,Experientia,13(1957)465.

[17] J.Willems, Discussions Faraday Soc., 25(1957)111.

[18] E.W.Fisher, Discussions Faraday Soc., 25(1957)204.

[19] E.W.Fisher, Kolloid-Z., 159(1958)108.

[20] J.C.Wittmann and B.Lotz J. Polymer Sci. Polymer Phys. Ed., 19(1981)1853.

[21] J.C.Wittmann, A.M.Hodge and B.Lotz, J. Polymer Sci. Polymer

Phys. Ed., 21(1983)2495.

[22] J.A.Koutsky, A.G.Walton and E.Baer, J. Polymer Sci. part A-2, 4(1966)611.

[23] J.A.Koutsky, A.G.Walton and E.Baer, J. Polymer Sci. Part-B, 5(1967)177.

[24] K.Kiss, S.H.Carr, A.G.Walton and E.Baer, J. Polymer Sci. Part-B, 5(1967)1087.

[25] S.H.Carr, A.G.Walton and E.Baer, Biopolymers, 6(1968)469.

[26] F.Rybnikar and P.H.Geil, J. Polymer Sci. Part A-2, 10(1972)961.

[27] K.A.Mauritz, E.Baer and J.Hopfinger, J. Polymer Sci. Polymer Phys. Ed., 11(1973)2185.

[28] K.A.Mauritz and A.J.Hopfinger, J. Polymer Sci. Polymer Phys. Ed., 13(1975)787.

[29] P.R.Baukema and A.J.Hopfinger, J. Polymer Sci. Polymer Phys. Ed., 20(1982)399.

[30] R.B.Richards, J. Polymer Sci., 6(1951)397.

[31] T.Takahashi, M.Inamura and I.Tsujimoto, J. Polymer Sci. Part-B 8(1970)651.

[32] G.Broza, U.Rieck, A.Kawaguchi and J.Petermann, J. polymer Sci. Polymer Phys. Ed. 23(1985)2623.

[33] J.Petermann, G.Broza, U.Rieke and A.Kawaguchi, J. Mater. Sci. 22(1987)1477.

[34] A.Keller, Phil. Mag., 2(1957)1171.

[35] R.Hosemann, Polymer, 3(1962)349.

[36] C.W.Bunn, Trans Faraday Soc., 35(1939)482.

[37] Y.Harita, High Polymers, Japan 38(1989)948.

[38] N.Gemma, K.Mizushima, A.Miura and M.Azuma, Synth. Met., 18(1987)809.

[39] Y. Miyadera, High Polymers, Japan, 38(1989)952.

[40] K.B.Blodgett, J. Amer. Chem. Soc., 57(1935)1007.

[41] K.B.Blodgett and I.Langmuir, Phys. Rev., 51(1937)964.

[42] K.B.Blodgett, J. Phys. Chem., 41(1937)975.

Chapter 1. Epitaxial Growth of Normal Paraffins From the Melt on Uniaxially Drawn Films of Polyolefins

1.1. Introduction

A number of polymers are epitaxially crystallized on various substrates of organic and inorganic materials and polymers[1]. In particular, epitaxial growth of polyethylene (PE) onto a uniaxially oriented isotactic polypropylene (iPP) is interesting for its practical importance in the adhesion of polymer laminates [2]. For the epitaxy, it has been demonstrated that crystallites of helical iPP chains possess a crystallographical plane on which the side methyl groups form straight rows along which linear PE chains can align [2-5]. It has also been found that when some n-paraffins crystallize onto oriented helical polyolefins, they align perpendicular to the substrate surface with an epitaxial correlation[6]. Though n-paraffins and PE differ in their chain length, they are analogous in chemical and crystallographic structure, except in the chain folding of PE. Nevertheless, the epitaxial growth behavior of n-paraffins onto the oriented helical polyolefins is in sharp contrast to that of PE. The dissimilarity in molecular orientation is puzzling in the

interpretation of the epitaxial growth behavior of n-paraffins and PE according to the mechanism proposed for PE/iPP epitaxy.

In the present work, epitaxial crystallization of n-paraffins of various chain lengths onto uniaxially oriented polyolefins (PE, iPP, poly-1-butene (PB) and poly-4-methyl-1-pentene(P4MP)) was conducted. Various epitaxial growth features were observed, depending on the kind of polymer substrates and the chain length of the paraffins. They are classified into several modes. Through the present observation, the factors affecting the epitaxial growth of long-chain molecules are discussed.

1.2. Experimental

Oriented thin films of PE, iPP, PB and P4MP were prepared by the method developed by Petermann and Gohil [7]. A small amount of the n-paraffin solution of 1-2 wt% in benzene or n-hexane was dropped on the oriented thin polymer films. In a few cases, n-paraffins were crystallized with an epitaxial orientation on the polymer substrates singly by evaporating the solvent, for example in the case of n-$C_{36}H_{74}$ in benzene. In most cases, however, an n-paraffin layer deposited after evaporation of the solvent was heated above the melting temperature of n-paraffins and subsequently cooled down so that n-paraffin crystals were epitaxially grown on the polymer substrates. The specimens obtained by these growth process were observed with an electron microscope (JEOl JEM-200CS). X-ray diffraction was applied to the

polymer films on which n-paraffin crystals were thickly grown from highly concentrated solutions.

n-Paraffins with carbon numbers of 20 through 50 were purchased from Tokyo Kasei Kogyo Co., Ltd.

1.3. Classification of epitaxial modes

Figure 1-1 shows a dark field electron micrograph and the corresponding electron diffraction (ED) pattern of the PE thin film on which n-hexatriacontane $C_{36}H_{74}$ (hereafter n-paraffin C_nH_{2n+2} is abbreviated to C_n) is epitaxially crystallized. The bright dots in Fig. 1-1 denote PE crystallites of a few tens of nm in width and a large and bright region of n-paraffin platelet extending to a few μm. As a C_{36} platelet covers so many tiny PE crystallites, the epitaxial compatibility between both never holds over the entire surface. The ED pattern (magnified in Fig. 1-2a) shows that the PE fiber pattern and the *hk*0 net pattern of C_{36} crystals overlap with their 110 spots coincident on the equator. The coincidence of the 110 spots evidences that the polymer substrate induces C_{36} molecules to crystallize epitaxially on it with a definite crystallographic orientation. Since the fiber pattern is cylindrically symmetric about the fiber axis, however, this overlapping does not always indicate that the epitaxial growth of n-paraffin crystals originates from the bright PE crystallites in Fig. 1-1. The mode of epitaxy cannot be determined only from the ED pattern, because (1) the surface of the polymer substrate is not defined by a unique

single crystallographic plane and (2) the surface planes bounding individual polymer crystallites in the fiber are unknown.

Prior to detailing the observed epitaxial growth of n-paraffin/polymer systems, we first outline the basic ideas to derive the growth modes in Fig. 1-2. In schematic drawings of ED patterns in Figs. 1-2 to 1-9, the solid circles denote the diffraction spots of the polymer substrates and the open circles those of n-paraffin crystals. In Fig. 1-2a, the C_{36} ED pattern is composed of two *hk*0 net patterns in a twin relation with respect to one of the {110} planes. The hk0 net pattern from C_{36} crystals is observed when the crystals are orthorhombic and their molecular axis is oriented normally to the substrate surface. Hence, the (001) basal plane of the C_{36} crystals is parallel to the PE substrate surface. Their 110 reflections might be simultaneously excited in the above way by C_{36} and PE crystals, i.e. the 110 planes for both crystals are located at the same position on the contact plane between them. Therefore, the epitaxial growth is defined straightforwardly as:

$(001)_{C36}//(310)_{PE}$, $[110]_{C36}//[001]_{PE}$

It has not been observed, however, that the {310} planes manifest themselves as the bounding planes of a single PE lamella grown from the solution or the melt. A lozenge-shaped lamellar crystal of PE grown from the solution is sectored with {110} planes and a truncated lamella with {110} and (100) planes. In the light of Wulff's theorem[8], it is reasonable that polymer crystals are bounded with these planes indexed with low Miller

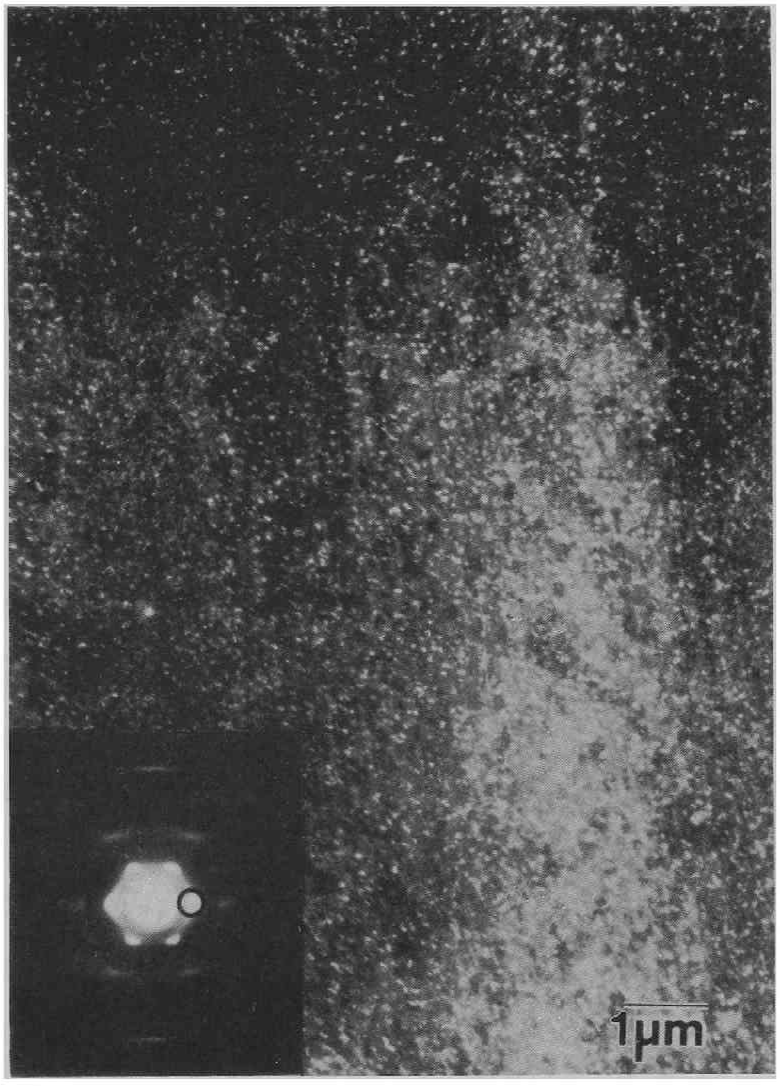

Fig. 1-1. Dark-field electron micrograph of the PE thin film on which C_{36} crystals were grown, taken with the enclosed 110 spot in the inserted ED pattern.

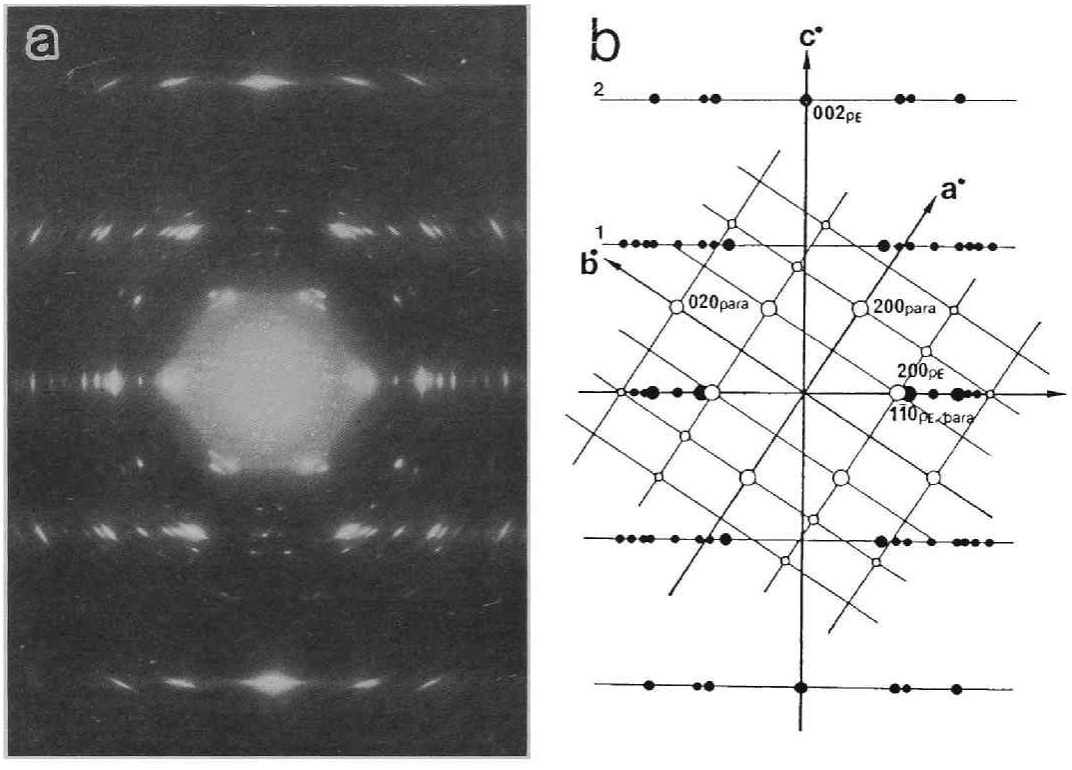

Fig. 1-2. ED pattern of the PE thin film on which C_{36} is epitaxially grown and (b) the schematic drawing corresponding to it. The real diffraction pattern of the C_{36} crystals is twinned with respect to the (110) plane.

indices. C_{36} crystals may epitaxially grow on the (110) plane of drawn PE in the relation:

$(001)_{C36} /\!/ (110)_{PE}$, $[110]_{C36} /\!/ [001]_{PE}$.

It is assumed that n-paraffins crystallized epitaxially on polymer crystal planes that are the growth faces of polymer lamellae grown from the solution or the melt are indexed with low Miller indices. Furthermore, these planes can be the (*hk*0) planes because the polymer substrate has a fiber texture. Thus, the {110} and (100) planes were chosen as candidates for the crystallite surfaces of drawn PE, (010), (100) and {210} for PP, (100) and {210} for PB and (100) and {110} for P4MP. Accordingly, epitaxial modes of various n-paraffin/polymer systems are classified below.

1.3.1. Polyethylene (PE)

Three epitaxial relationships of n-paraffin/PE were observed and designated as modes A_1, A'_1 and A_2.

1.3.1.1. Modes A_1 and A'_1

One of the two epitaxial modes, A_1, is attributed to the crystal growth giving rise to the ED pattern modeled in Fig.1-2b, and the other, A'_1, whose ED pattern is in a twin relationship with respect to that in Fig.1-2b, has {110} twin planes. In Fig. 1-2a, the two patterns overlap, because these modes gave rise to coincided 110 reflections of n-paraffin and PE crystals as detailed in the C_{36}/PE epitaxial relationship. Thus, this

epitaxial relationship is defined as:

$(001)_p // (110)_{PE}$, $[110]_p // [001]_{PE}$,

where the subscript p stands for n-paraffins. In the above discussion, the {310} PE planes were not adopted as the contact surface with n-paraffin crystals. However, the {310} planes play an important role in the growth behavior of n-paraffin and PE crystals, e.g. (310) twinning [9,10] and [310] striations [11,12]. As n-paraffins and PE form (310) twins, it is likely that the outer surfaces of PE crystallites are bounded with the {310} planes. From the lattice energetic consideration, Boistelle [13] pointed out that the boundary surface of the (310) twins is possibly composed of (110) and (100) microfacets alternating along the mean $[\bar{1}30]$ direction. This suggests that the {110} planes becomes substantially the outer surface of PE crystallites in the fiber.

Wittmann and Lotz[14] observed that when PE was evaporated in vacuum, fibrillar PE crystals were grown on the (110) surface of a flat n-paraffin single crystal with their (110) planes parallel to it. In contrast, n-paraffin crystals were grown on the PE substrate in the present study. The epitaxial orientation between n-paraffins and the PE crystals of both cases, however, is completely identical. This supports the fact that the above epitaxial growth mode is possible.

1.3.1.2. Mode A_2

Figure 1-3a shows that the *hk*0 net pattern of C_{50} crystals

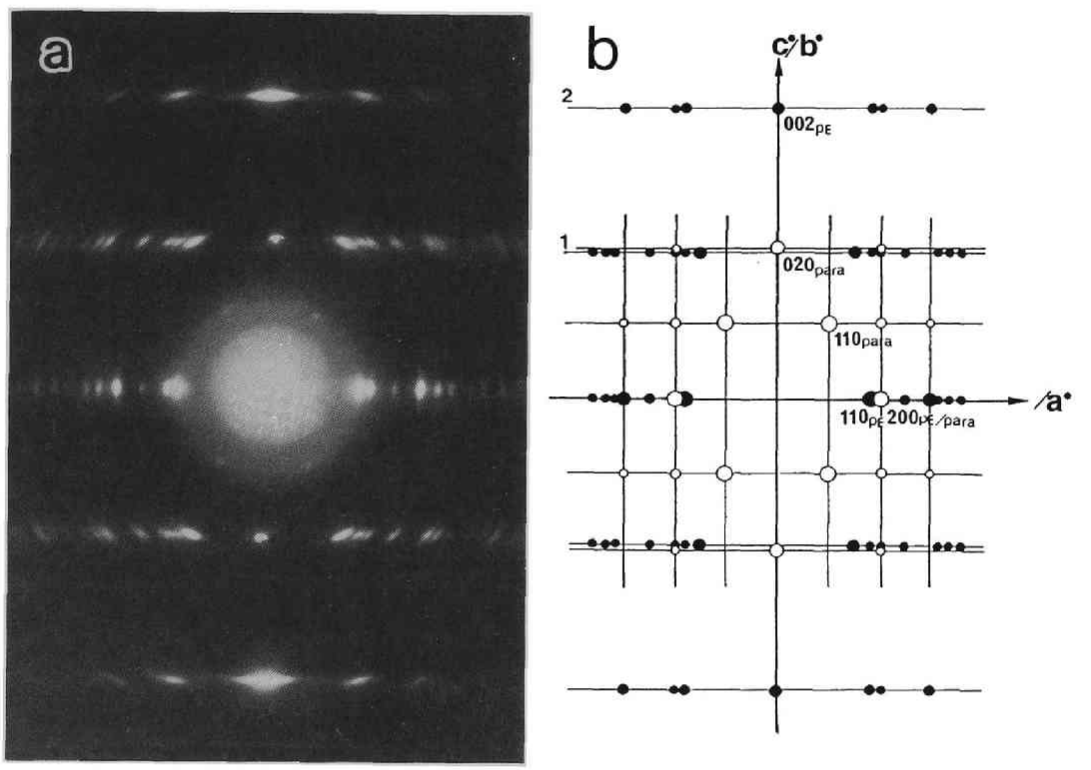

Fig. 1-3. (a) ED pattern of the PE thin film on which C_{50} crystals are over-grown, and (b) the schematic drawing corresponding to (a).

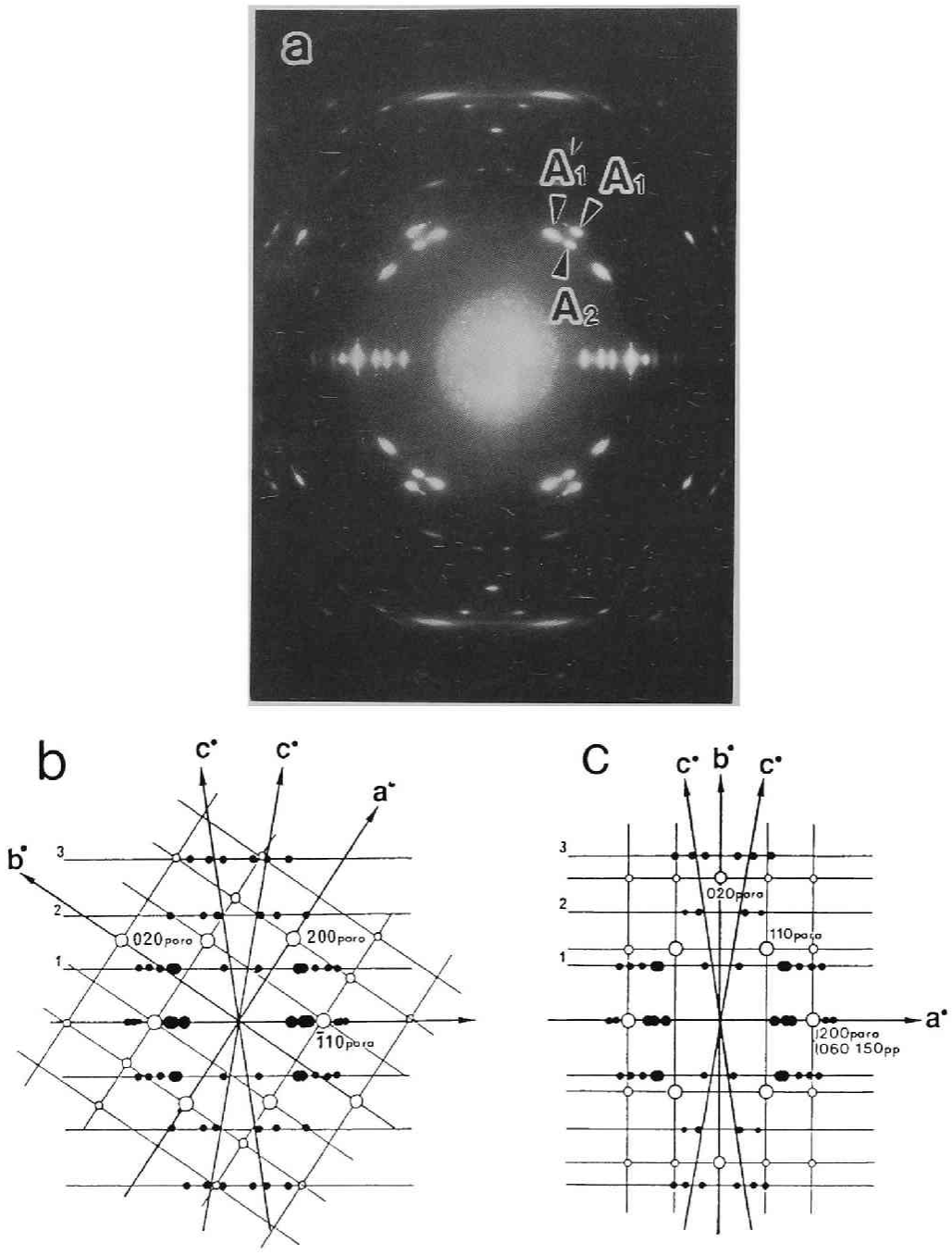

Fig. 1-4. (a) ED pattern of the iPP thin film on which C_{36} is epitaxially crystallized. The schematic drawings of (b) and (c) denote the orientation of the hk0 net pattern from the C_{36} ED pattern (a).

overlaps on the PE fiber pattern in a different way from that in Fig. 1-2a. The 020 reflection of C_{50} in the meridian is strong, while the 110 reflections are weak. The 200 reflection of C_{50} may be weaker, although its intensity cannot be estimated because of its proximity to the 200 reflection of PE. The ED pattern having this feature indicates a second epitaxial mode in the n-paraffin/PE system. The intensity relation among these spots implies that monoclinic C_{50} crystals [15] grow with the (001) plane parallel to the polymer substrate. This was proven by the X-ray diffraction study described below. Since the 100 lattice spacings of PE and C_{50} are almost the same, this epitaxial growth may occur in such a way that these planes are adjusted at the C_{50}/PE interface. However, attention must be paid to the strong 020 reflection of C_{50} in the meridian. The 001 lattice spacing of PE, $d_{PE}(001)$, is 0.254 nm at room temperature and the 010 lattice spacing of C_{50}, $d_{C50}(010)$, is 0.494 nm. The lattice misfit between $2d_{PE}(001)$ and $d_{C50}(020)$ is 0.14 nm, which is small enough to cause the epitaxial growth. Thus, this mode of epitaxy is defined generally as:

$(001)_p // (110)_{PE}$, $[010]_p // [001]_{PE}$.

1.3.2. Isotactic Polypropylene (iPP)

For the sake of convenience, the six epitaxial modes observed in the n-paraffin/iPP systems are designated as A_1, A'_1, A_2, A_3, A'_3 and B in this discussion.

1.3.2.1. Modes A_1, A'_1 and A_2

Although the *hk*0 net patterns of C_{36} crystals in Fig.1-4a are quite complicated, precise analysis has enabled the isolation of two *hk*0 net patterns of orthorhombic C_{36} crystals, which are in different orientations with respect to the iPP fiber axis. The first is explained in terms of the reciprocal lattice in Fig. 1-4b and the second in Fig. 1-4c.

In Fig. 1-4b, the [110] direction of the C_{36} crystals is parallel to the fiber axis of the PP substrate, and the epitaxial mode is named as A_1 analogous to the A_1 mode of n-paraffin/PE epitaxy. A twined C_{36} ED pattern with respect to the {110} planes is seen in Fig. 1-4a and the A'_1 mode is in the $(1\bar{1}0)$ twin relation to the A_1 mode.

In Fig. 1-4c, the 020 reflection of C_{36} is approximately in the meridional direction, whereas the 200 spot is on the equator and coincides with the 060 or 150 spot of iPP. As the difference between d_{C36} (0.376 nm) and $d_{iPP}(600)$ (0.327 nm) is small enough, epitaxial growth may occur to adjust the two lattice planes at the boundary surface. However, it follows that the [010] direction of the C_{36} crystal is parallel to the iPP fiber axis. Thus, the epitaxy is defined as the A_2 mode in the relation: $(001)_p // (010)_{iPP}$, $[010]_p // [001]_{iPP}$.

1.3.2.2. Modes A_3 and A'_3

The *hk*0 net pattern in Fig. 1-5a shows that an orthorhombic C_{26} crystal is formed to align normal long chains perpendicular

to the iPP substrate surface. The intensities of the diffraction spots corresponding to the 111 reflection or the composite reflection of 041 and $\bar{1}31$ of the monoclinic iPP lattice are asymmetric about the meridian. The asymmetry results from the overlapping of the C_{26} net pattern on the iPP fiber pattern so that the $\bar{1}10$ spot of C_{26} spot coincides with the 111 or 041 or $\bar{1}31$ spot of PP. The coincidence of these spots proves the epitaxial growth of C_{26} crystal on drawn iPP. The vector from the origin to the 110 spot of C_{26} makes an angle of 40° with the equator of the iPP fiber pattern. The epitaxial A_3 mode of the n-paraffin/iPP systems is thus characterized by its ED pattern.

The complicated ED pattern of the C_{35} crystal in Fig. 1-5b basically consists of two different *hk*0 net patterns. The key diffraction spots of one *hk*0 pattern are labelled with A_3 and indexed as 110 of the orthorhombic C_{35} crystal as explained in terms of the reciprocal lattice in Fig. 1-5c. These spots belong to the n-paraffin crystals in the epitaxial A_3 mode. Other key spots of the *hk*0 net pattern are labelled with A'_3 and are indexed as 200. Here, it is noted that the coincidence of the 110 spot with the 110 or 041 or $\bar{1}31$ spot of iPP is still retained in the latter *hk*0 net pattern. Both *hk*0 net patterns are in a twin relation with respect to the {110} planes of Fig. 1-5c. Accordingly, the epitaxial mode for the latter was named A'_3. Two modes of epitaxial growth distinguishable from the same point of view were also observed on the n-paraffin/PB systems.

Wittmann and Lotz[3] and Petermann et al.[2] proposed that

PE epitaxially crystallizes on the (010) plane of the iPP substrate. In reality, the (010) plane is the growth face, i.e. the fold plane, of lath-shaped iPP single crystals grown from solution [18,19]. The plane may be preferential over others as a bounding plane of iPP crystallites in fibers. In assuming that n-paraffins also crystallize on the (010) plane, this epitaxial mode of the n-paraffin/iPP system is in the relation:

$(001)_p /\!/ (010)_{iPP}$, $[110]_p \measuredangle 50°\ [001]_{iPP}$

where $\measuredangle 50°$ means that the direction $[110]_p$ makes an angle of 50° with $[001]_{iPP}$

1.3.2.3 Mode B

Figure 1-6 exemplifies the ED pattern characterizing another epitaxial mode of n-paraffin/iPP systems. No hk0 net pattern of C_{50} crystals is observed, and the 020 reflection of C_{50} is just on the second layer line of the iPP fiber pattern and as a result, in the direction at an angle of 46° from the equator. When PE is epitaxially crystallized from the melt onto the drawn iPP thin film, a similar ED pattern is observed(Fig. 1-6b)[3]. Thus, the ED pattern of the C_{50}/iPP system can be interpreted in terms of the same molecular orientation as in the case of the PE/iPP system. On the assumption that the n-paraffin grows on the (010) plane of iPP as well, the epitaxial mode is defined as:

$(100)_p /\!/ (010)_{iPP}$, $[010]_p \measuredangle 46°\ [001]_{iPP}$

However, the possibility of the epitaxial overgrowth of n-paraffins on other planes such as (100) and (210) is not

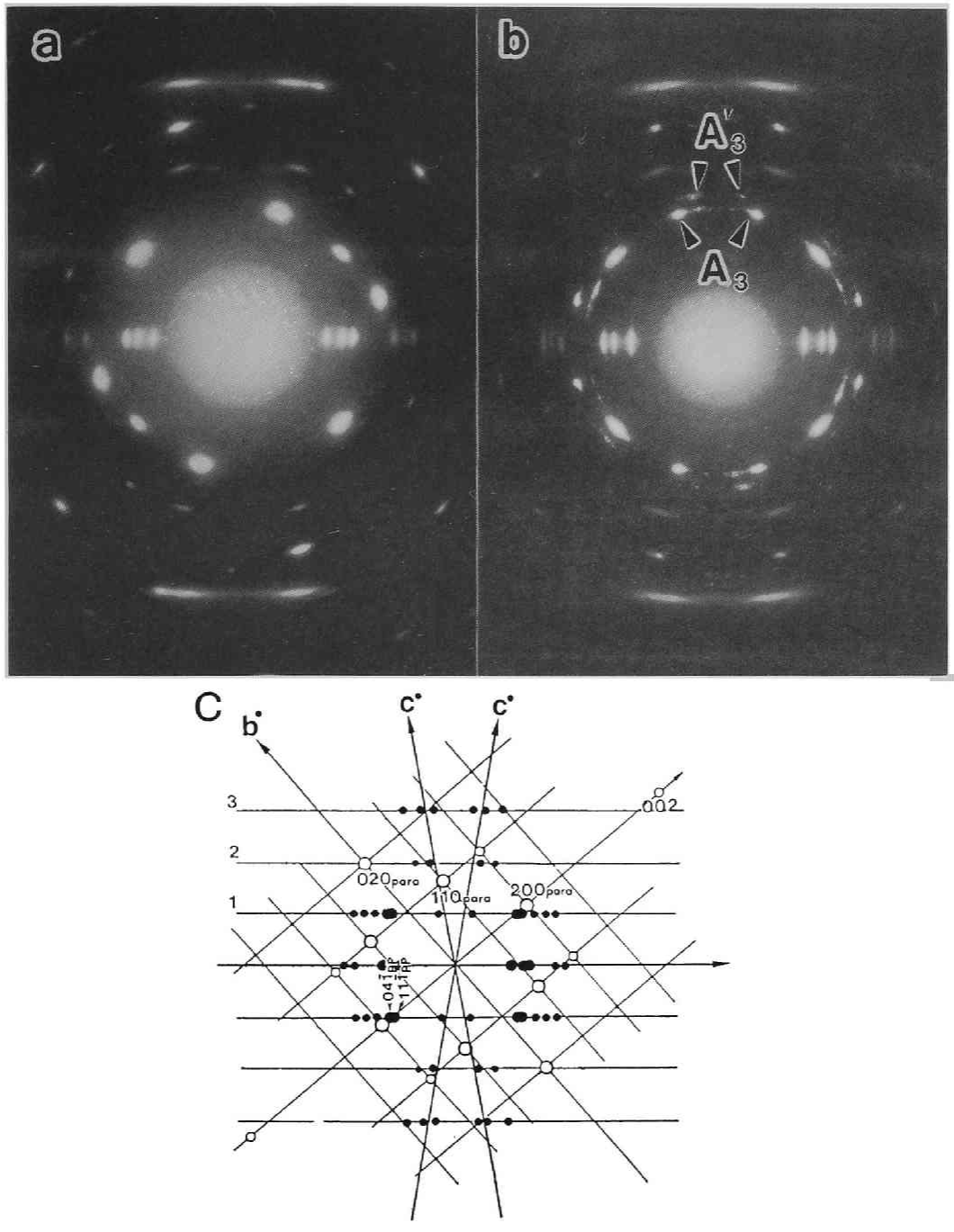

Fig. 1-5. ED patterns of iPP thin films on which n-paraffins are epitaxially crystallized; (a) C_{26} and (b) C_{35}. The schematic drawing (c) corresponds to (a). Spots labeled with A_3 and A'_3 in (b) indicate diffraction spots from C_{35} crystals grown in the A_3 and A'_3 modes, respectively.

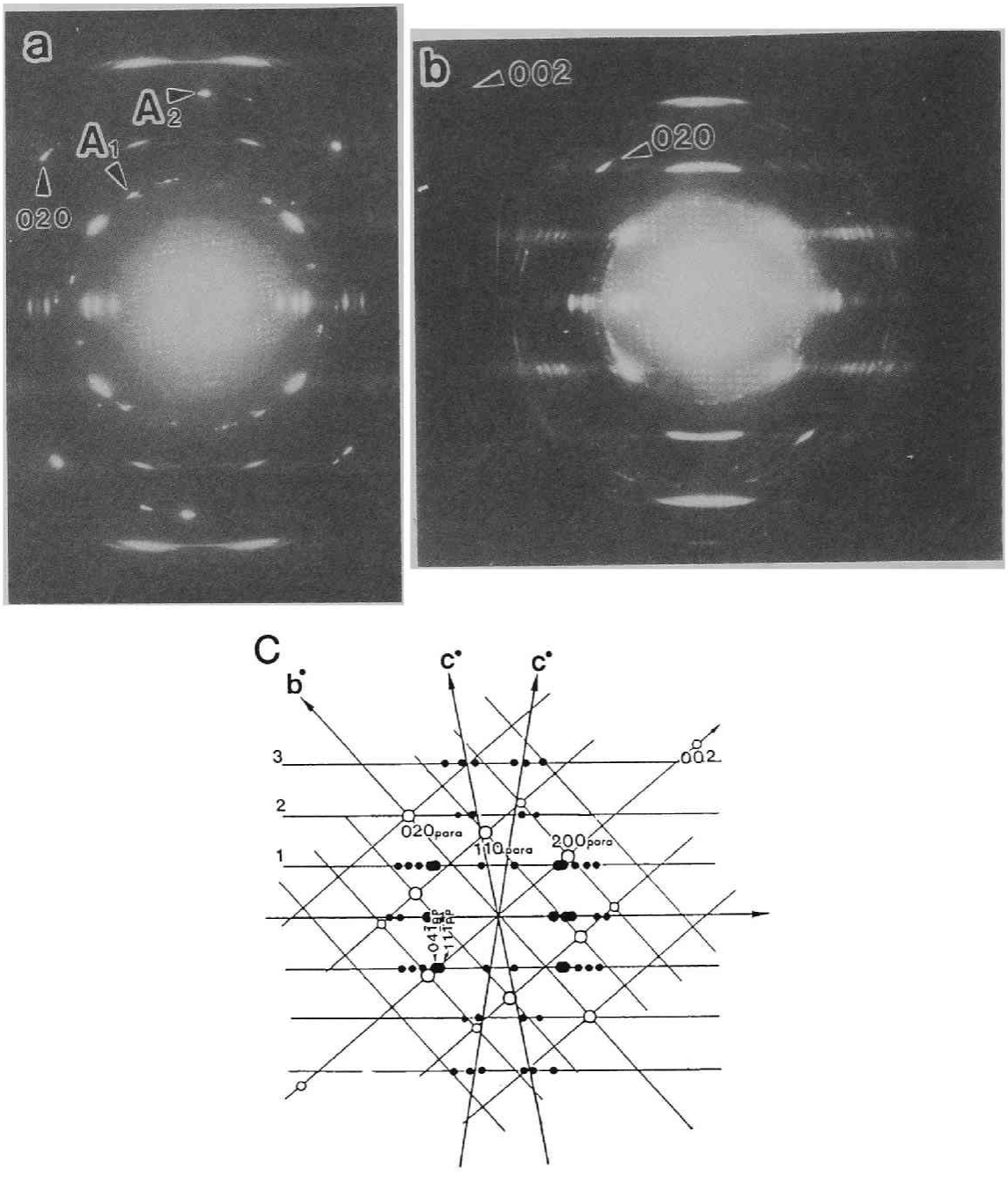

Fig. 1-6. (a) ED pattern of the iPP thin film on which C_{50} is epitaxially crystallized, and (b) PE on iPP. (c) The schematic drawing corresponding to these ED patterns. Arrows with A_1 and A_2 in (a) show reflections produced by crystals of the A_1 and A_2 modes, respectively.

excluded.

1.3.3. Polybutene-1 (PB)

Three epitaxial modes observed in n-paraffin/PB systems are named A_2, A_3 and A'_3.

1.3.3.1. Mode A_2

Figure 1-7 represents the ED pattern of the first epitaxial mode of n-paraffin/PB systems. The *hk*0 net pattern of an orthorhombic C_{28} crystal overlaps on the PB fiber pattern in the way that the 200 spot of C_{28} coincides with the 410 spot of PB. Otherwise, the overlapping is characterized by the [010] direction of the n-paraffin crystals, which is oriented parallel to the PB fiber axis. When the (001) plane of orthorhombic crystals of the n-paraffin is in contact with the (210) plane of PB at the n-paraffin/PB interface, the 200 reflection of the n-paraffin and 410 of PB are excited almost simultaneously. Thus, this epitaxial mode is defined as:
$(001)_p // (210)_{PB}$, $[010]_p // [001]_{PB}$.

1.3.3.2. Modes of A_3 and A'_3

The ED pattern of Fig. 1-8a is characteristic of the A_3 epitaxial mode of n-paraffin/PB systems. The 211 spots of the PB hexagonal modification are not balanced on the left and right sides with respect to the meridian, as seen in Fig. 1-5a. The hk0 net pattern of orthorhombic C_{28} crystals overlaps on the PB fiber

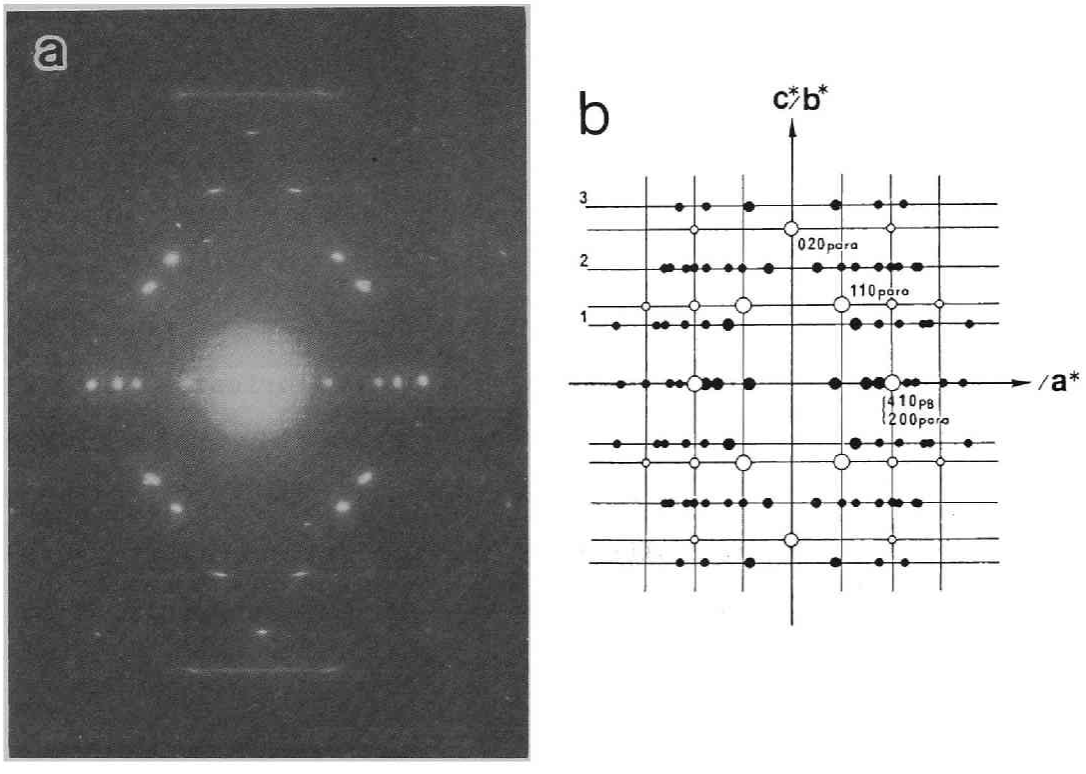

Fig. 1-7. (a) ED pattern of the PB thin film on which C_{28} crystals are crystallized, and (b) the schematic drawing corresponding to (a).

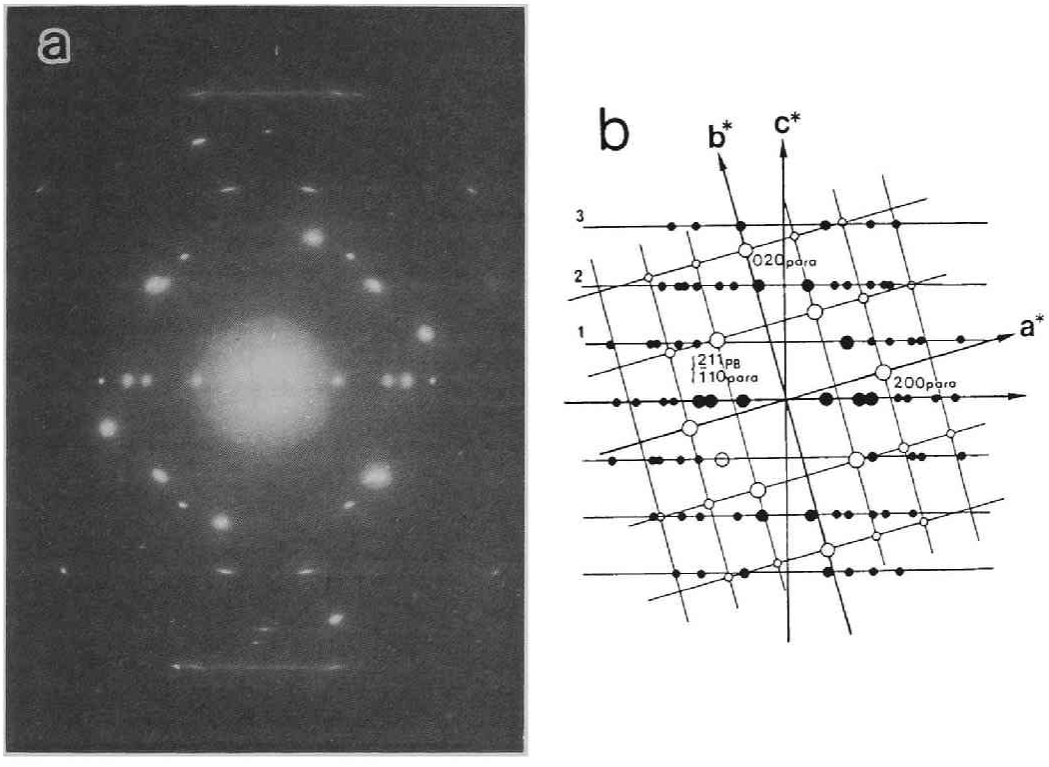

Fig. 1-8. (a) ED pattern of the PB thin film on which C_{28} crystals are epitaxially grown, and (b) the schematic drawing corresponding to (a).

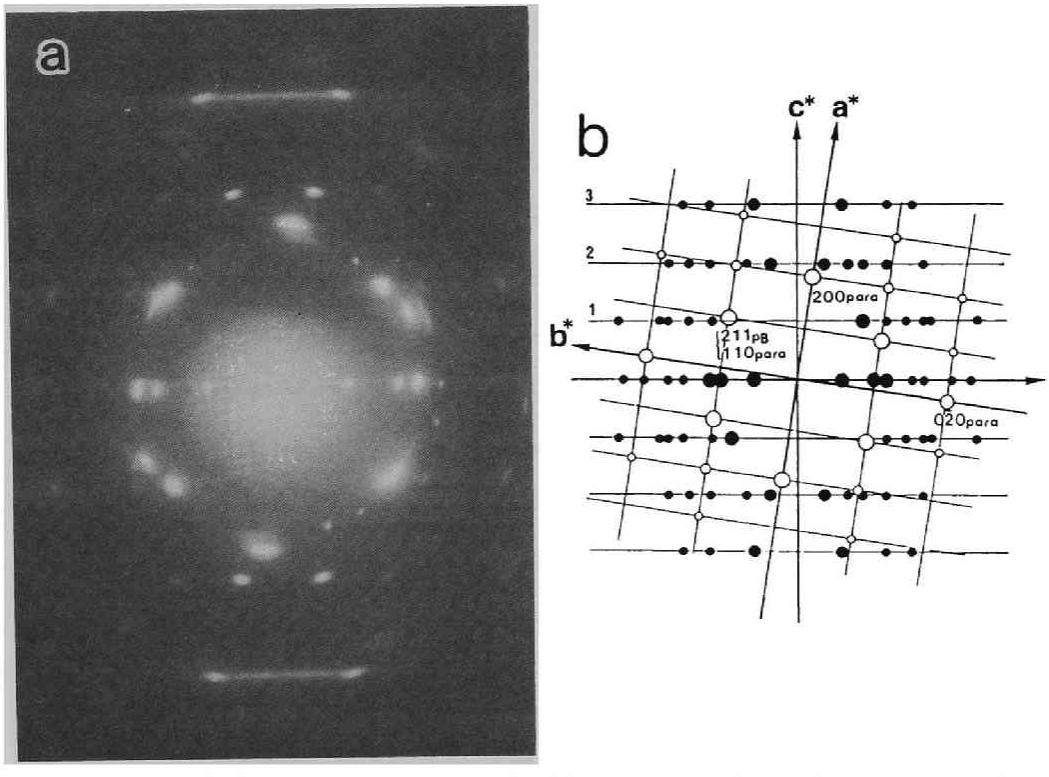

Fig. 1-9. (a) ED pattern of the PB thin film on which C_{24} crystals are epitaxially grown, and (b) the schematic drawing corresponding to (a).

pattern so that the 110 spot of C_{28} coincides with 211 of PB on the left side, as depicted in Fig. 1-8b. Consequently, the vector from the origin to the 110 spot of C_{28} makes an angle of 42° with the equator. It seems to be important for this epitaxy that the lattice spacings of (110) of the n-paraffin and (211) of PB are nearly equal; $d_p(110)$=0.411nm and $d_{PB}(211)$=0.431nm[20]. In reality, however, an *hk*0 plane of PB plays an important role in this epitaxy. Molecular chains are most densely packed in the {210} planes of the hexagonal PB crystals. These planes become the growth face of the solution-grown PB single crystal. Thus, one possible epitaxial mode is defined as follows:

$(001)_p /\!/ (210)_{PB}$, $[110]_p \lessdot 48° [001]_{PB}$

Figure 1-9 shows the ED pattern corresponding to the A'_3 mode. The reciprocal axis a^* of an n-paraffin crystal is close to the equator of the PB fiber pattern in Fig. 1-8 and nearly in the meridian in Fig. 1-9. The two *hk*0 net pattern of the n-paraffins in Figs. 1-8 and 1-9 are related to each other by a mirror symmetry with respect to the {110} planes, retaining the coincidence of the 110 spot of the n-paraffin with 211 of PB. This twin relationship implies that n-paraffin crystals of one mode, which are formed under the influence of the substrate, may produce those of the other by twinning on their {110} planes. Of course, the orientation of n-paraffin crystals which are caused by the twinning is really observed. However, since the ED patterns in Figs. 1-8 and 1-9 are interpreted in terms of different *hk*0 net patterns of n-paraffins, respectively, it

follows that n-paraffin crystals of each epitaxial mode grow independent of each other as their orientation is affected by the substrate surface. It is interesting here that n-paraffin crystals grown in either of the two mode of epitaxy maintain the coincidence of the 110 spot of n-paraffin and the 211 spot of PB. Though the present identification of the epitaxial mode is based on the (210) plane, the possibility on other planes such as (110) is not excluded.

1.3.4. Poly-4-methyl-1-pentene (P4MP)

As explained for Fig. 1-10, the 110 spot of orthorhombic C_{26} crystals coincides with the 331 spot of P4MP on the first layer line of the fiber pattern[21]. This epitaxial mode is characterized by an angle of 27° which the vector from the origin to the 110 spot makes with the equator of the P4MP fiber pattern. When the (001) basal plane of an orthorhombic C_{26} crystal is in close contact with the P4MP (110) plane, the condition that these two reflections be excited at the same time is fulfilled. At the present time, this coincidence is identified in the diffraction patterns of other n-paraffin/P4MP systems. The epitaxy mode is named the A_3 mode in a relation such as:

$(001)_p // (110)_{P4MP}$, $[110]_p \measuredangle 73°\ [001]_{P4MP}$

However, P4MP lamellar crystals grown from solution have a tetragonal shape whose edges are {100} planes[22]. Thus, further studies are needed to clarify the epitaxial growth of n-paraffin/P4MP systems on the basis of various planes including

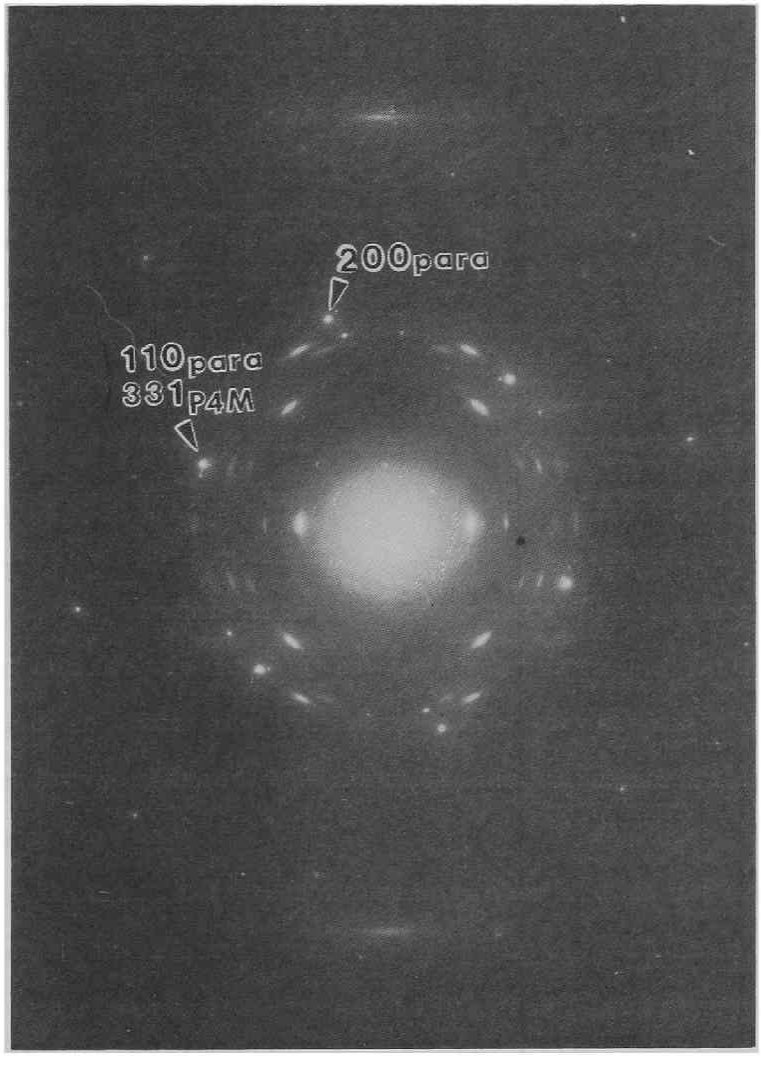

Fig. 1-10. ED pattern of the P4MP thin film on which C_{26} is grown.

Table 1-1. Epitaxial types of n-paraffins on the polymer substrate PE, iPP and PB.

	Modification	PE	iPP	PB
C_{20}	Triclinic	A_1	A_3	A_3
C_{22}	Triclinic	A_1	A_3	A_3
C_{24}	Triclinic, Monoclinic	A_1	A_3	A_2, A_3
C_{25}	Orthorhombic	A_1, A_2	A_3	A_2, A_3
C_{26}	Monoclinic	A_1, A_2	A_3	A_2, A_3
C_{27}	Orthorhombic	A_1, A_2	A_2, A_3	A_2, A_3
C_{28}	Monoclinic	A_1, A_2	A_2, A_3	A_2, A_3
C_{35}	Orthorhombic	A_1, A_2	A_1, A_2, A_3	A_3
C_{36}	Orthorhombic, Monoclinic	A_1, A_2	A_1, A_2, A_3	A_2, A_3
C_{40}	Orthorhombic	A_1, A_2	A_1, A_2, A_3	A_2, A_3
C_{44}	Orthorhombic	A_1, A_2	A_2, A_3	A_2, A_3
C_{50}	Orthorhombic	A_1, A_2	A_2, A_3	A_2, A_3

this one.

The two epitaxial modes in a twin relation are basically same in their growth mechanism, because both exhibit a common diffraction coincidence as described above. n-Paraffin crystals extend over the substrate surface in one growth direction under its control and in another direction by the growth nature of their own. The two epitaxial modes are classified only by a difference in the latter growth direction not affected by the substrate. By neglecting the distinction in the growth process, various epitaxial modes except the B mode in the n-paraffin/iPP system are unified into the following three types, A_1, A_2 and A_3, irrespective of the polymer substrates:

A_1: $(001)_p$//SS, $<110>_p$//FA,

A_2: $(001)_p$//SS, $[010]_p$//FA,

A_3: $(001)_p$//SS, $<110>_p \measuredangle \alpha$ FA,

where SS and FA denote the substrate surface and the fiber axis of a polymer substrate, respectively. In the A_3 types, the angle depends on and is inherent to the kind of the polymer. The observed epitaxial types are summarized in Table 1. Here, it should be noted that the $<110>_p$ of n-paraffin crystals largely contributes to their epitaxy on the polymer substrate.

1.4. Discussion

As shown in Table 1, n-paraffins crystallize differently, i.e. in triclinic, monoclinic and orthorhombic forms, depending on the chain length and crystallization condition [14,23]. The

most stable n-paraffin crystals grown under normal crystallization conditions are not always orthorhombic. Except in cases of longer n-paraffins on the PE substrate, the observed crystalline form of n-paraffins is orthorhombic. While n-paraffin crystals are being examined in an electron microscope, the diffraction pattern changes drastically from time to time, especially in the case of shorter paraffins, and settles in a pattern belonging to the orthorhombic form. The phase change from some form to the orthorhombic one easily takes place due to electron irradiation [24]. From an experimental point of view, a problem arises on whether or not the ED patterns of Figs. 1-2 to 1-10 result from phase changes induced by electron irradiation. Here it is stressed that these n-paraffins are carefully examined so as to prevent the phase changes. Most n-paraffins crystallize originally in the orthorhombic form on polymer substrates. This means that the interaction between methyl end groups of n-paraffins and the surface of the polymer substrate is so strong that the substrate forces the long chains of n-paraffins to align normal to the surface.

Figures 1-11a, 1-11b and 1-11c show the X-ray diffraction patterns of the PE films on which C_{24}, C_{28} and C_{50} are crystallized, respectively. As (00*l*) reflections due to the unit cell are seen in a line in the direction perpendicular to the substrate surface, n-paraffins are layered with their chain axes perpendicular or inclined to the surface. The measured lattice spacings are 3.035, 3.756 and 5.670 nm for C_{24}, C_{28} and

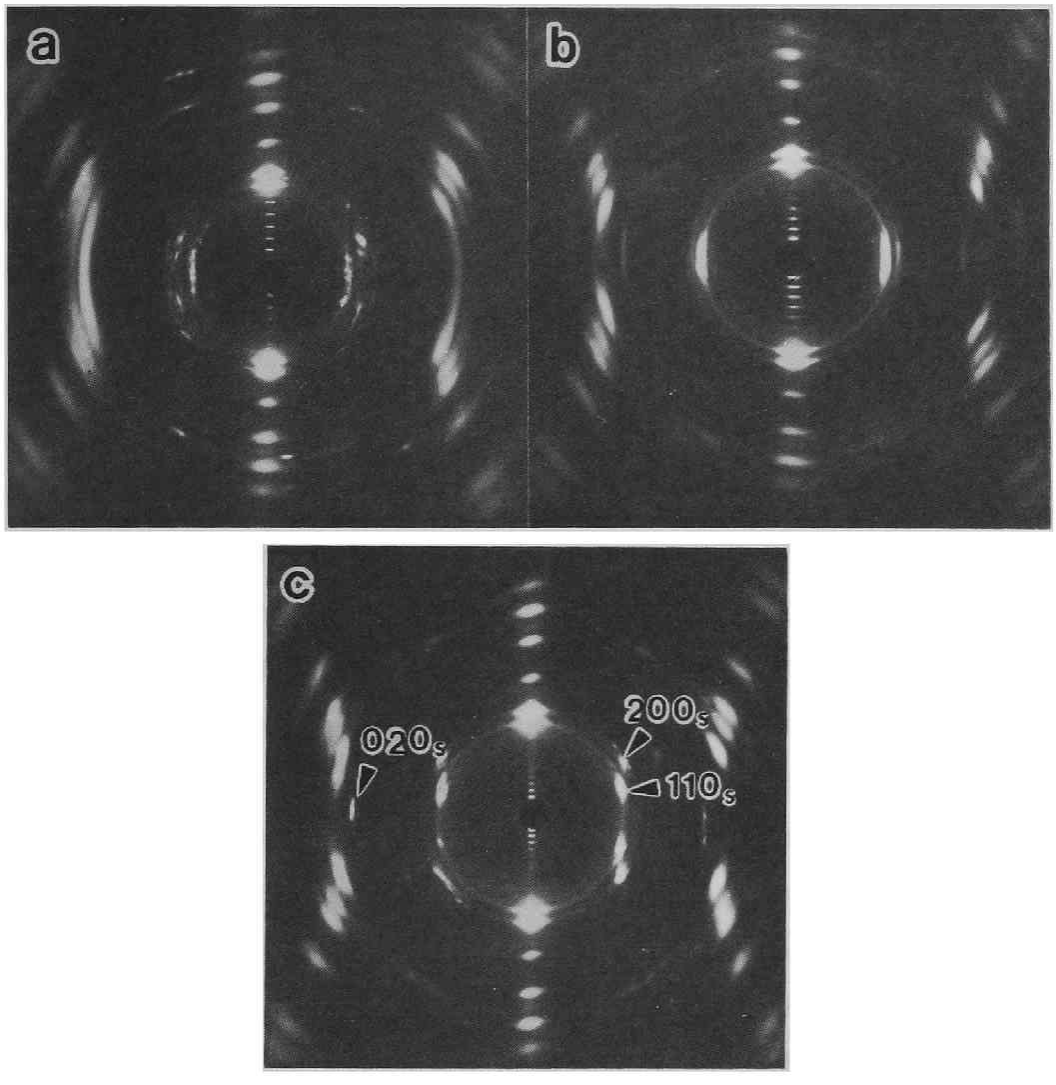

Fig. 1-11 X-ray diffraction patterns of the PE film on which various n-paraffins were epitaxially crystallized: (a) C_{24}, (b) C_{28} and (c) C_{50}. The PE film is set in such a way that the drawing direction (molecular direction) is horizontal and the normal to the film surface is vertical. The X-ray beams are incident parallel to the film surface, i.e. normal to these patterns. The 200_s and 020_s in (c) denote the 200 and 020 spots of the n-paraffin subcell[23], respectively.

C_{50}, respectively. From these values, it was found that C_{24}, C_{28} and C_{50} crystallized in the triclinic, orthorhombic and monoclinic forms, respectively[25]. In Fig. 1-11c, the 200_s reflection of the subcell is observed in the direction off from the substrate surface, and the 020_s one on it and in the direction of the PE molecular axis. This explains the weak 200 and strong 020 spots of the C_{50} ED pattern in Fig. 1-3a. In the case of C_{24}, the normal chain orientation is revealed by electron diffraction (see Fig. 1-9a) and the inclined one by X-ray diffraction. While the examination by electron diffraction is restricted to a small domain close to the interface, the bulky region is surveyed by X-ray diffraction. In view of the difference in the domain size of examination, the above inconsistency in orientation is not always surprising. The molecular orientation in n-paraffin crystals grown on the substrate is affected only in a short range from the interface. Thus, when n-paraffin molecules crystallize far from the interface, their crystallization behavior is determined by molecular interactions of their own. Polytypes and polysynthetic twins occur very often in n-paraffin crystals[13]. Through these mechanism, changes in the growth direction of n-paraffin crystals take place, leading to randomized molecular orientations and to the stable form in large specimens.

The various modes of epitaxy in Table 1 exhibit the following tendency. On the PE substrate, the A_1 mode occurs in all the n-paraffins and the A_2 mode appears in the n-paraffins

having larger number of hydrocarbons. On the iPP substrate, the A_3 mode occurs frequently in all n-paraffins. Further, it is noted that the n-paraffins longer than C_{40} can crystallize in the same way as PE [6]; n-paraffin chains align lying along the iPP surface with an inclination angle of 46° to the iPP fiber axis. On the PB substrates, the A_2 mode prevails in the all n-paraffins. In this regard, the crystallization temperature, at which the epitaxial growth is induced, may be an important factor. It appears that the longer the n-paraffin molecules, the higher the crystallization temperature. At higher temperatures, thermal motions of polymer chains in the substrate are activated, resulting in a change in the unit cell dimensions and in the molecular arrangement at the n-paraffin/polymer interface. PE has a negative thermal expansion of the c-axis (in the chain direction) of the unit cell [26]. At higher temperatures, the cell dimension along the PE chain axis decreases and, on the contrary, the *b*-axis dimension of the n-paraffins increases. Consequently, lattice fitting between the *c*-axis of PE and the *b*-axis of n-paraffins may be favorable to activate the A_2 epitaxial mode in the longer paraffins. When n-paraffins differing in chain length are overgrown on the same substrate, the change in the epitaxial mode according to the chain length may be caused by the change in the feasibility of lattice fitting between the n-paraffin crystals and the polymer substrate, which change is related to the crystallization temperature.

As for the molecular model of n-paraffin/PE epitaxy, the

adsorption model of an n-paraffin on the (001) basal plane of n-paraffin crystals is very instructive[27]. From the energy calculation of the adsorption, it appears that the most favorable orientation of the n-paraffin is described by the chain axis parallel to the [110] direction in the (001) crystal face. This orientation of methylene sequence is quite analogous to that of the PE chain to the (001) basal plane of a n-paraffin in the case of n-paraffin/PE epitaxy. In next chapter crystallization of long-chain compounds on the PE (110) plane which is one of the growth faces of PE single crystal was examined.

Wittmann and Lotz[3] and Petermann et al.[2] proposed a molecular model of epitaxial growth of PE onto drawn iPP. On the basis of this model, we examined the epitaxial growth mechanism of n-paraffins on the iPP substrate, paying attention to the way of deposition of n-paraffin molecules on their contact plane. In Fig. 1-12, the atomic arrangement on a (010) plane of the monoclinic iPP lattice is depicted. Methyl side groups of iPP chains, which are directed upward from the figure, are aligned in a line. As for the atomic arrangement on the (010) plane, a two-dimensional lattice with a rectangle unit cell of ABCD is set up. The direction AB makes an angle of 50° with the iPP molecular axis, and accordingly, the AD direction makes an angle of 40° . Geometrically, the two-dimensional coincidence of the n-paraffin lattice on the plane is described as follows;

$d_{AB}(0.846\text{nm}) \approx 2d_p(110)(0.411\text{nm})$

and

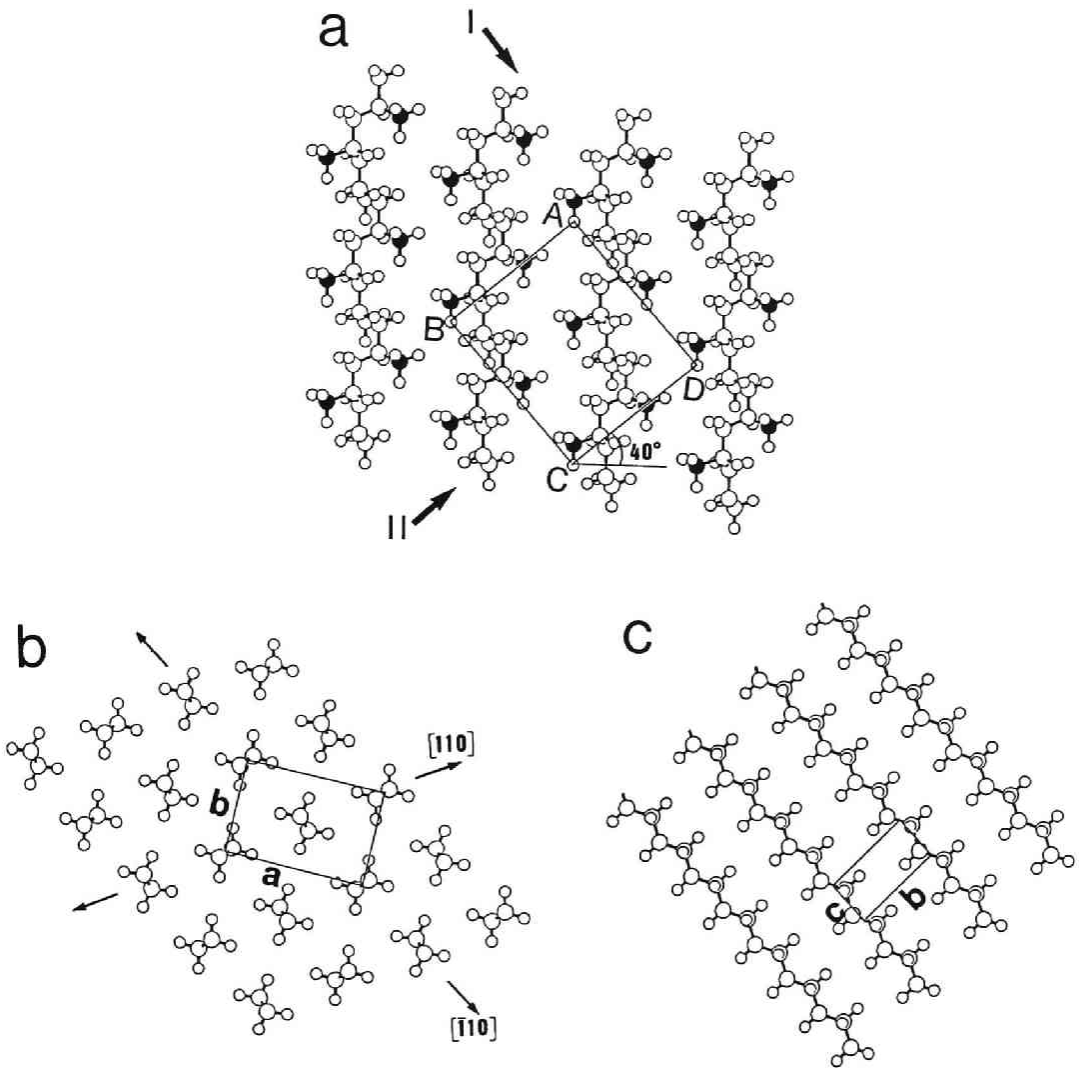

Fig. 1-12. (a) Schematic drawing of a (010) plane of monoclinic PP. Large and small circles denote the carbon and hydrogen atoms, respectively. Solid large circles mean the carbon directed upward. A rectangle shows the two-dimensional unit cell on the surface; AB = 0.846 and AD = 1.005 nm. The angle which AB (and CD) makes with the molecular axis of iPP is 40°. (b) The schematic drawing of the n-paraffin crystal lattice with the orthorhombic form, which is projected on the (001) basal plane. The rectangle denotes the projected unit cell (a = 0.742 and b = 0.496 nm). (c) The schematic drawing of the n-paraffin crystal lattice with the orthorhombic form, which is projected on the (100) plane. The rectangle denotes the b-c plane of the unit cell; b = 0.496 and c = o.254 nm. These three drawings correspond to one another with the orientation as described in the text.

$d_{AD}(1.005nm) \approx 2d_p(010)(0.492nm)$

$4d_p(001)(0.254nm)$.

In the first coincidence, when the (001) plane of n-paraffin lattice is in contact with the (010) iPP plane, the [110] direction of the n-paraffin lattice is aligned parallel to the AD direction. When the n-paraffin crystals grow maintaining the lattice coincidence with the iPP crystal, the 110 diffraction spots of the n-paraffin are observed in the direction at an angle of 40° from the equator of the iPP fiber pattern. n-Paraffin crystals epitaxially grown on the iPP substrate in the A_3 mode show this orientational relationship of the diffraction spots. It is noted from Fig. 1-12b that the methyl end groups of n-paraffins are most closely aligned along the <110> directions in the (001) n-paraffin plane. When one of the close-packed [$\bar{1}$10] lines is fitted in any of the "channels" which are formed by side methyl groups of iPP chains as specified by the direction I in Fig. 1-12a, all other [$\bar{1}$10] lines also fit in respective channels at the interface (the commensurate adjustment). No lattice fitting is detectable in other directions. Namely, the commensurate adjustment is responsible for the A_3 epitaxial growth of n-paraffin/iPP systems. The other growth direction of n-paraffin crystals is not influenced by the substrate surface, but determined according to their own crystallization behavior. Two different modes of n-paraffin/iPP epitaxy, A_3 and A'_3, are thus caused by the difference in other growth direction.

As for the second coincidences, it is first considered that

the b-axis of the n-paraffin lattice is in the AB direction. When the c-axis of the n-paraffin lattice, i.e. the molecular axis, is laid down on the (010) surface of iPP as shown in Fig. 1-12c, n-paraffin chains are arranged parallel to the substrate surface and at an angle of 50° from the iPP chain axis, so that they coordinate along the channel II as in Fig. 1-12a. This coordination of planar zigzag methylene chains on the iPP surface was proposed by Wittmann and Lotz [3] and Petermann et al.[2]. Otherwise, it is considered that n-paraffin chains can align along the channel I so that the c-axis coincides with the AD direction. The PE/iPP and the mode B of n-paraffin/iPP epitaxiy can be explained on the basis of these models. Only the atomic arrangement in the (010) plane of monoclinic iPP has been discussed. Further studies on other iPP planes are needed to draw a clear conclusion. The epitaxial growth behavior of n-paraffin crystals on other oriented helical polyolefins, PB and P4MP, could be explained on the basis of a similar channel model. Since alkyl side groups of these polymers are arranged in a more complicated manner, even on planes with low Miller indices, a detailed examination is required to explain their epitaxial growth in the future.

Another problem is whether the epitaxial growth occurs to attain the thermodynamic stability between n-paraffin crystals and the polymer substrate or from the kinetic origin. The nucleation on the substrate is speculated as follows: for longer n-paraffins, nuclei where n-paraffin molecules are aligned

parallel to the substrate are more stable than those in which chains are perpendicular to the substrate. From this view of nucleation, it is assumed that longer n-paraffins form the nuclei with their chain axis lying down on the polymer substrate, leading to B mode epitaxy on the iPP substrate. However, the nucleation rate depends on the interfacial energy at the contact plane between the n-paraffins and the substrate. Hence, detailed studies to elucidate the mechanism of epitaxy are needed in the future.

References

[1] K.A. Mauritz, E. Baer and A.J. Hoffinger, J.Polymer Sci. Macromol. Rev. 13(1978) 1;

B. Wunderlich, Macromolecular Physics, Vol. 1(Academic Press, New York,1973).

[2] J. Petermann, G. Broza, U. Rieke and A. Kawaguchi, J.Mater. Sci. 22(1987)1477.

[3] J.C. Wittmann and B. Lotz, J.Polymer Sci. Polymer Phys. Ed. 23(1986)205.

[4] B. Lotz and J.C. Wittmann, J.Polymer Sci. Polymer Phys. Ed. 24(1986)1541.

[5] B. Lotz and J.C. Wittmann, J.Polymer Sci. Polymer Phys. Ed. 24(1986)2559.

[6] G. Broza, U. Rieke, A. Kawaguchi and J. Petermann, J.Polymer Sci. Polymer Phys. Ed. 23(1985)2633.

[7] J. Petermann and R.M. Gohil, J.Mater. Sci. 14(1979)2260.

[8] C. Herring, Phys. Rev. 82(1951)87.

[9] D.C. Bassett, F.C. Frank and A. Keller, Phil. Mag. 8(1963)1739.

[10] D. Bloor and G.D. Dean, J.Mater. Sci. 5(1970)752.

[11] D.J. Blundell and A. Keller, J. Macromol. Sci. -Phys. B25(1986)1.

[12] D. Dorset, J. Macromol. Sci. - Phys. B25(1986)1.

[13] R. Boistelle, in: Current Topics in Materials Science, Vol. 4, Ed. E. Kaldis(North-Holland, Amsterdam, 1980).

[14] J.C. Wittmann and B. Lotz, J. Polymer Sci. Polymer Phys. Ed.

23(1985) 205.

[15] H.M.M. Shearer and V. Vand, Acta Cryst. 9(1956) 379.

[16] G. Natt and P. Corradini, Nuovo Cimento Suppl. 15(1960) 40.

[17] Z. Mencik, J. Macromol. Sci. - Phys. B6(1972)101.

[18] D.R. Morrow, J.A. Sauer and A.F. Woodward, J. Polymer Sci. B3(1965)463.

[19] M. Kojima, J. Polymer Sci. B5(1967)245.

[20] G. Natta, P. Corradini and I.W. Bassi, Nuovo Cimento Suppl. 15(1960)52.

[21] H. Kusanagi, M. Takase, Y. Chatani and H. Tadokoro, J. Polymer Sci. Polymer Phys. Ed. 16(1978)131.

[22] D.C. Bassett, F.R. Dammont and R. Salovey, Polymer 5(1969)597.

[23] P.W. Teare, Acta Cryst. 12(1959)294.

[24] A. Kawaguchi, S. Isoda, M. Ohara and K. Katayama, Bull. Inst. Chem. Res., Kyoto Univ. 59(1981)284.

[25] G.M. Broadhurst, J. Res. Natl. Bur. Std. (US)66(1962)241.

[26] Y. Kobayashi and A. Keller, Polymer 11(1970)114.

[27] R. Boistelle and H.E.L. Madsen, J. Crystal Growth 43(1978)141.

Chapter 2. Crystallization Behavior of Long-Chain Compounds on the (110) plane of polyethylene

2-1. Introduction

When polyethylene(PE) is epitaxially crystallized from the melt on oriented isotactic polypropylene(iPP), the chain stems align parallel to the substrate surface and edge-on lamellae are formed [1]. In order to elucidate the overgrowth mechanism of PE onto iPP, we studied the growth behavior of n-paraffins which play the role of a model substance for PE. n-Paraffins are analogous to PE in chemical and crystallographical structures, except for chain folding [2]. When n-paraffins are crystallized from the melt on various polyolefin substrates, shorter homologues stand perpendicular to the substrate surface. This is in contrast to longer homologues, which maintain lattice coincidence at the n-paraffin/polymer interfaces. The longer homologues having more than 40 carbon atoms lying down on the iPP substrate as PE does. The oriented overgrowth of n-paraffins on drawn PE was first observed by Richard [3]. Willems attempted to epitaxially overgrow organic materials on cold-drawn polymers [4,5]. In their reports and in Chapter 1, however, the surfaces

of polymer substrates, on which n-paraffins were epitaxially crystallized, were not well-defined crystallographically in the uniaxially drawn polymers examined, because the constituting polymer crystallites were randomly arranged around the drawing axis (i.e. fiber orientation). In order to elucidate the epitaxial growth mechanism more precisely, we crystallized n-paraffins on the PE substrates with a crystallographically well-defined surface [6].

Two interactions between the methyl end groups of n-paraffins and the polymer substrates, and between methylene sequences of hydrocarbon chains and polyolefin chains play an important role in the oriented overgrowth of n-paraffins on PE. Accordingly, we expect that other long-chain compounds such as n-alcohols and n-carboxylic acids may crystallize epitaxially on the polymer substrates. We report here that the normal long-chain alcohols and carboxylic acids crystallized epitaxially on the PE substrates. Their epitaxial crystallization behavior and its mechanism are discussed.

2.2. Experimental

The procedure to prepare thin PE films with the surface bounded by the {110} planes is sketched in Fig. 2-1. (a) An NaCl crystal with a fresh (001) cleavage surface was immersed for 3-5 min. in a 0.01 wt% p-xylene solution of high density PE (Sholex 6050 with a melt index of 50, produced by Showa Denko Co., Ltd.) at about 80℃. Then, PE lamellae were epitaxially grown in an

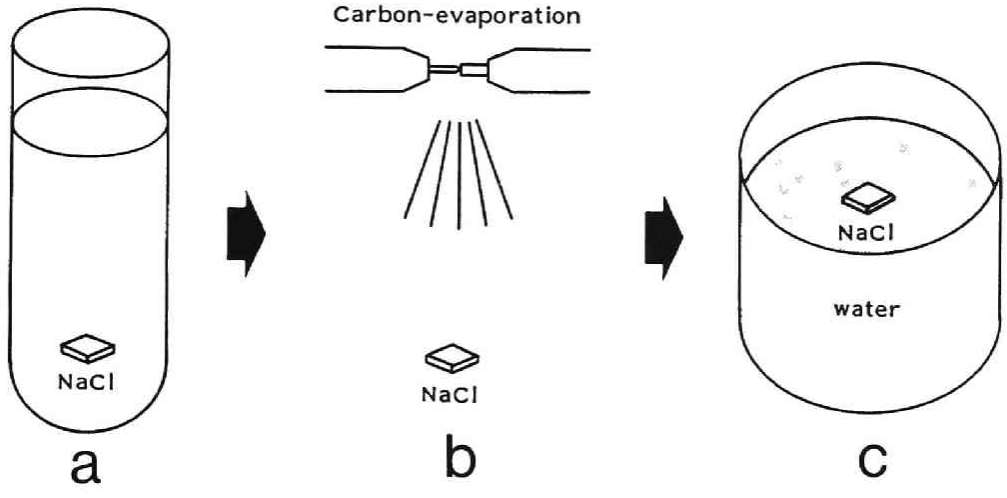

Fig. 2-1. Procedure to make a thin PE film bounded by {110} planes (detailed in text).

edge-on wise on the NaCl surface. (b) After being taken out of the solution and dried, the NaCl crystal was heat-treated at 125 for 1 hr to perform better orientation of PE, and was coated with a thin carbon film by evaporation. (c) The NaCl crystal was put on the water surface so that it dissolved, allowing the thin, carbon-coated PE film to float off. The PE film was picked up on a copper grid for electron microscopy. The long-chain compounds were epitaxially crystallized onto the PE film surface which had been in contact with the NaCl surface in the following ways:

(1) by direct vapor-deposition at reduced pressure onto the substrate which was kept at various temperatures;

(2) by slow cooling from the melt, which was produced by heating above the melting points of the organic compounds that had been deposited on the substrate by the method (1);

(3) by evaporation of the solvent from a solution.

The epitaxial growth morphologies of the specimens thus prepared were observed with a transmission electron microscope JEOL JEM-200CS and a scanning electron microscope Hitachi S-310.

We examined n-paraffins n-C_nH_{2n+2} of C_{22} to C_{50}, n-alcohols n-$C_nH_{2n+1}OH$ with n of 23 to 30 and n-carboxylic acids n-$C_{n-1}H_{2n-1}COOH$ with n of 17 to 30, all of which were purchased from Tokyo Kasei Kogyo Co., Ltd. Hereafter, these compounds are designated as n-C_n, n-C_nOH and n-$C_{n-1}COOH$ with the constituent carbon number n.

2.3. Result

2.3.1. n-Paraffins

The structure of the PE substrate is first discussed. Figures 2-2a and 2-2b show a transmission electron micrograph of a thin PE film and the corresponding electron diffraction (ED) pattern, respectively. The thin PE film is composed of edge-on chain-folded lamellae with the thickness of a few tens of nm. The lamellae were arranged in a cross-hatched array and densely packed with their long sides perpendicular to one another. The diffraction spots in Fig. 2-2b were indexed on the basis of the orthorhombic unit cell [7]. The 002 spots of PE observed in two perpendicular directions indicate that the PE chains lay parallel to the substrate surface in two mutually perpendicular directions. In all the PE substrates used here, the 110 diffraction spots were never observed, but both or either of the 210 and 310 spots were observed in most cases. In the PE crystal lattice, the (110) plane intercept almost perpendicularly (87°) to the $(\bar{2}10)$ plane, and makes an angle of 97° with the $(\bar{3}10)$ plane. Thus, we concluded that the wide PE surface in contact with the (001) plane of NaCl were bounded by {110} planes.

Figure 2-3a shows a transmission electron micrograph of vapor-deposited n-C_{50} crystals on the PE substrate at 40℃. The 00*l* reflections of the corresponding ED pattern in Fig. 2-3b, resulting in a long spacing of 3.39 nm, were lined up in the direction of the 002 spot of PE. No strong *hk*0 reflection was observed, except for the 210 spot. Thus, it was determined that

n-C_{50} molecules formed orthorhombic crystals, the chain axis being parallel to the PE substrate with the following coincidence relation:

$(001)_p//(110)_{PE}$, $[001]_p//[001]_{PE}$.

Here p and PE denote n-paraffins and PE, respectively. Although this epitaxial relationship was defined as the mode B in the n-C_{36}/PE system[6], we redefine it as B_1, because this is a different epitaxy mode in which the molecular chains are parallel to the PE substrate surface. Grown from vapor phase on the substrate kept at room temperature, n-paraffins of C_{26} to C_{50} exhibited the B_1 epitaxial mode.

Two different ED patterns shown in Fig.2-4 were very often observed in shorter n-paraffin/PE systems at room temperature, but not exclusively in cases of higher homologues. These patterns reveal two different modes of epitaxy. In Fig. 2-4a, the 110 spot of the *hk*0 net pattern of n-C_{26} is perpendicular to the 002 spot of PE. This epitaxial mode was referred to as the mode A_1 which was observed in the n-C_{36}/PE system [2], being characterized as:

$(001)_p//(110)_{PE}$, $[110]_p//[001]_{PE}$.

Another mode of epitaxy, A_2 [2], was also observed, particularly between longer n-paraffins/PE;

$(001)_p//(110)_{PE}$, $[010]_p//[001]_{PE}$.

Previously, the A_1 and A_2 epitaxial modes were discussed from the viewpoint of the thermodynamical stability of the crystal shape, i.e., in terms of Wulff's theorem [8]. It was concluded that these modes of epitaxy should occur on the most

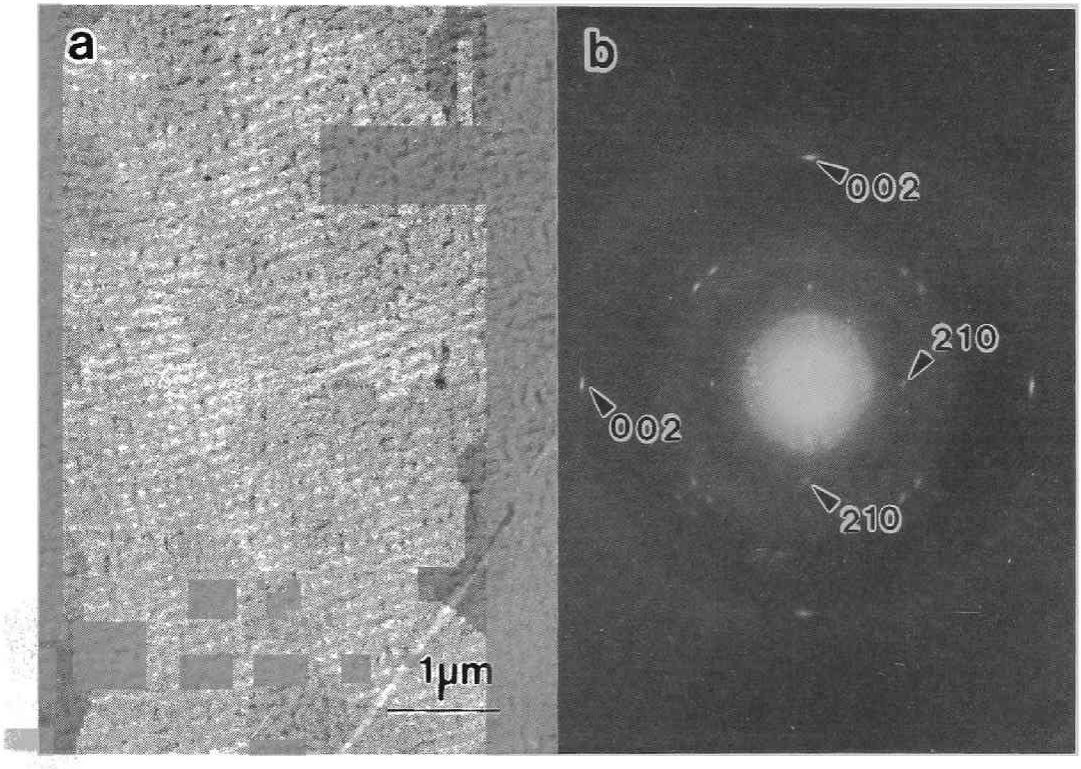

Fig. 2-2. (a) Transmission electron micrograph of the PE substrate. The tiny hillocks running in vertical and horizontal directions are edge-on PE lamellae. (b) Corresponding ED pattern.

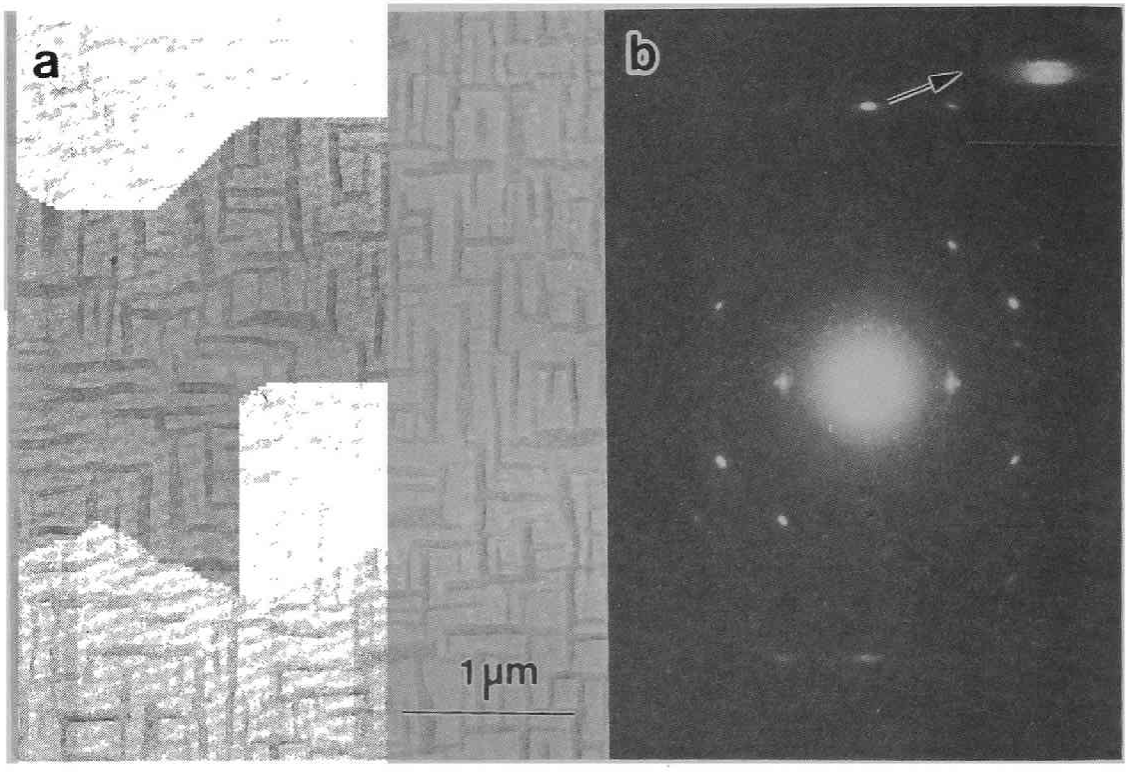

Fig. 2-3. (a) Transmission electron micrograph of n-C_{50} crystals vapor-deposited on the PE substrate at 40°C. Crystallites grew with their long axes parallel to the chain axis of PE; vertical and horizontal. (b) ED pattern. The low order of 00*l* reflections are not reproduced in the photograph because of their weakness and the strong halation due to the incident beams, although discerned in the original negative. Instead, higher order of 00*l* reflections around the first layer line of PE are shown in a enlarged inset.

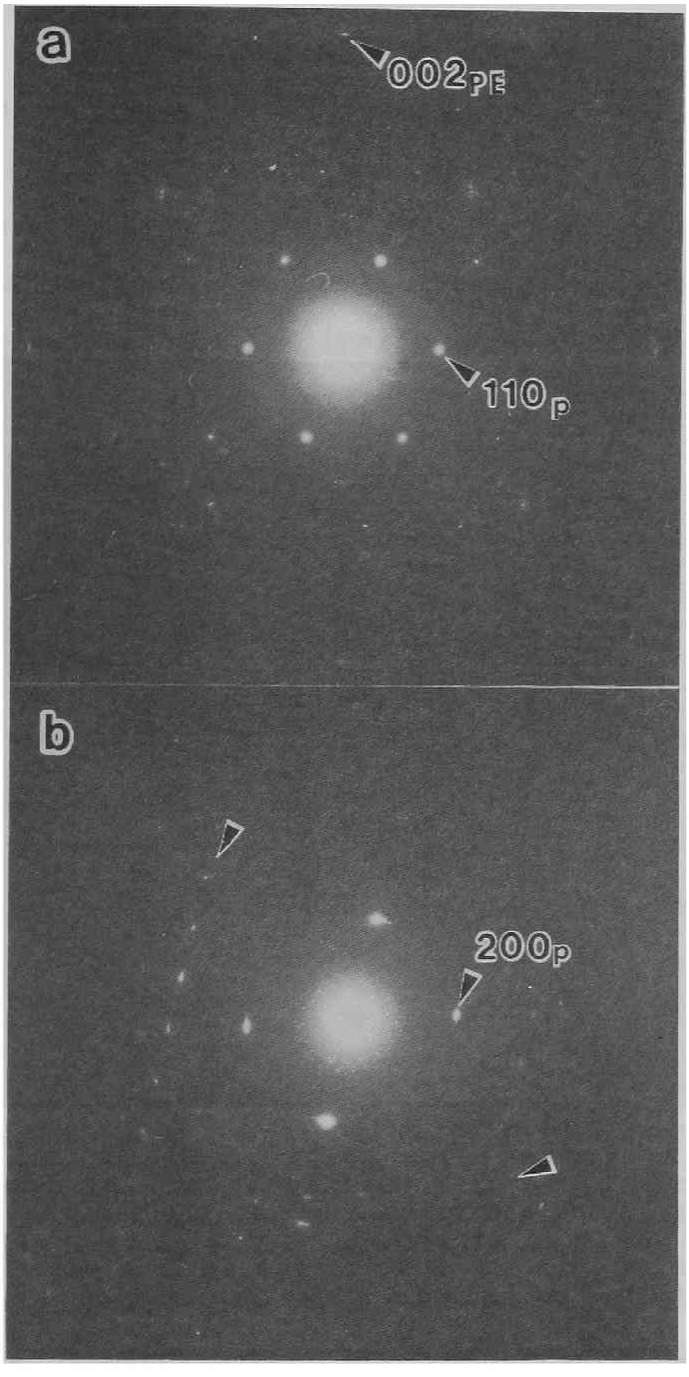

Fig. 2-4 ED patterns of n-C_{26} crystallites grown by vapor-deposition on the substrate at 30°C In (a), the *hk*0 net pattern of n-C_{26} is observed with the 110 spot perpendicular to the 002 spot of PE. In (b), lined-up spots shown by arrows are indexed as *hk*14 spots of n-C_{26} crystal, and the 200 spot is perpendicular to the 002 spot of PE.

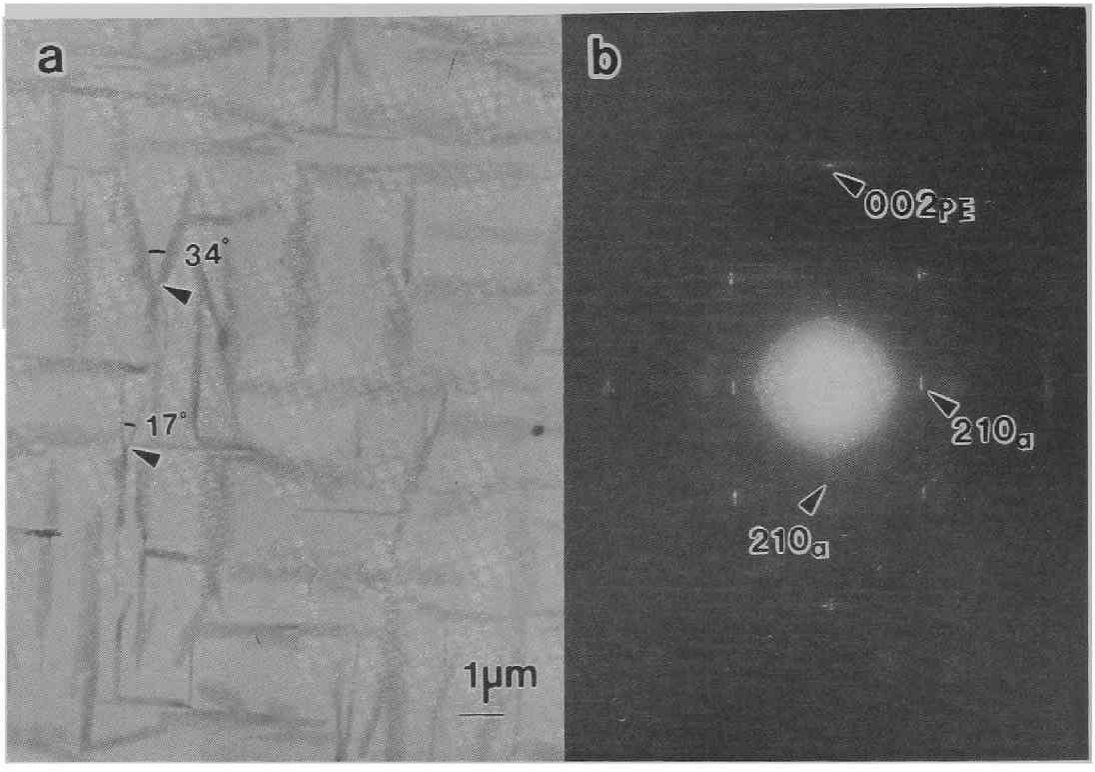

Fig. 2-5. (a) Transmission electron micrograph of n-C_{23}OH crystals grown by vapor-deposition, and (b) the ED pattern corresponding to the encircled area. In the figures, the PE chain axis is vertical and horizontal. Crystallites oriented vertical and horizontal are in the β-form, and oblique ones branched from them, as indicated by arrows in (a), are in the α-form.

stable {110} planes which could be exposed as the surface plane of crystallites in uniaxially oriented PE.

There is another mode of epitaxy that is characterized by the ED pattern in Fig. 2-4b. The arrowed spot corresponds to a lattice spacing of 0.374 nm and consequently, these are indexed with the 200 reflection of either orthorhombic or monoclinic modification[9]. No other *hk*0 spots except *h*00 are observed. This suggests that molecules crystallized in the monoclinic form (the M_{011} type[10,11]) with their axes tilted to the substrate surface. When the (001) basal plane is set parallel to the substrate surface, the *hk*14 spots can be observed lining up as shown by thin arrows in Fig. 2-4b. Although the crystalline form was not determined definitely, the above conclusion is most plausible, because the (001) basal plane tends to be parallel to the substrate surface when n-paraffins are crystallized from the melt[2]. The ED patterns in Fig. 2-4b indicate that the [110] direction of n-paraffin coincides with [001] of PE. Consequently, the following epitaxial growth mode was deduced:
$(001)_p // (110)_{PE}$, $[110]_p // [001]_{PE}$.
This mode is defined as A_1, although the crystalline modification is different.

Among the various modes of epitaxy examined here, the B_1 mode was more populated at low temperatures, and the A_1 and A_2 modes at high temperatures. "Low temperature" here means a temperature far below the melting temperature. We observed no sharp transition temperature where the epitaxial mode changed

from B_1 to any of the A modes. For example, the A_1 and/or A_2 modes prevail over B_1 at temperatures above 40 and 45℃ for n-C_{36} and n-C_{50}, respectively. The A modes of epitaxial growth occurred more frequently from vapor phase with increasing substrate temperature, and occurred exclusively in crystallization from the melt. It should be noted that odd-numbered n-paraffins behaved in the same way in the epitaxial crystallization as even-numbered ones, crystallizing in the orthorhombic form in most cases.

2.3.2. Normal long-chain alcohols

Figure 2-5 shows an electron micrograph and the corresponding ED pattern of n-tricosanol (n-C_{23}OH) crystallized by vapor-deposition. The crystals are arranged in a cross-hatched way as seen in the cases of n-paraffins in Fig. 2-3. The ED pattern exhibits the 00*l* and 210 reflections. The 00*l* spots are lined up in the direction normal to the long side of the crystallite and parallel to the 002 spot of PE. The measured long spacing of 6.2 nm indicates the β-form of n-C_{23}OH crystals[12](This form is designated as α-form in ref. [13]). Similarly to the n-paraffin/PE system, the diffraction features show that the n-C_{23}OH crystals grew with the molecular chain parallel to the PE molecules. Further, it was concluded from the observation of the 210 reflection that $(110)_a$//(110)PE coincidence (the subscript a refers to n-alcohols) was attained. Thus, the B_1 mode was also observed in the β-form of odd-numbered n-alcohols; $(110)_a$//$(110)_{PE}$, $[001]_a$//$[001]_{PE}$.

Since the unique angle β of the unit cell of the monoclinic β form of n-C_{23}OH is 91°, the crystal structure is very close to the orthorhombic n-paraffin[12]. This may explain that the odd-numbered n-alcohols epitaxially crystallize on PE in the same morphology as the n-paraffins. As indicated by the arrows in Fig. 2-5a, there are crystallites which are branched from the end of β-form crystallites at about 34° or from the side at a inclination angle of 17°. Their long spacing was measured at 6.09 nm. This value indicates that the crystalline form is the monoclinic α-form whose long spacing value is 5.982 nm[12]. The corresponding lattice planes are parallel to the long side of the inclined crystallites as well. Because the molecular chains are highly tilted on the basal plane in the crystal structure, the molecular chain in the α-form of n-C_{24}OH crystals is also aligned parallel to the PE chain axis.

When the alcohols with such an oblique crystal structure are crystallized with the chain axis parallel to the substrate, the orientation of the resulting crystallites is complicated, as observed in the crystallization of even-numbered alcohols. Figure 2-6a shows an electron micrograph of n-tetracosanol (n-C_{24}OH) crystals grown at 40℃ by vapor-deposition. Most crystallites reveal a ribbon morphology extended presumably in the [110] direction. We divided the crystallites into three groups taking into account the relative orientations of the ribbon-like growth hillocks; (P,P'), (T_1,T_2) and (T'_1,T'_2). This designation originates from the orientational relationship of the ribbon axes

with respect to the PE chain axes. P and P' denote the orientation perpendicular to the horizontal and vertical PE axes, respectively. The T_1 and T_2 crystals are tilted at angles of $\pm 120°$ with respect to the horizontal PE axis, and T'_1 and T'_2 at angles of $\pm 120°$ with respect to the vertical one. In the above notation, both T_1-T'_1 and T_2-T'_2 make a right angle.

The ED pattern of Fig. 2-6b was taken from the P crystallite in Fig. 2-6a. The low order of 00*l* reflections gives a long spacing of 6.49 nm comparable to that of the orthorhombic β-form(6.5nm)[12]. The space group of the β-form is P2/C. In the crystal lattice, molecules linked by hydrogen bonding between OH groups are stacked in the chain direction, maintaining the 2_1 screw axis. Thus, the low order 00*l* (*l*=2n) spots are observed. Although the β-form is not identified in higher members of even-numbered n-alcohols[12], it is shown here that the alcohols can be crystallized in the orthorhombic β-form when they are deposited throughly evaporation onto the substrate at 40℃. It should be noted that, in the original negative of the ED pattern (Fig. 2-6b), additional weak 00*l* spots with *l*=2n+1 were recognized in between the strong 00*l* reflections with *l*=2n, especially around the first layer line of the PE diffraction pattern. This involves the default of the 2_1 screw symmetry in the chain direction. A possible structural irregularity to cause the symmetrical deficiency is such a stacking disorder as a polytypic structure, as observed in normal alkanes [13-15] and stearic acids[16].

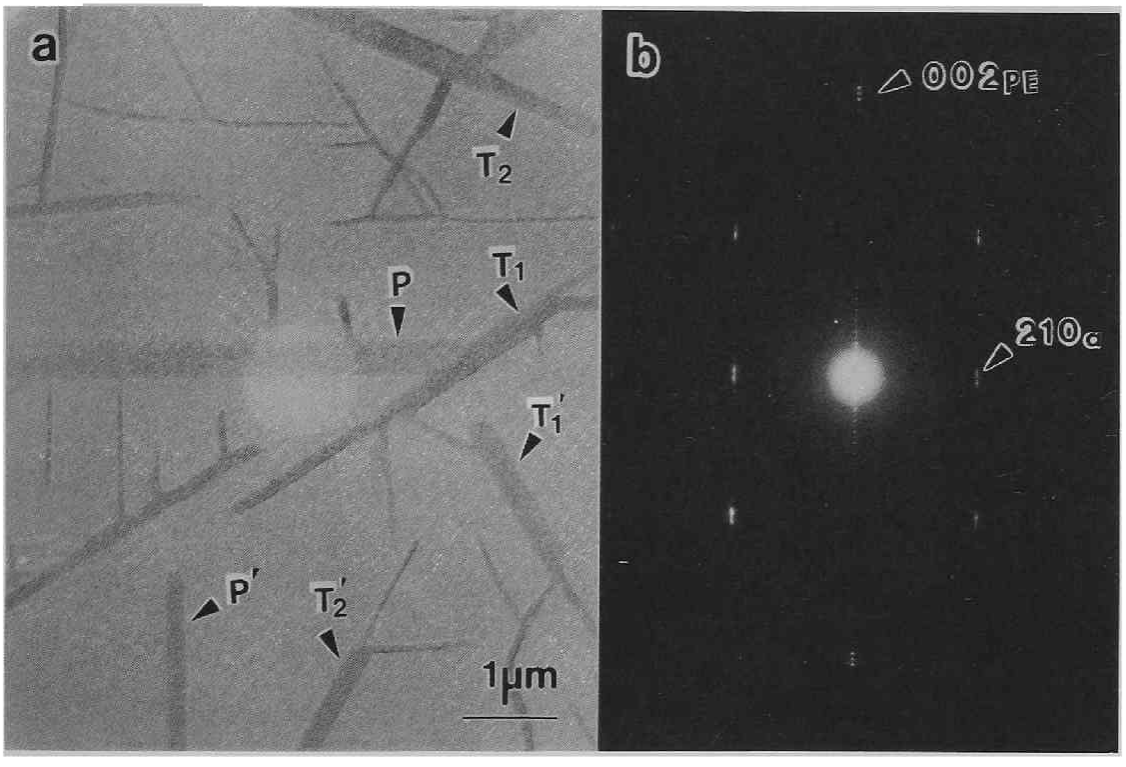

Fig. 2-6. (a) Transmission electron micrograph of n-C_{24}OH crystals grown by vapor-deposition, and (b) the ED pattern corresponding to the encircled area. PE chain axes are vertical and horizontal.

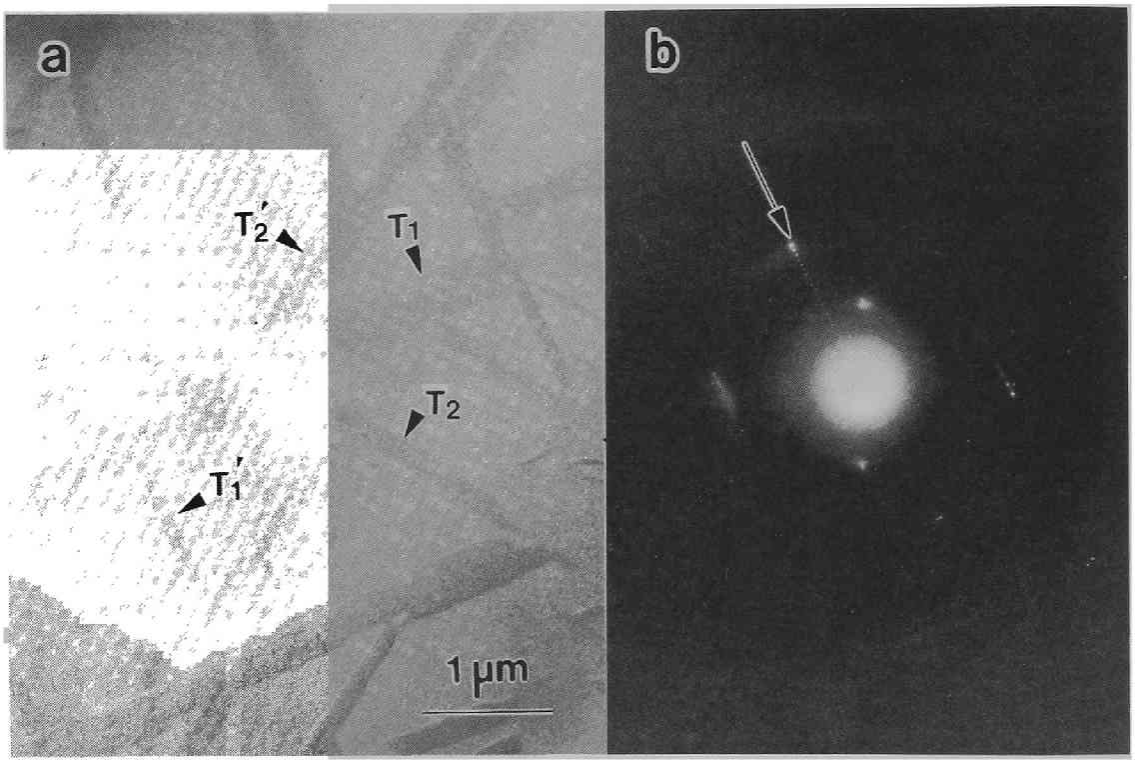

Fig. 2-7. (a) Transmission electron micrograph of n-C_{26}OH crystallites grown at 40℃ by vapor-deposition. They are designated as (T_1, T_2) and (T'_1, T'_2), according to the present notation that their inclination angles are 120° with respect to the PE *c*-axis: vertical and horizontal. (b) ED pattern corresponding to the encircled area. The arrowed 00*l* spots are lined up with an angle of 30° with the polyethylene *c*-axis.

The epitaxial relationship between the (P,P') crystallites of n-C_{24}OH and PE crystals equals the B_1 mode. On the other hand, the (T_1,T'_1) crystallites exhibited the 00*l* spots in a line perpendicular to their long side, having the long spacing of 5.4 nm which indicates the γ_1-form [12,16]. (This form is referred to as β-form in ref. [13].) Figure 2-7a shows an electron micrograph of n-hexacosanol (n-C_{26}OH) crystallites grown on the substrate at 40℃ by vapor-deposition. Their preferential orientations are divided into four groups, matching those in the n-C_{24}OH/PE system. The long side of the T-crystallites were tilted by 120° from the chain axis of PE. The 00*l* spots are lined up perpendicular to the long side and tilted by 30° from the 002 spot of PE. The long spacing of 6.14 nm obtained from them is comparable to the reported value of the γ_1- form (5.8 nm)[12]. These results show that the T-crystallites have the γ_1- form and that alcohol molecules are aligned parallel to the chain axis of PE.

The crystallization behavior of n-alcohols on the (110) surface of PE depends strongly on the temperature of the substrate. When vapor-deposited at 25℃ , n-C_{24}OH partly crystallized, exhibiting a halo in the ED pattern. Obviously, this temperature is too low for complete crystallization. When vapor-deposited onto the substrate at elevated temperatures, both even- and odd-numbered n-alcohols are no longer oriented parallel to the substrate surface, but are aligned with their molecular axes perpendicular or inclined to the surface. Figure 2-8 shows

the ED patterns of n-C_{24}OH crystals vapor-deposited on a PE film kept at 50°C. The 00*l* spots did not appear; instead, the *hk*0 net patterns appeared with a distinct orientational relationship with respect to the PE pattern. We notice again that the 110 and 020 spots are in the direction parallel to the direction of 002 of PE in Figs. 2-8a and 8b, respectively. These orientational relationships are identical to the A_1 and A_2 modes of epitaxy observed in n-paraffin/PE systems[2,6].

There was no sharp transition temperature where the epitaxial mode changed from B_1 to any of A-series of modes; only the population of the former mode decreased with increasing temperature, depending on the chain length. On inorganic substrates such as alkali halides, these normal long-chain compounds are also crystallized epitaxially in the parallel orientation at low temperatures and in the perpendicular orientation at high temperatures[18,19]. This tendency seems to be common to the epitaxy of these compounds, irrespective of the kind of substrate surface. The *hk*0 net patterns in Fig. 2-8 show a perpendicular molecular orientation; therefore, the crystalline form revealing the A series of modes may be the orthorhombic or β-form. In addition to the above patterns, another pattern was often observed in melt-crystallized n-alcohols, indicating a tilted molecular orientation on the substrate. This pattern was quite similar to those in Fig. 2-4b. This suggests that there is another mode of epitaxy in which monoclinic crystals grow with the $(001)_a$ plane being parallel to $(110)_{PE}$, as discussed for the

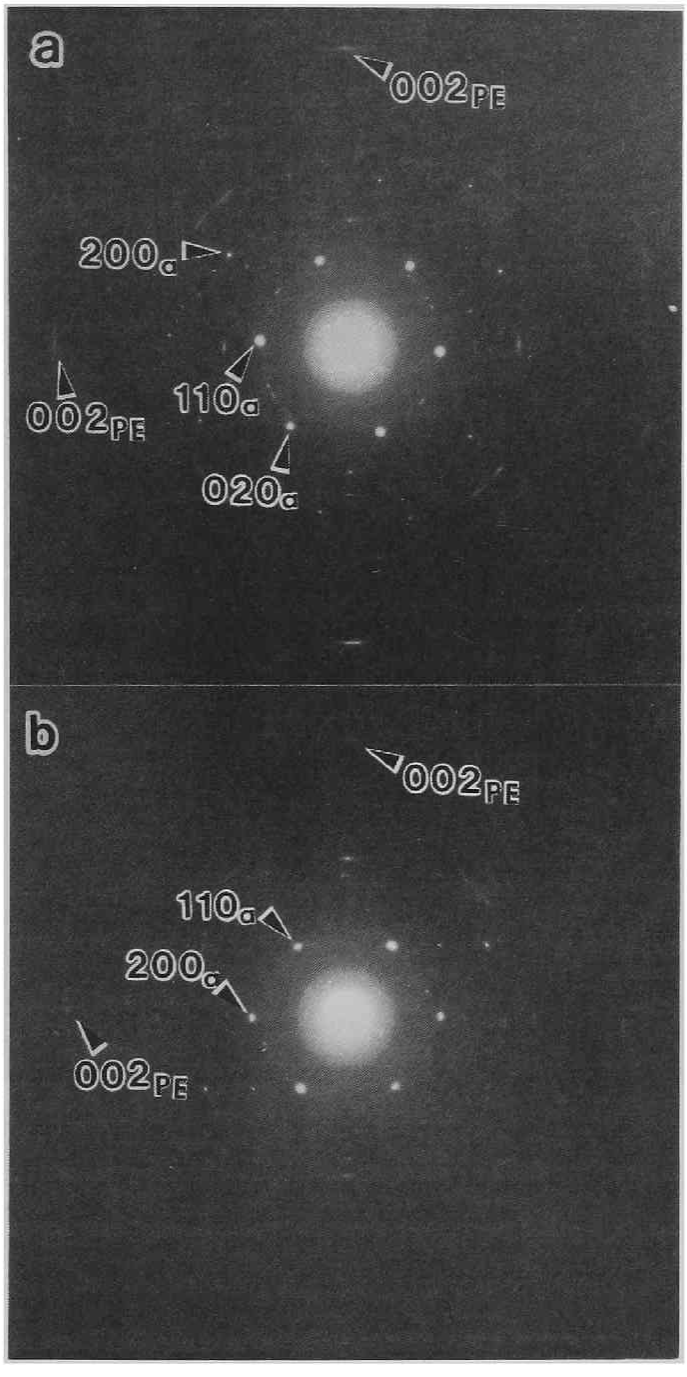

Fig. 2-8. ED patterns of n-C_{24}OH crystallites grown on the PE substrate at 50°C by vapor-deposition. The 110 spot in (a) and the 200 spot in (b) are perpendicular to the direction of the 002_{PE} spot, corresponding to the epitaxies of A_1 and A_2, respectively. In these figures, the polyethylene *c*-axis is vertical and horizontal.

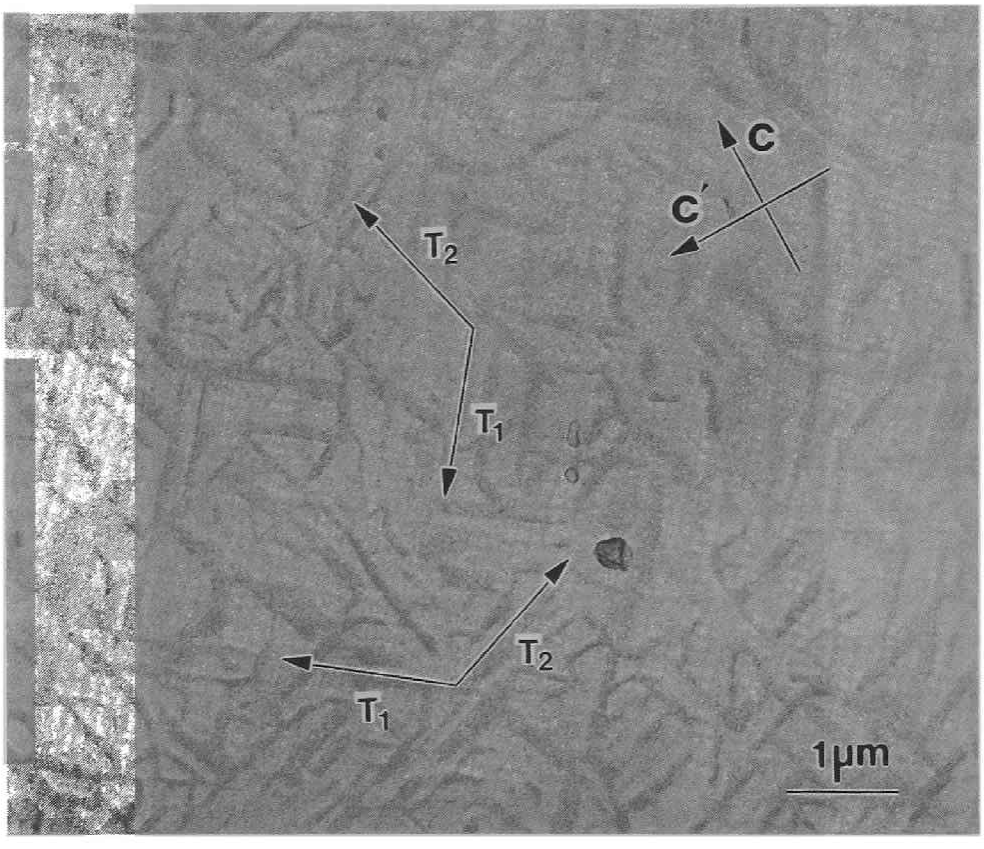

Fig. 2-9. Transmissiion electron micrograph of n-tetracosanoic acid crystallites grown by vapor-deposition. The arrows C and C' denote the directions of chain axis of PE. Two pairs of arrows, (T_1, T_2) and (T'_1, T'_2), stand for the average directions of long sides of the crystallites, and each pair makes an identical angle of 125° .

n-C_{26}/PE system.

2.3.3. Normal Long-Chain Carboxylic acids

There are many crystalline modifications in n-carboxylic acids that depend on the chain length and the number (odd or even) of carbon atoms. The carboxylic acids that crystallize with the orthorhombic subcell are the B'- and C'-forms in odd-numbered homologues [20,21] and B- and C-forms in even-numbered homologues [22-24]. The subcell and molecular staggering in the unit cell of carboxylic acids studied here is analogous to either of the α- and γ_1-forms of n-alcohols. Hence, the morphology observed in the epitaxial crystallization has been interpreted in the same way as those of n-paraffins and n-alcohols. Fig. 2-9 shows an electron micrograph of n-tetracosanoic acid (n-C_{23}COOH) crystals grown at 40℃ by vapor-deposition, exhibiting elongated crystallites that are arranged with their long sides oriented in four different directions. According to the same notation used in the n-alcohol cases, the crystals were classified into two pairs, (T_1,T_2) and (T'_1,T'_2). The PE chains run in the directions bisecting the angle, 125° , which the average directions of long sides of respective crystallites, paired as (T_1,T_2) and (T'_1,T'_2), make with one another. In more detail, all crystallites are oriented to make an angle of 117.5° with the PE chain axis, i.e., T-designated crystallites are oblique to the PE *c*-axis and T'-designated ones to the *c*'-axis. The angle is very close to the angle of 117.2° , which the molecular chains make

with the (001) basal plane of the B-form [21,23]. This orientation relation is similar to that observed in the monoclinic γ_1-form of n-alcohol/PE systems. This implies that carboxylic acid crystals with the B-form grew on the PE substrate in the B_1 mode of epitaxy. The carboxylic acids with n = 18,19,26 and 30, deposited in the same way, also crystallized epitaxially in a similar morphology.

2.3.4 Epitaxial growth from vapor phase on a uniaxially drawn film of PE

Figure 2-10 show an electron micrograph of n-hexatriacontane deposited on a uniaxially drawn film of PE and corresponding ED pattern. This diffraction pattern indicates that molecular chains of the n-paraffin lie parallel to the c-axis of PE. This result corresponds to the morphology in which n-paraffin lamellae grew edge-on on the PE substrate with their chains parallel to the c-axis of PE. This orientation is different from the case of n-paraffins crystallized on a drawn film of PE from the melt. In melt-crystallization, molecular chains of n-paraffins stood perpendicular to the surface of the PE film (see chapter 1). These crystallization behaviors of n-paraffins on the drawn PE film are the same as those on the (110) plane of PE. From this, it is concluded that the epitaxial growth on the (110) plane of PE is predominant for epitaxial growth when long-chain compounds crystallized on a uniaxially drawn film of PE.

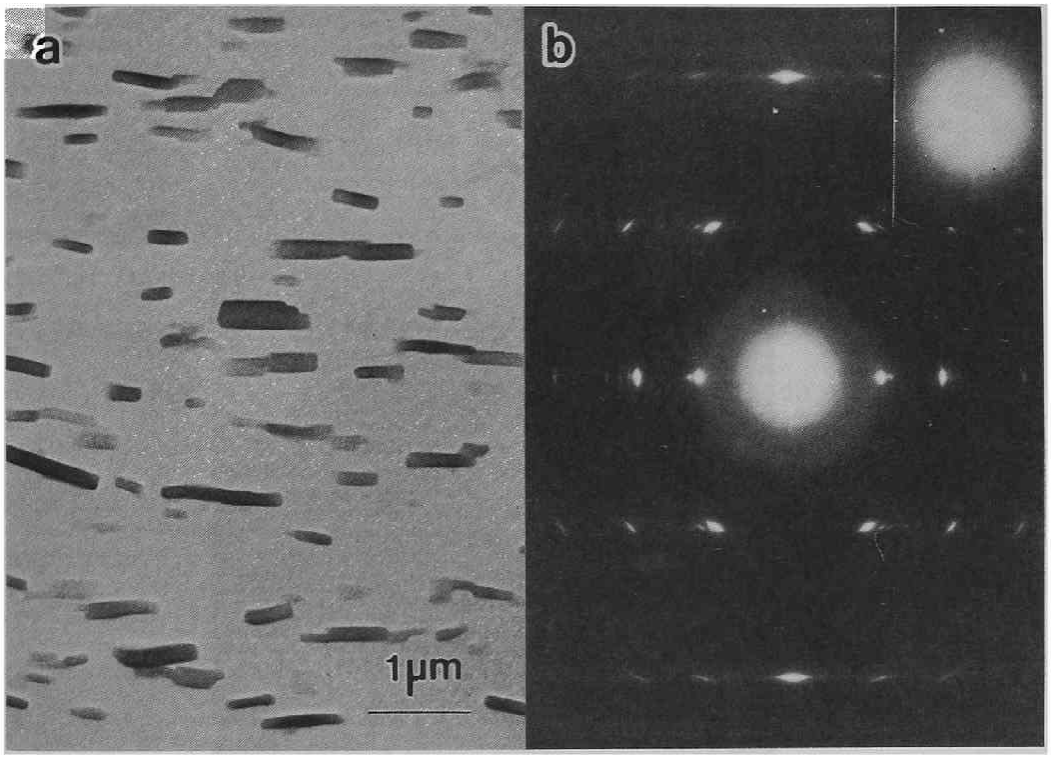

Fig. 2-10 (a) Transmission electron micrograph of n-hexatriacontane crystallites grown on the uniaxially drawn PE film, and (b) the corresponding ED pattern.

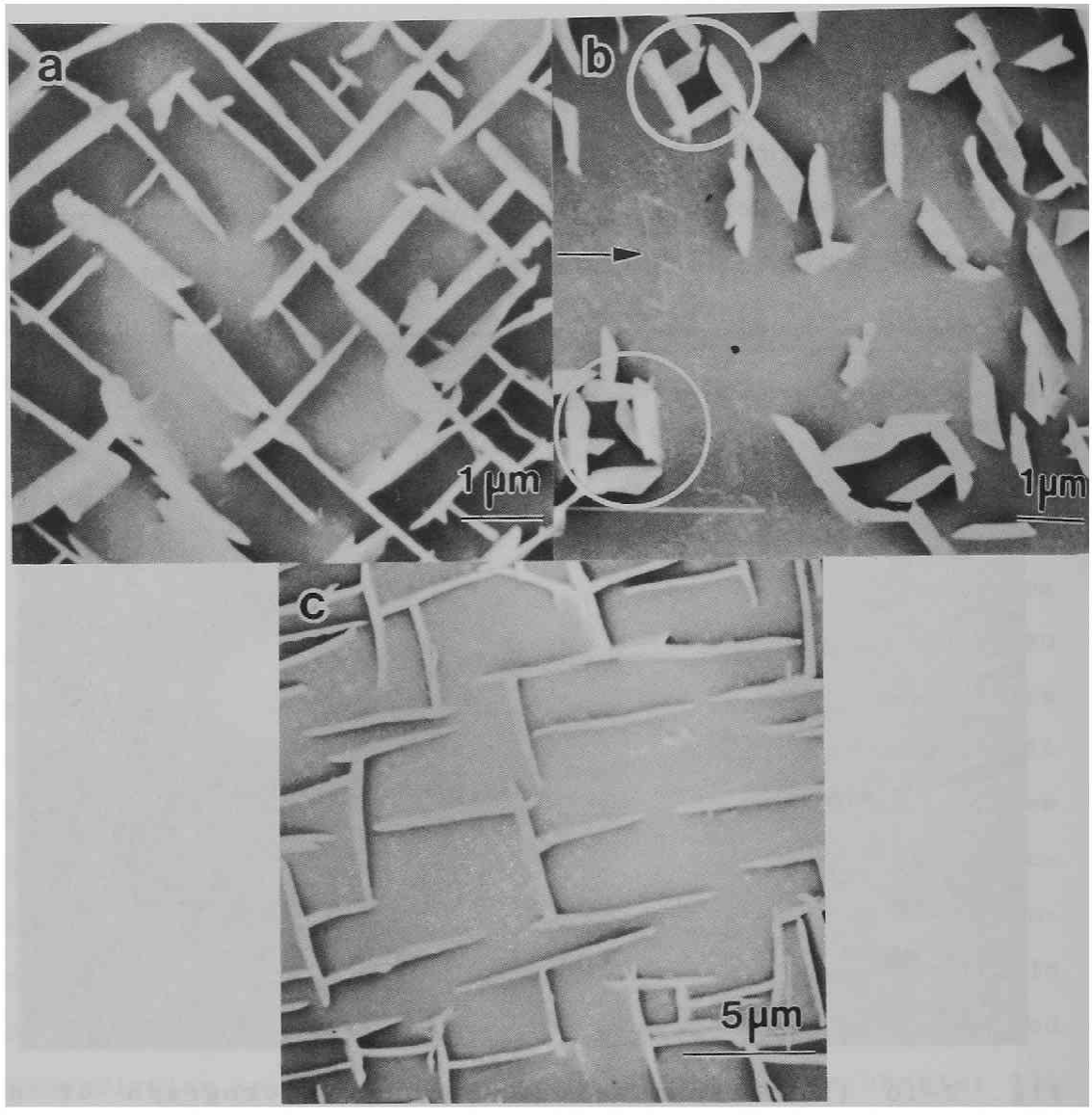

Fig. 2-11. Scanning electron micrographs of (a) n-C_{35}, (b) n-$C_{24}OH$ and (c)n-$C_{18}COOH$ crystals grown on the (110) PE surface from an n-heptane solution by evaporation of the solvent. In (a) and (c), two kinds of platelets crossed perpendicularly grew edge on. In (b), four differently oriented edge-on platelets are discerned. The encircled four edge-on platelets are arranged to form a rectangular box. Two of them, being face to face, were tilted in opposite directions towards the substrate. The difference in the tilting direction is due to the difference in growth manner between II and II' (see text). The morphology of edge-on platelets is parallelogrammic, as seen from the morphology of tumbled platelets, trimmed with white lines as shown with an arrow.

2.3.5 Epitaxial growth from solution

Figures 2-11a, 11b and 11c show electron micrographs of epitaxial solution-growth of n-paraffins, n-alcohols and n-carboxylic acids, respectively. They were grown by placing a drop of a saturated solution in n-heptane or benzene on a PE substrate, and subsequently evaporating the solvent at room temperature. The characteristic array of plate-like crystals resulted from the epitaxial overgrowth on the PE lamellae that are arranged in the cross-hatched way. Generally, when the normal long-chain compounds were slowly crystallized from solution, the rate of homogeneous nucleation was slow compared with that of heterogeneous nucleation and subsequent crystal growth. As a result, large and thin plates were formed edge-on with their side surface in contact with the substrate surface in the present solution crystallization. The plates were as thin as the PE lamellae, i.e., about 20 nm in thickness. This implies that the growth rate in the direction perpendicular to the chain axis is larger than that in the chain direction.

2.4. discussion

The normal long-chain compounds crystallize either in the orthorhombic form or in the monoclinic one. Both forms have a common orthorhombic subcell that corresponds to the PE orthorhombic unit cell [7]. In the B_1 epitaxial mode, the orthorhombic and monoclinic crystals of the compounds are formed with their (110) plane in contact with the (110) plane of PE, so

that their molecular chains are arranged parallel to the PE chains. The orientation of crystallites, the molecular orientation within them, and the orientation relative to the PE chain axis are illustrated in Fig. 2-12, in which the shapes I, II and II' denote the postulated morphologies of the orthorhombic and monoclinic crystallites. The long side of these shapes correspond to the (001) basal surface. When the orthorhombic platelets grow edge-on on the substrate surface, their long sides are perpendicular to the PE chain axis(type I). In the monoclinic crystal, the laterally packed molecules are staggered in the molecular direction, and consequently tilted to the basal plane. Hence, the long side of the resulting crystallites tilt against the PE chain axis. Two different orientations with the same tilting angle (types II and II') arise, depending on the type of the lattice coincidence between the molecular chains in the crystallites and the PE crystal. The monoclinic platelets of types of II and II' might nucleate and grew at the same probability. A complicating factor is that the present PE substrate comprised edge-on lamellae arranged in two perpendicular ways(see Fig. 2-2). In the orthorhombic form, some crystallites grow on the PE lamellae ordered in one direction, taking the perpendicular orientation of type I in Fig. 2-12. Simultaneously and independently, crystallites grow in a similar way on PE lamellae ordered in the other (perpendicular) direction. Thus, the crystallites of two kinds oriented perpendicular to each other grow at the same time, and hence, the

morphology and orientation of the crystallites were complex (see e.g., Figs. 2-3,2-5 and 2-11a).

In the case of the monoclinic form, four differently oriented crystallites appear due to a combination of types II and II' of the crystallites and the two chain-orientations of the PE substrate, as observed in the case of hexacosanol and tetracosanol crystals (Figs. 2-7 and 2-11b) and tetracosanoic and nonadecanoic acid crystals (Figs. 2-9 and 2-11c). Consequently, both the orthorhombic and monoclinic crystals cause six kinds of different orientations(Figs. 2-5 and 2-6). The oblique angles θ in Fig. 2-12 may depend on the tilting angles of the molecular chains to the basal plane of the unit cell, which differ in the various monoclinic forms. Hence, the crystalline modification can be identified by measuring the oblique angle θ with respect to the PE axis, if the normal-long chain compounds are epitaxially crystallized.

In the B_1 mode, there are two different crystallographic correlations between the crystallite and the PE substrate, depicted as types I and II in Fig. 2-12, caused by two kinds of side-by-side molecular packing: (a) a continuous coherent lattice and (b) twinning with respect to the (110) plane. In the monoclinic crystal, the two lateral stacking manners lead to two different oblique orientations (Fig. 2-12). The two types of lattice coincidence are unified on the basis of the subcell as follows;

$(110)_{sc}//(110)_{PE}$, $[001]_{sc}//[001]_{PE}$,

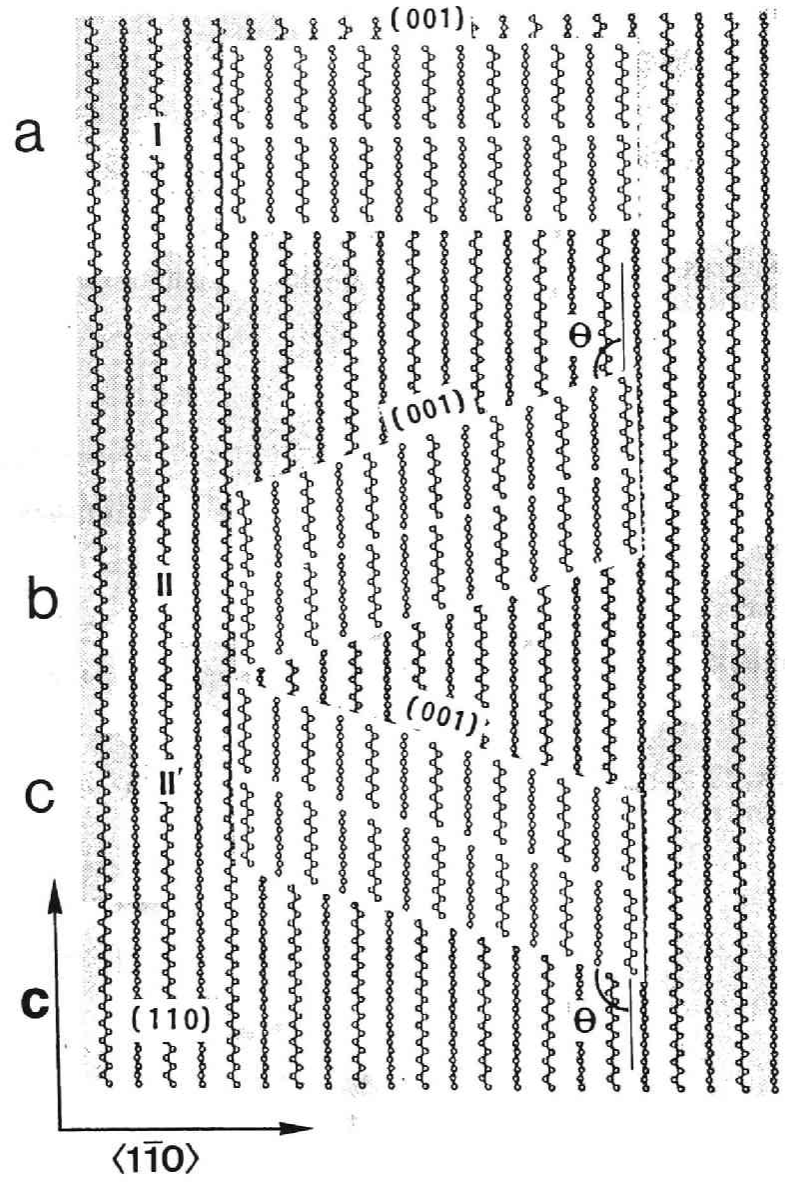

Fig. 2-12. Models of the shape and orientation of normal long-chain crystallites epitaxially grown on the (110) surface of PE and the molecular orientation within them: (a) an orthorhombic unit cell, and (b) and (c) a monoclinic unit cell. The shapes drawn in white denote crystallites. θ denotes the angle which the projected basal surface of crystallites makes with the PE chain axis. The arrow c denotes the PE *c*-axis.

where sc denotes the subcell. This lattice matching is the origin of the B_1 mode of epitaxy.

Through the present results, it can easily be envisaged that various normal long-chain compounds, which differ in the kind of end group, carbon number of hydrocarbon chain and crystalline modification, all can be crystallized at low temperatures in the B_1 epitaxial mode: their chains lie down parallel to the PE chains, maintaining the above unified lattice coincidence at the interface. The lattice dimensions of the subcells of these compounds strongly depend on the temperature, but the variation in their values and those of PE is only a few percent in the low temperature range of crystallization. From the viewpoint of the unit cell dimensions, it is understood that the compound crystals grow laterally on oriented PE through the lateral packing modes (1) and/or (2) without producing serious lattice strains. We, therefore, predict that other normal long-chain compounds with an orthorhombic subcell will crystallize epitaxially on PE in this way. Indeed, we succeeded in epitaxially crystallizing other types of normal long-chain compounds not described here, such as normal long-chain alkyl halides and esters, on the PE substrate. Figure 2-13 shows ethyl tetracosanate crystals grown from solution on the PE (110) plane.

The epitaxial growth due to the above subcell matching suggests that the length of hydrocarbon chain affects the epitaxial crystallization, because the polymorphic modification depends on the chain length. In fact, the short chain compounds

which usually crystallize in the triclinic form with the triclinic subcell do not grow epitaxially on PE, because the triclinic subcell is not compatible with the orthorhombic PE unit cell.

Edge-on PE lamellae of several hundred nm in width and a few tens of nm in thickness are arranged in a cross-hatched array on the substrate(Fig. 2-2). If the subcell matching drives the present epitaxy of normal long-chain compound crystals on the PE substrate, their size is to be limited within the lamellar thickness in the direction of PE chain. Nevertheless, the compounds grown by vapor-deposition over the above site were limited to several hundred nm in the thickness direction. They also extended into ribbon-like crystals in excess of the limited length of lattice compatibility in the direction perpendicular to the PE chains (see Figs. 2-3,2-5,2-6,2-7,2-9 and 2-11). Thus, the epitaxial lattice matching was not always maintained over the entire interface between the compound crystals and the PE substrate surface. Although defined as the {110} planes, the exposed surface of individual lamellae may not be smooth in molecular dimension but micro-faceted by other crystallographic planes, leading to step formation. The fact that hydrocarbon chains of normal long-chain compounds are oriented to be parallel to the PE chains, performing the lattice coincidence $(110)_{SC}//(110)_{PE}$, proves that PE chains on the exposed {110} planes controlled the oriented crystallization of the compounds. Even so, the growth mechanism through heterogeneous nucleations

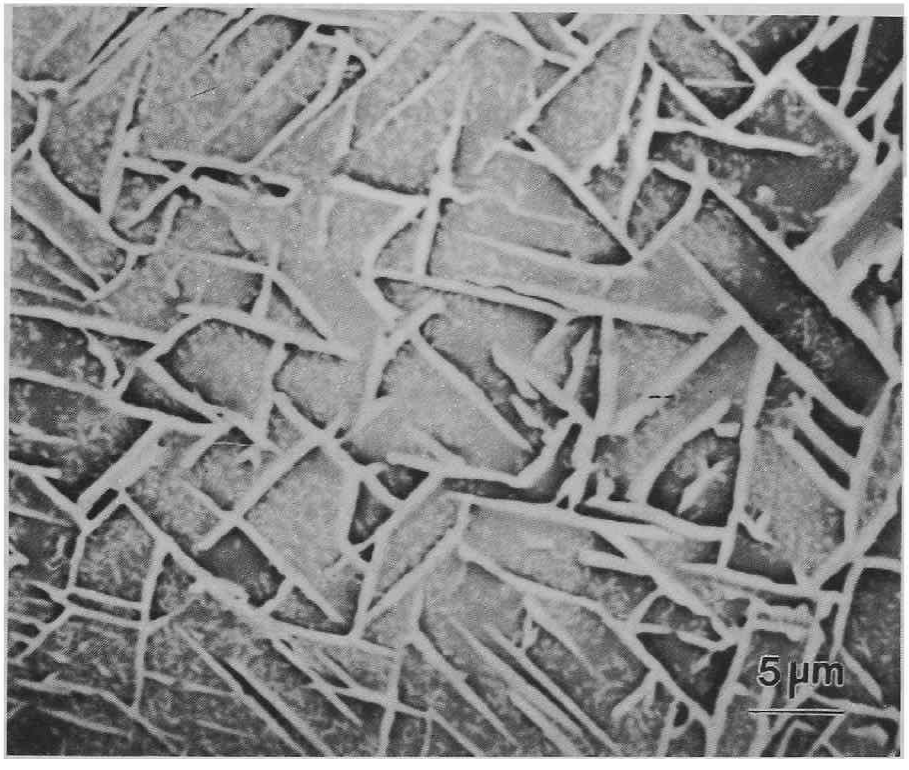

Fig. 2-13 Scanning electron micrograph of the morphology of crystals of ethyl tetracosanate grown on the PE (110) plane.

(1) on the {110} planes and (2) at the steps or kinds is considered. As mentioned above, the size of the compound crystallites is not so tiny as edge-on PE lamellae and their molecular orientation is not so frequently changed from part to part as that of PE lamellae. Thus, we have to consider that the epitaxial growth was controlled by the primary nuclei formed through either and/or both of above mentioned heterogeneous nucleation processes. When these compounds are slowly crystallized from solution, plates as thin as the PE lamellae were observed. Generally, when normal long chain compounds are crystallized from solution, thin lozenge-shaped plates which are bounded by {110} planes extend widely in the direction perpendicular to the molecular axis [14,25]. In the present epitaxial crystallization from solution, thin crystals may grow edge-on in the same growth form as in the homogeneous crystallization from solution. Indeed, lozenge-shaped n-C24OH platelets bounded with the {110} planes grew edge-on with the (110) plane in contact with the substrate surface.

The smooth lattice continuity shown in Fig. 2-14 is not retained in the epitaxial modes of A_1 and A_2. We assumed that the favorable molecular arrangement at the interface minimizes the interactions between the normal long-chain compounds standing on the substrate and the PE chains. Hence, we calculated the interfacial energy by the pair-wise summation of the interatomic interactions between a compound and the PE crystal, using the following equation:

$U(r)=\sum_{ij}\sum u(r_{ij})$

Here $u(r_{ij})$ is the interatomic potential between the i-th atom in the compound crystal and j-th atom of the PE crystal. For calculating the interfacial energy, the orientation of an n-paraffin crystal with respect to the PE substrate is fixed as observed; $(001)_p//(110)_{PE}$ and $[110]_p//[001]_{PE}$. It was assumed, further, that a cylindrical crystallite with a diameter of 3 nm was comprised of long-chain molecules longer than one half of the diameter, e.g., n-C_{13}. The assumption is set to sum Van der Waals interaction of atomic pairs within 1.5 nm and to exclude the effect of methyl groups at the other molecular end (not connected with PE) in the interfacial energy. Under the assumption, we computed the interfacial energy by changing the relative shift between the compound and PE crystals and the separation between them. An energy contour map computed at the separation of 0.4 nm is shown in Fig. 2-15 as a function of respective relative shifts $\triangle x$ and $\triangle y$ in the direction of c-axis and in the direction perpendicular to it. In the calculation, we used the interatomic potential given by Williams[26] (see Table 2-1) and the crystallographic data of the n-paraffin n-C_{36}[27] and PE at room temperature[7] (see Table 2-2). The minimum in Fig. 2-15 shows the stable disposition of the compound and PE crystals at the separation of 0.4 nm between them. We searched the smallest value of the minima calculated by changing the separation. Actually, the minimum of Fig. 2-15 corresponds to it. Thus, the most stable atomic arrangement for the epitaxial mode A_1 was obtained as .pa

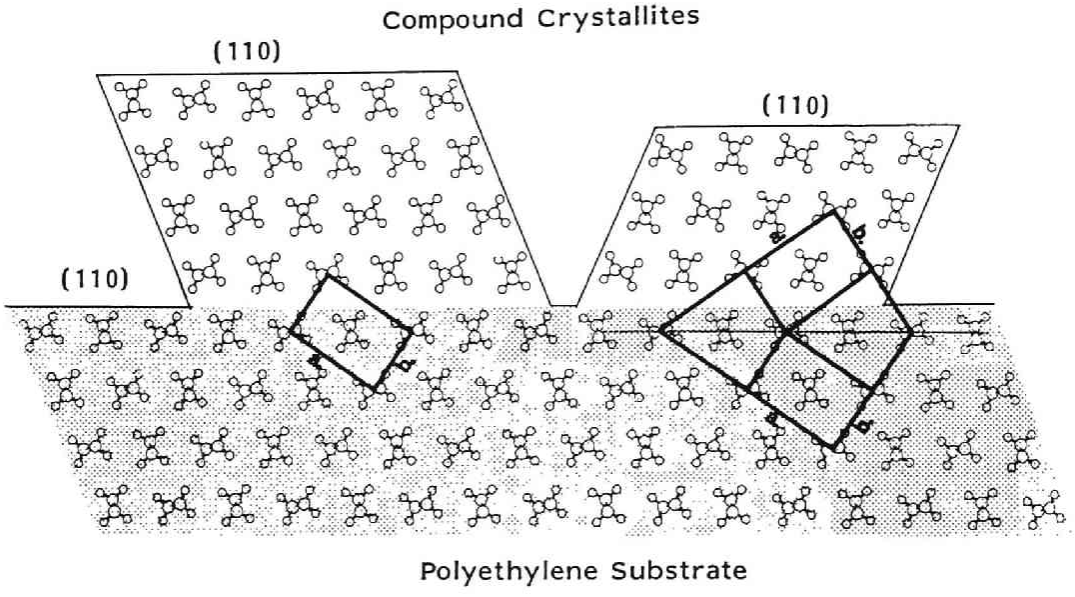

Fig. 2-14. Subcell-matched model at the interface between the compound crystallites and the PE substrate, which is shown as the projection onto the cross-section along the molecular axes; the (001) plane of PE. The shaded part is the PE substrate. Large and small open circles denote carbon and hydrogen atoms, respectively. Structural motifs made of two large circles and four small ones are methylene units projected onto the plane.

illustrated in Fig. 2-16. The minimum energy is 18 kcal/mol unit cell area of the (001) n-paraffin plane. We concluded that the epitaxy takes place so that the lines defined by methyl end groups in n-paraffins, which are most densely aligned in the [110] direction, are incorporated into the potential valleys which are formed between extended PE chains in the [001] direction. In a similar calculation, we found that the epitaxy mode A_2 is such that linear arrays of methyl end groups in the [010] direction of the n-paraffin crystals fit in the potential valleys. In a calculation of the adsorption energy, Boistelle and Madsen [26] showed the energetically favorable site and orientation, in which an n-alkane molecule is adsorbed on the (001) face of crystals of a long-chain alkane. The most favorable orientation of the molecule is with the long axis being parallel to the <110> direction on the (001) plane and the second one in the [010] direction. In the present experiment and computation, the reverse process that the (001) plane of long-chain compounds comes to be in contact with the (100) plane of PE containing the hydrocarbon chains was followed, but the orientational relationship between the methyl end groups on the (001) plane of long-chain crystals and the methylene sequences of the PE substrate is the same. Thus, although the present calculation was too simplified, Fig. 2-13 substantially reproduces the experimental data for the epitaxial modes of A_1 and A_2.

The lattice misfits for the A_1 mode are 0.063 nm in the [001] direction of PE ($d[110]_p$=0.45 nm and $2d[001]_{PE}$=0.508 nm)

Table 2-1 Potential function used for calculation and its parameter

$U(r)=Ar^{-6}+Bexp(-Cr)$

interaction	A	B	C
H···H	-27.3	2654	3.74
C···H	-125	8766	3.67
C···C	-568	83630	3.60

Table 2-2 Lattice parameters of $n\text{-}C_{36}$ and polyethylene

	a(nm)	b(nm)	c(nm)
$n\text{-}C_{36}$ (ortorhombic)	0.742	0.496	9.514 (0.254)
polyethylene	0.742	0.494	0.254

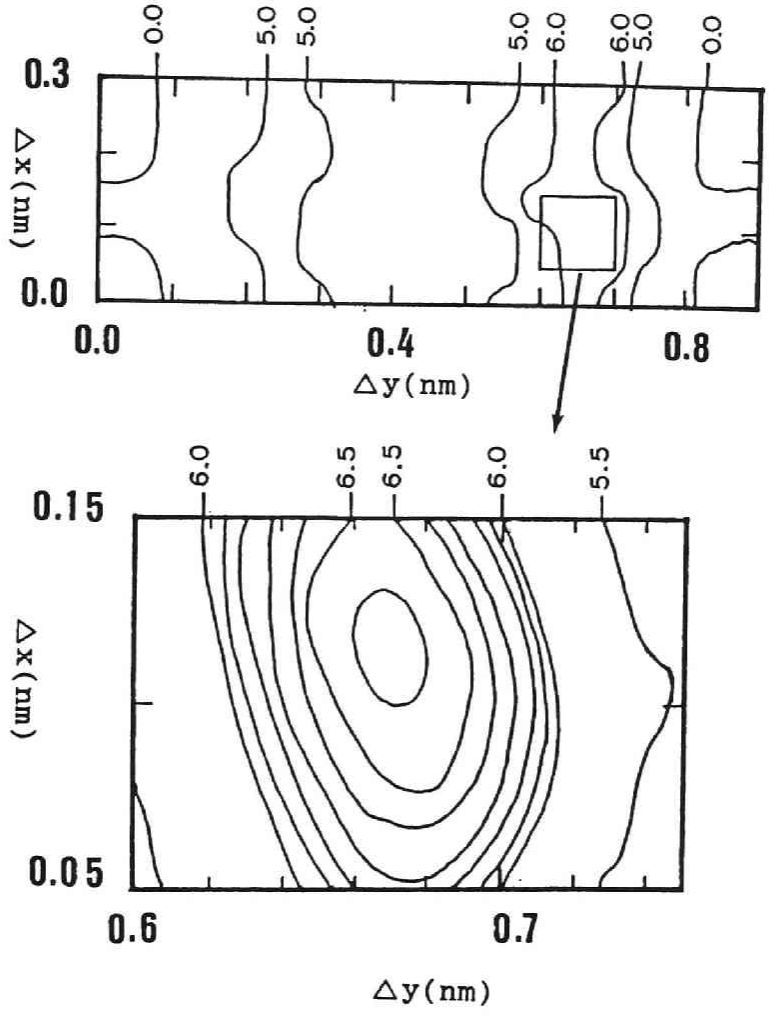

Fig. 2-15 Contour map of interfacial energy between paraffin (001) and PE (110) planes. Δx and Δy mean relative shifts in the c-axis of PE and in the direction perpendicular to it, respectively. The position where the origins of the (001) basal plane of n-paraffin and of the (110) plane coincide is taken as the origin of (a). Energy is represented by kcal per a mole of pairs of end methyl groups on the (001) plane of n-paraffin crystal.

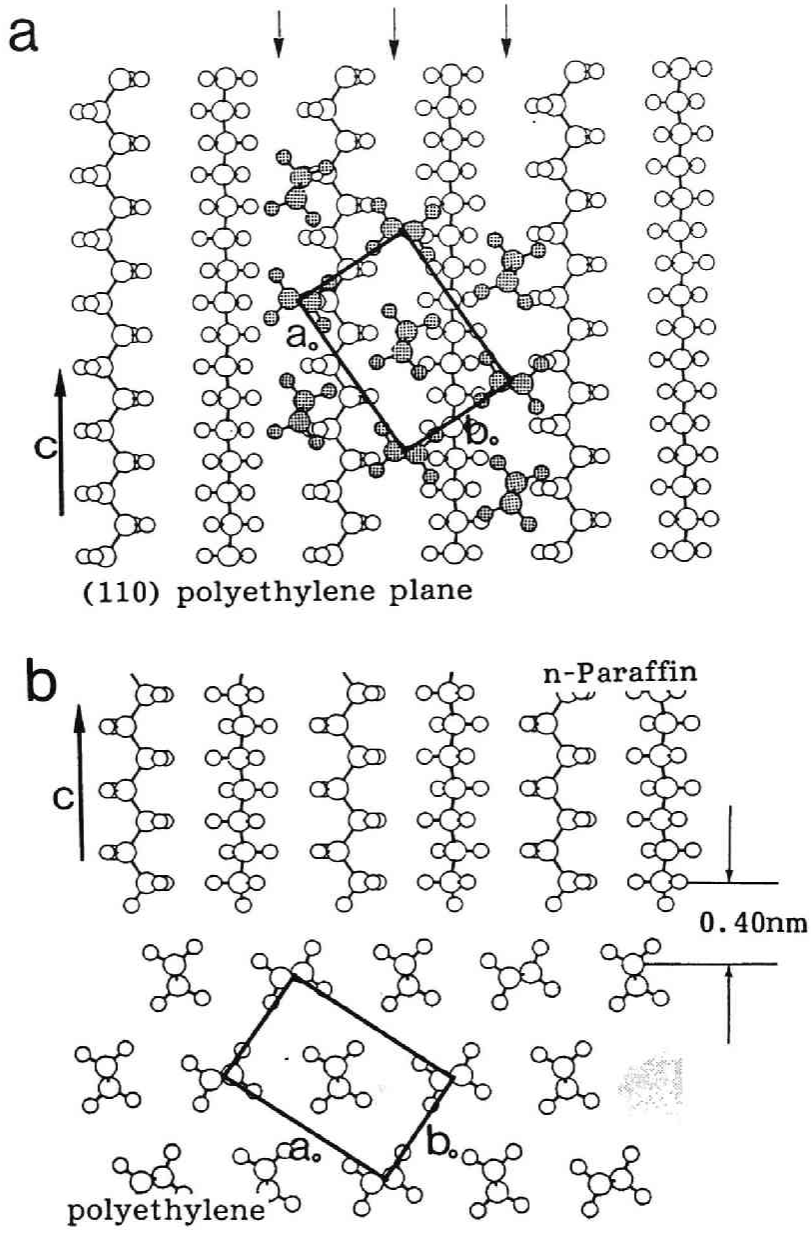

Fig. 2-16. Lattice matching model of the epitaxial mode A_1 as the projection (a) on the (110) plane of PE and (b) on the plane perpendicular to the PE chain axis. Large and small open circles denote carbon and hydrogen atoms, respectively. In (a), shaded circles show the atomic arrangement of n-paraffins projected on the (001) basal plane. Thin arrows show the potential valleys in the (110) plane of PE. The arrowed c directions in (a) and (b) are the PE and n-paraffin molecular axes, respectively.

and 0.07 nm in the [110] direction of PE(2 × the direction normal to the (110) compound plane = 2 × 0.411 nm and $d[110]_{PE}$ = 0.89 nm). On the other hand, the lattice misfits for the mode A_2 are 0.04 in the former direction ($d[010]_p$=0.494 nm and $2d[001]_{PE}$= 0.508 nm) and 0.15 nm in the latter direction ($d[100]_p$= 0.74 nm and $d[110]_{PE}$= 0.89 nm), respectively. These lattice misfits may indicate that the A_2 epitaxial mode is less probable.

As to the epitaxial modes A_1 and A_2 of n-alcohols and n-carboxylic acids, we did not calculate the interfacial energy and have no direct information about the nature of the molecular contact at the interface between their crystals and PE. One may infer, however, that the same argument as that for n-paraffins holds in these compounds, since their epitaxial crystallization behavior was quite identical to that of n-paraffins. This may be accounted for by the fact that n-alcohols and n-carboxylic acid form dimers by coupling polar OH and COOH groups, arranging the methyl end groups at their end surfaces.

In next chapter we discussed another PE plane. It is the (100) plane which appeared if the PE single crystal was truncated.

References

[1] J. Petermann, G. Broza, U. Rieke and A. Kawaguchi, J. Mater. Sci. 22(1987)1477.

[2] A. Kawaguchi, T. Okihara, M. Ohara, M. Tsuji, K. Katayama and J. Petermann, J. Crystal Growth 94(1989)857.

[3] R.B. Richard, J. Polymer Sci. 6(1951)397.

[4] J. Willems, Disc. Faraday Soc. 25(1958)111.

[5] J. Willems, Kolloid-Z.Z. Polymere 251(1973)496.

[6] Proc. 9th Intern. Conf. on Crystal Growth (ICCG-9), Sendai, 1989, Eds. I.Chikawa, J.B.Mullin and J.Woods[J. Crystal Growth 99(1990)].

[7] C.W. Bunn, Trans. Faraday Soc. 35(1939)482.

[8] C. Herring, Phys. Rev. 82(1951)87.

[9] G.M. Broadhurst, J. Res. Natl. Bur. Std. (US) 66(1962)241.

[10] H.M.M. Shearer and V. Vand, Acta Cryst. 9(1956)379.

[11] P.K. Sullivan and J.J. Weeks, J. Res. Natl. Bur. Std. (US) 74A(1970)203.

[12] K. Tanaka, T. Seto, A. Watanabe and T. Hayashi, Bull. Inst. Chem. Res. Kyoto Univ. 37(1959)281.

[13] S. Amelinckx, Acta Cryst. 8(1955)530.

[14] M. Kobayashi, T. Kobayashi, Y. Itoh, Y. Chatani and H. Tadokoro, J. Chem. Phys. 72(1980)2024.

[15] M. Kobayashi, K. Sakagumi and T. Tadokoro, J. Chem. Phys. 78(1983)6391.

[16] M. Kobayashi, T. Kobayashi, Y. Itoh and K. Sato, J. Chem. Phys. 80(1984)2897.

[17] S. Abrahamsson, G. Larsson and E. von Sydow, Acta Cryst. 13(1960)770.

[18] Y. Uyeda and M. Ashida, J. Electron Microsc. 29(1980)38.

[19] M. Okada, T. Inoue and K. Yase, Oyo Buturi 58(1989)391.

[20] E. von Sydow, Acta Cryst. 7(1954)823.

[21] E. von Sydow, Acta Cryst. 8(1955)810.

[22] E. von Sydow, Acta Cryst. 8(1955)557.

[23] M. Goto and E. Asada, Bull. Chem. Soc. Japan 51(1978)2456.

[24] V. Malta, G. Gelotti, R. Zannetti and A.F. Martelli, J. Chem. Soc. (B)(1971)548.

[25] S. Amelinckx, Acta Cryst. 9(1956)217.

[26] D.E. Williams, J. Phys. Chem. 47(1967)4680.

[27] P.W. Teare, Acta Cryst. 12(1959)294.

[28] Boistelle and Madsen, J. Cryst Growth, 43(1978)141.

Chapter 3. Crystallization Behavior of Long-Chain Compounds on the (100) Plane of Polyethylene

3.1. Introduction

In Chapter 2, the epitaxial crystallization of long-chain compounds on the (110) plane of polyethylene(PE) is described. We found that the normal long-chain compounds epitaxially crystallized with two different types of lattice coincidence on the (110) plane of PE: with molecules of the compounds being parallel and normal to the substrate surface [1]. Generally, PE crystallized from solution forms a lozenge-shaped lamella whose sides are bounded by the {110} planes. However, the (100) plane also becomes a crystallographic plane bounding the surface of PE crystallites: lozenge-shaped lamellae are truncated in the *a*-axis direction with the (100) plane when they are grown from solution at rather high temperatures [2]. In order to clarify further the epitaxial crystallization of normal long chain compounds on PE, it is shown here the crystallization behavior on the (100) plane of PE.

3.2. Experimental

A PE substrate used was an ultra-drawn, ultra-high molecular weight PE (UD-UHMWPE) film. It has been reported that this material reveals a double orientation with the molecular axis (*c*-axis) oriented in the drawing direction of draw and the a-axis perpendicular to the film surface. Thus, the surface is bounded with the (100) plane[3-5].

The PE film was prepared as follows: UHMWPE with $M=2\times10^6$ (Hizex Million, Mitui Petroleum Co., Inc.) was dissolved at a concentration of 0.2 wt% in *p*-xylene at its boiling point. Subsequently, the polymer was isothermally crystallized at 80℃, overnight. The precipitated mass was filtered, and so-called "dry-gel films" were obtained. These films were drawn up to a draw ratio of 120-130 at 130℃ using an Instron tensile-tester equipped with a temperature-controlled chamber. A similar kind of doubly oriented PE film with the (100) surface was prepared by pressing or rolling high density film[6]. However, the UD-UHMWPE film was mainly used as the substrate for the present epitaxial crystallization work because of its extremely high degree of molecular orientation. The film thickness was about 1 μm.

The normal long-chain compounds used in this study were the same as those employed in Chapter 2: n-paraffins (n-C_nH_{2n+2}), n-alcohols (n-$C_nH_{2n+1}OH$) and n-carboxylic acids (n-$C_{n-1}H_{2n-1}COOH$). Hereinafter, these compounds are abbreviated to n-C_n, n-C_nOH and n-$C_{n-1}COOH$, with the number of carbon atoms, *n*. These compounds were crystallized on the UD-UHMWPE films from solution and from

the melt. The molecular orientation and morphology of the epitaxially grown crystals were examined by X-ray diffraction and by optical and scanning electron microscopy.

3.3. Results

3.3.1. Structure of UD-UHMWPE film

Figure 3-1 shows the so-called *through* and *edge* wide-angle X-ray diffraction patterns (WAXDPs) of the UD-UHMWPE film on which n-pentacosane ($n\text{-}C_{25}$) was epitaxially crystallized. Clearly, the sharp, intense 020 reflection of PE is seen in the *through* pattern, while the 200 spot is absent. The *edge* pattern displays the reverse presence of reflections. These diffraction features indicate that the PE chains in the UD-UHMWPE films were well aligned parallel to the drawing direction, and that the (100) plane was oriented almost perfectly parallel to the film surface and the (010) plane normal to the film surface. From this sharp double crystalline orientation, it was concluded that the surface of the thin UD-UHMWPE films was bounded with the (100) plane, although its structure was not clarified as in the case with direct methods such as RHEED. All UD-UHMWPE films used here did not display this high degree of double orientation, but the 020 reflection of the used films was always sharp and stronger than the 200 one in the *through* WAXDP. Thus, we surely employed the PE films in which the (100) plane was preferentially oriented parallel to the surface.

3.3.2. Identification of epitaxial modes

3.3.2.1. n-Paraffins

Figures 3-2a and 3-2b show respectively optical and scanning electron micrographs of a thin UD-UHMWPE film, on which C_{25} was crystallized from an n-heptane solution. In Fig. 3-2a, the dark striations running perpendicular to the drawing direction correspond to n-C_{25} platelets standing edge-on on the film surface. Figure 3-2b clearly shows that the edge-on platelets are stacked with their long sides perpendicular to the drawing direction. After comparing Fig. 3-2 with an optical micrograph of paraffin wax crystals arranged on cold-drawn PE [7,8], it is concluded that the (100) plane is preferentially oriented parallel to the film surface of the cold-drawn PE. In the *through* WAXDP of Fig. 3-1a, the spot-like 00*l* reflections of the n-paraffin unit cell are seen only in a line parallel to the PE chain axis. The long spacing of 3.4 nm indicates that the n-C_{25} crystals are orthorhombic[9]. From Figs. 3-1a and 3-2, we discerned the first feature of epitaxial growth of n-paraffins: the molecules lie on the (100) surface of PE with their chain axes parallel to the PE chains. The arc-shaped, dotty 200 reflection of n-C_{25} is weak in Fig. 3-1a and strong in Fig. 3-1b. On the other hand, the dotty 020 reflection of n-C_{25} is completely absent in Fig. 3-1b, in accordance with the 020 spot of PE. The intensity relationship of these main spots shows another epitaxial growth feature: n-paraffin platelets grew with their (100) plane in contact with the (100) plane of PE, fitting

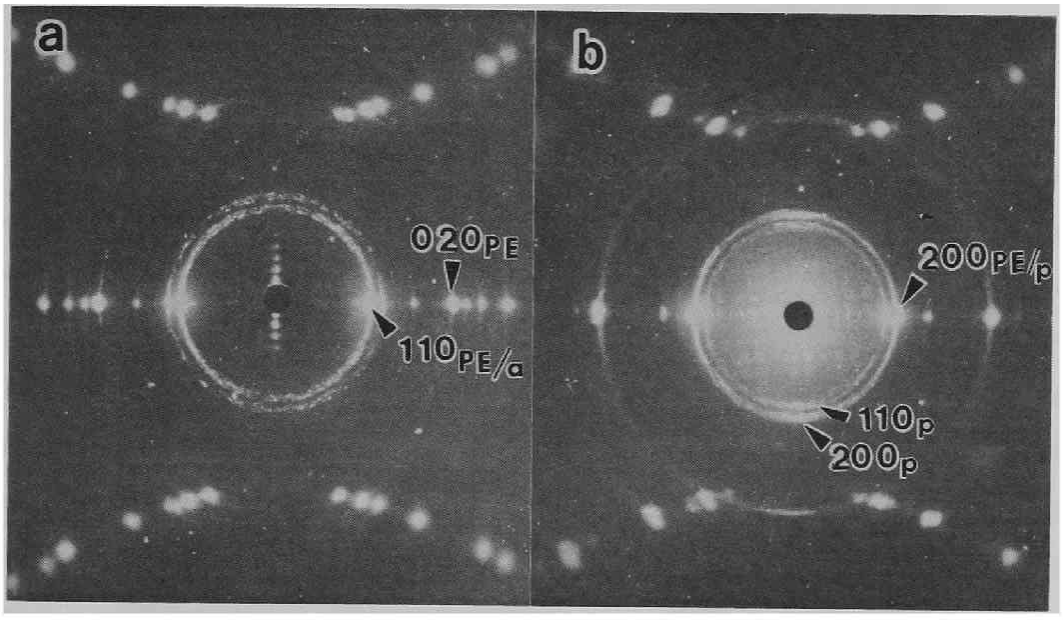

Fig. 3-1. (a) *Through* and (b) *edge* wide-angle X-ray diffraction patterns (WAXDPs) of ultra-drawn UHMWPE, onto which n-C_{25} was crystallized. In (a), X-rays are incident perpendicular to the film surface and in (b) perpendicular to the polyethylene chain axis on the edge. In both figures, the polyethylene axis is vertical and the incident X-rays are normal to the paper. The subscripts of indexed spots, PE and p, refers to the polyethylene and n-paraffin (n-C_{25}), respectively. Low angle reflections in the central part are 00*l* reflections.

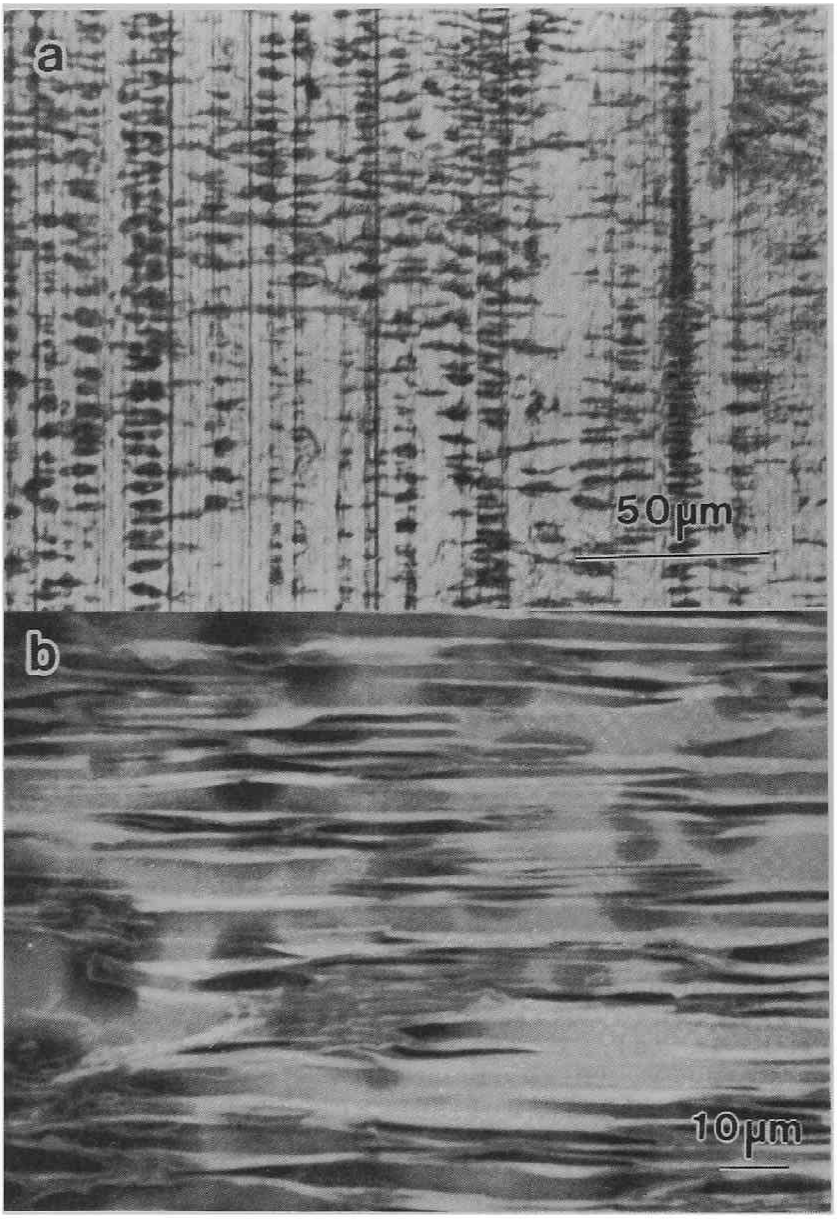

Fig. 3-2. (a) Optical and (b) scanning electron micrographs of n-C_{25} crystallites grown on UD-UHMWPE, corresponding to Fig. 2-1. The chain axis of PE, i.e. the drawing direction, is vertical.

the (010) plane with the (010) plane of PE. Hence, the epitaxy is performed with the following lattice coincidence:

$(100)_p // (100)_{PE}$, $[001]_p // [001]_{PE}$.

Here p and PE stand for n-paraffins and PE, respectively. This epitaxial mode is designated as B_2, which differs from B_1 (Chapter 2) in the sense that B_1 is characterized by lattice matching between the {110} contact planes of the n-paraffins and PE. Yet, the parallel orientation of methylene sequences of the n-paraffins and PE is retained similarly in B_1 and B_2.

In the *edge* WAXDP of Fig. 3-1b, the 00*l* unit cell reflections of n-C_{25} are arc-shaped, but their azimuthal intensity profiles reveal peaks both on the equator and meridian. The equatorial 00*l* reflections show that n-C_{25} molecules layered with their chain axis normal to the substrate surface, that is, flat-on platelets were produced. Flat-on n-paraffin platelets are really grown on the uniaxially drawn PE in the A_1 or A_2 epitaxial mode[10]. It might be possible if the PE substrate surface was not entirely bounded with the (100) plane only. However, this does not seem to be the present case, because when n-paraffins are crystallized from solution by solvent evaporation on a PE substrate limited with the {110} planes, the platelets stand edge-on as well [1]. It should be noted further that on the meridian, the 200 reflection of n-C_{25} is stronger than the 110 one. This means that the *a*-axis of the n-paraffin is preferentially oriented parallel to the *c*-axis of PE. This allowed us to deduce another epitaxial growth mode with the

following lattice coincidence:

$(001)_p//(100)_{PE}$, $[010]_p//[010]_{PE}$.

This epitaxy is designated as the A_3 mode. The directional correlation between the lattices of n-paraffins and PE is distinct from those of A_1 and A_2 in Chapter 1[10].

Other odd-numbered n-paraffins revealed the epitaxial crystallization on UD-UHMWPE from solution, forming both edge-on and flat-on platelets. The mode B_2 epitaxy was predominant in higher homologues(e.g., n-C_{35}).

Figures 3-3a and 3-3b show optical and scanning electron micrographs of n-hexatriacontane (n-C_{36}) crystals, respectively, which were grown at room temperature from n-heptane solutions. The n-C_{36} crystallites grew edge-on and were arranged slantly in two different orientations at angles of $\pm 117.5°$ with respect to the PE chain axis. The angle of 117.5° equals the unique angle β of the monoclinic unit cell of the n-paraffins[11]. Obviously, this textured morphology of edge-on n-paraffin platelets resulted from the oriented overgrowth induced by the PE substrate. Figure 3-3c shows the corresponding *through* WAXDP. The 00*l* reflections are lined up in an X-shape. The two directions are perpendicular to the long sides of the platelets and their azimuthal angle is 27.5° off from the meridian. The n-C_{36} crystals were monoclinic, because the long spacing was 4.2 nm [11]. In the *edge* WAXDP, the 00*l* reflections were completely absent. From this, we concluded that the n-paraffin crystals grew in the epitaxial mode:

$(010)_p//(100)_{PE}$, $[001]_p//[001]_{PE}$.

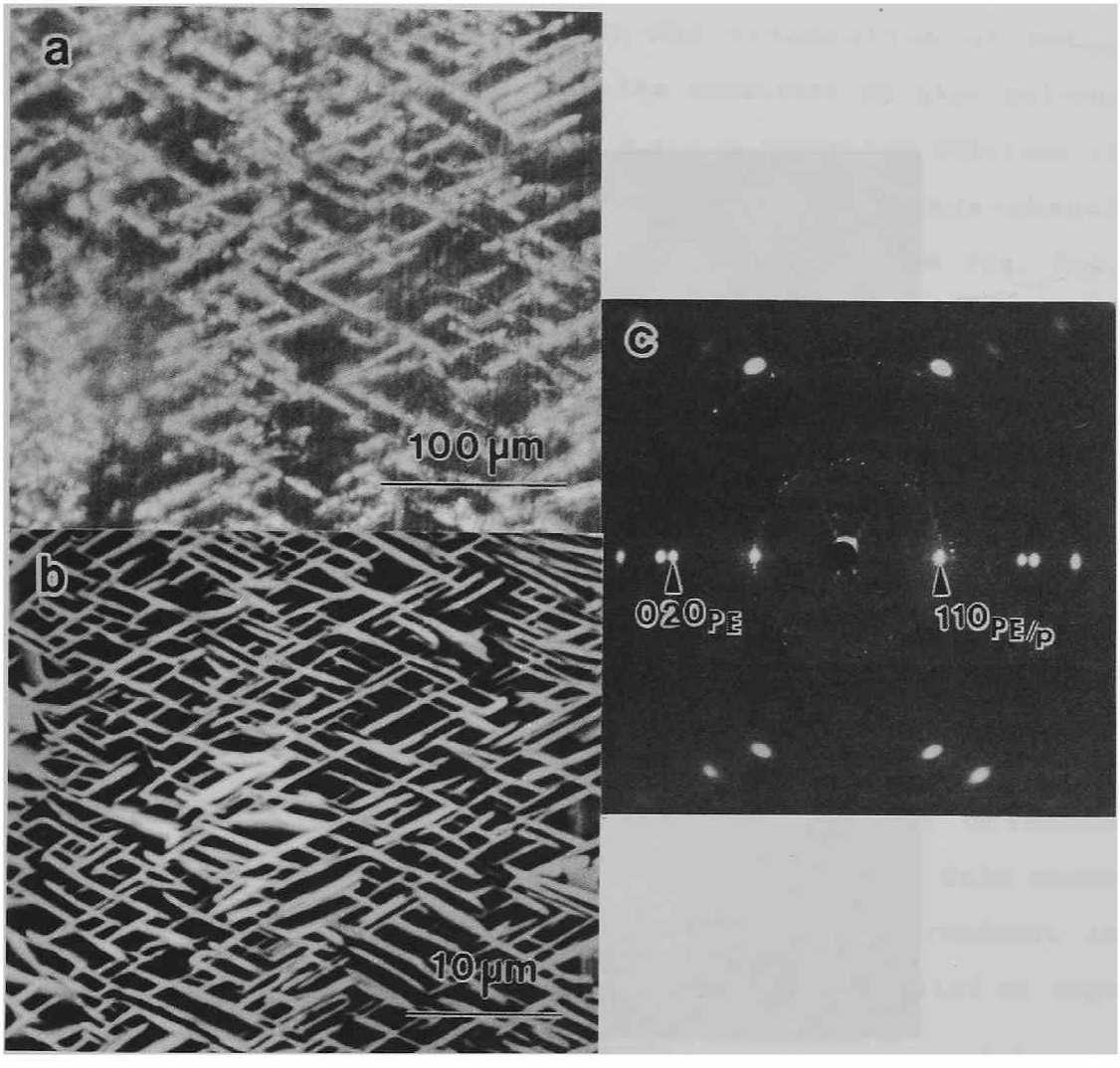

Fig. 3-3. (a) Optical and (b) scanning electron micrographs of n-C_{36} crystallites grown on UD-UHMWPE. The optical micrograph was taken under crossed polarizers; the polarizer was vertical and analyzer was horizontal. The bright striations which run slantly at angles of ±117.5° with respect to the PE *c*-axis (vertical) correspond to the n-C_{36} crystallites. It is clearly seen in (b) that they stand edge-on. (c) Corresponding *through* WAXDP. The PE c-axis is vertical and the incident X-rays are normal to the figure. Low angle reflections seen in an X-shaped in the central part correspond to 00*l* reflections.

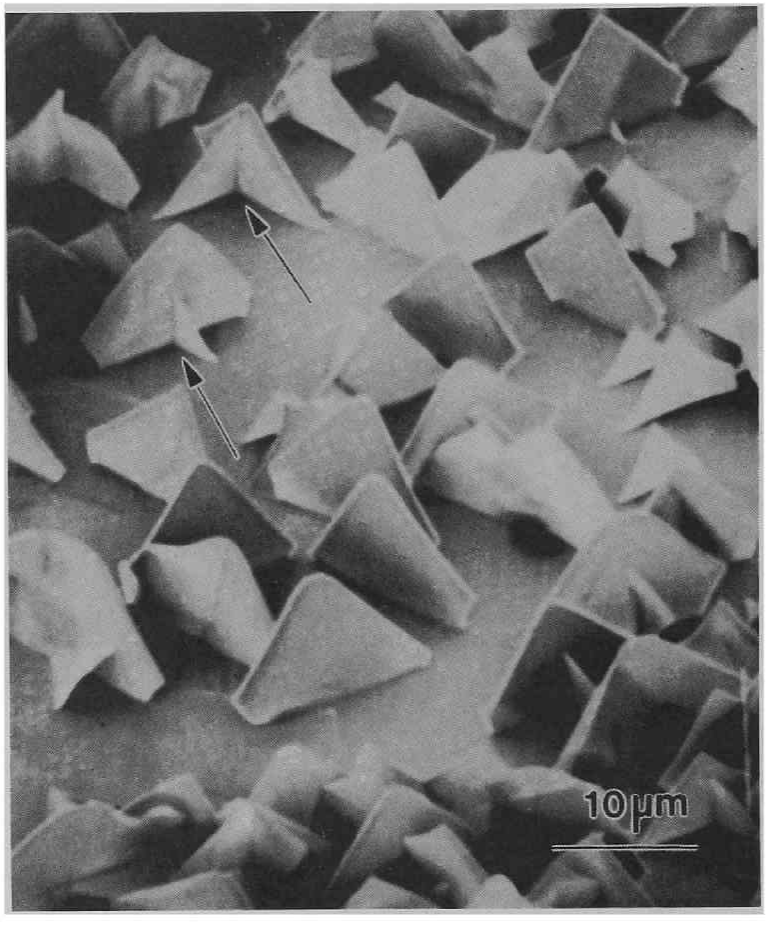

Fig. 3-4. Scanning electron micrograph of n-C_{36} platelets grown from a dilute solution in n-heptane. The photo was taken viewing in the direction tilted by 30° toward the PE *c*-axis from the normal to the substrate surface. Lozenge-shaped platelets stand edge-on with the (100) truncation plane in contact with the substrate and with their roots inclined with respect to the PE c-axis. Two edge-on platelets (shown by arrows) intersected each other, keeping the growth shape.

This epitaxy is designated as B'_2.

Figure 3-4 shows the habit and orientation of n-C_{36} platelets which grew edge-on onto the substrate by slow solvent evaporation of a dilute solution, e.g., a saturated solution in n-heptane, at room temperature. Normally, lozenge-shaped platelets are homogeneously grown from solution. From Fig. 3-4, we see that the lozenge-shaped platelets truncated with the (100) plane stand edge-on with the plane in contact with the saturate. This explains the above epitaxial mode morphologically.

Figure 3-5 shows the morphology of n-C_{36} crystals grown by solution evaporation at 50°C and the corresponding WAXDP. We observed from the figure that the epitaxial modes of B_2 and B'_2 concurrently occurred.

The n-paraffins of n-C_{22} to n-C_{50} were systematically examined. We found that the even-numbered, shorter paraffins of n-C_{22} to n-C_{26} did not exhibit the distinctly oriented crystallite arrangement as the long homologues did. This means that the epitaxial lattice compatibility was less prominent in the n-paraffins. We also found that the B_2 mode prevailed at high temperatures and for higher homologues.

The n-paraffins solution-crystallized on UD-UHMWPE films were once heated above their melting point and cooled down to induce the recrystallization from the melt. Figure 3-6a shows the melt-crystallized n-C_{36} crystals, whose morphology is different from that of solution-grown crystals. Rather thick platelets grew edge- on as well, stacking compactly onto themselves, with their

long sides perpendicular to the PE chain axis. In the *through* WAXDP of the sample of Fig. 3-6a, the lined-up 00*l* reflections are observed in the direction parallel to the PE chain axis. They correspond to a long spacing of 4.7 nm which indicates the orthorhombic crystal modification[11]. The 110 and 020 reflections of the n-paraffin are seen with rather high intensities, though arc-shaped, and the 200 spot is observed only faintly. The diffraction features show that the epitaxial growth of n-paraffin crystals on PE takes place in the mode B_2 from the melt. Odd- and even-numbered n-paraffins longer than n-C_{26} crystallized from the melt gave similar X-ray diffraction patterns indicating the epitaxial overgrowth in the B_2 mode. It is worthy to note that when n-paraffins are epitaxially crystallized from the melt on the (110) surface of PE, they are aligned normal to it in the epitaxial mode A_1 and/or A_2, which are largely different from the growth on the (100) plane of PE(Chapter 2).

3.3.2.2. n-Alcohols

Figure 3-7a shows a scanning electron micrograph of n-tricosanol (n-C_{23}OH) crystals grown from an n-heptane solution, and Figs. 3-7b and 3-7c display the corresponding *through* and *edge* WAXDPs, respectively. In Fig. 3-7a, the edge-on n-C_{23}OH crystallites are piled up along the PE chain axis, showing the same morphological features as the n-paraffins in Fig. 3-2b. Similarly, in Fig. 3-7b, the 00*l* reflections are lined up along

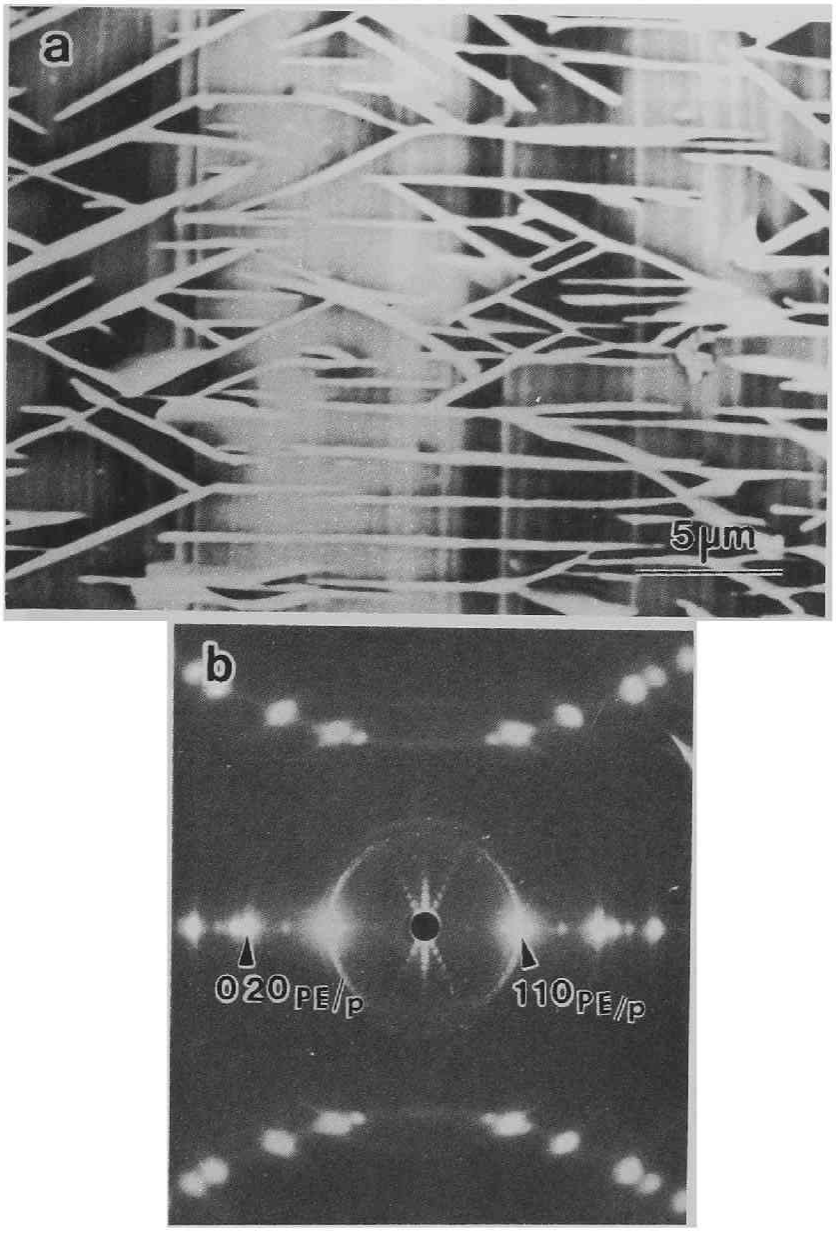

Fig. 3-5. (a) Scanning electron micrograph of n-C_{36} platelets grown on the UD-UHMWPE at 50℃ and (b) the corresponding WAXDP. The PE chain axis is vertical. Vertical 00l reflections are produced by the horizontal edge-on platelets, giving a long spacing of 4.7 nm, and hence they are orthorhombic. The inclined platelets are monoclinic, as the long period is 4.2 nm. The two types of platelets are connected one another by branching or by changing the growth direction.

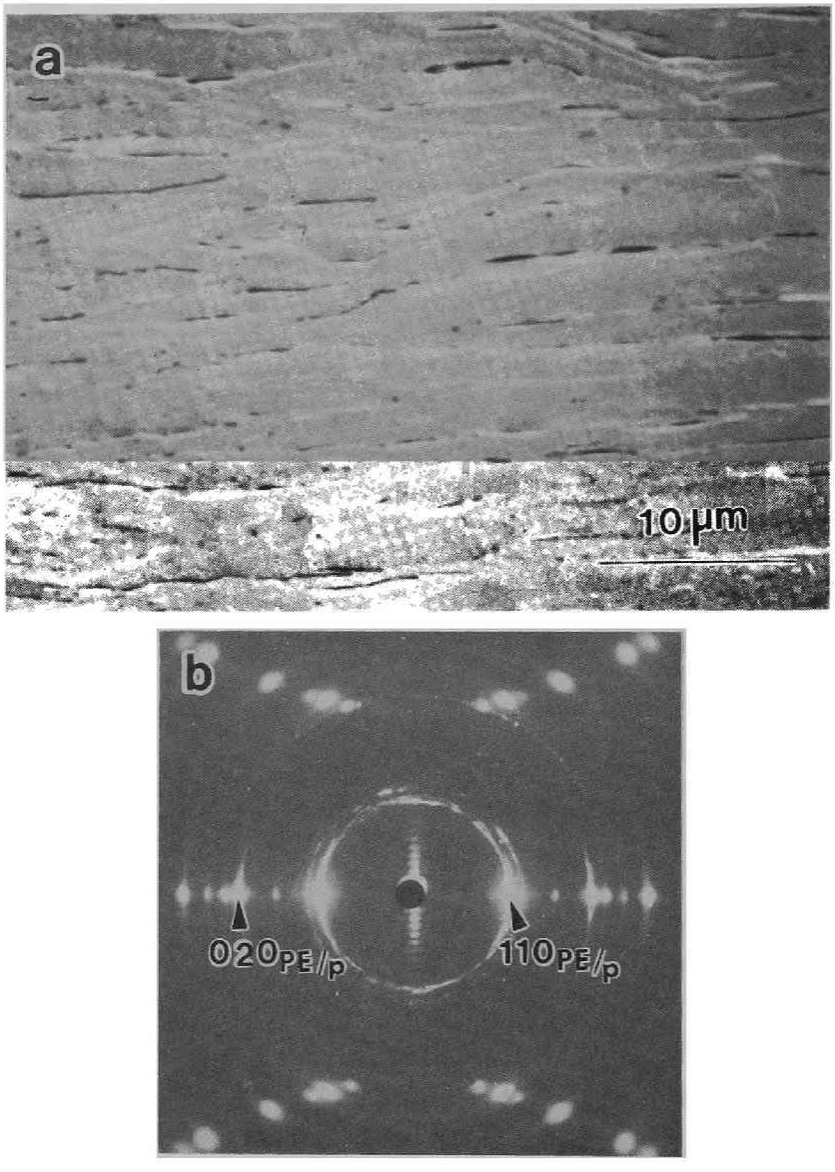

Fig. 3-6. (a) Scanning electron micrograph of melt-crystallized n-C_{36} and (b) the corresponding *through* WAXDP. The PE chain axis is vertical.

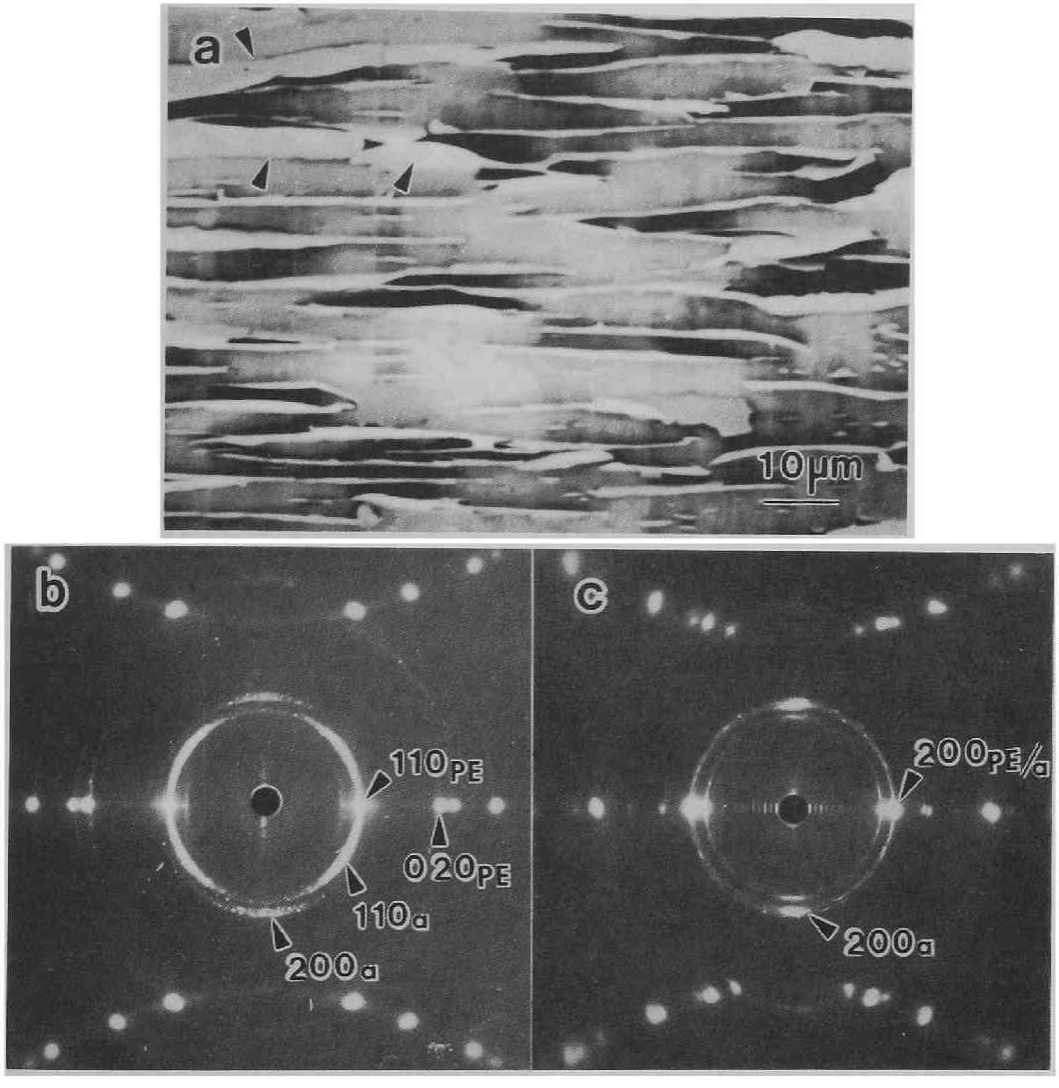

Fig. 3-7. (a) Scanning electron micrograph of n-C_{23}OH crystals grown on UD-UHMWPE, and the corresponding (b) *through* and (c) *edge* WAXDPs. In all these figures, the PE chain axis is vertical. Platelets are edge-on, and some are going to tumble, as shown by arrows in (a). The subscript a denotes an n-alcohol(n-C_{23}OH).

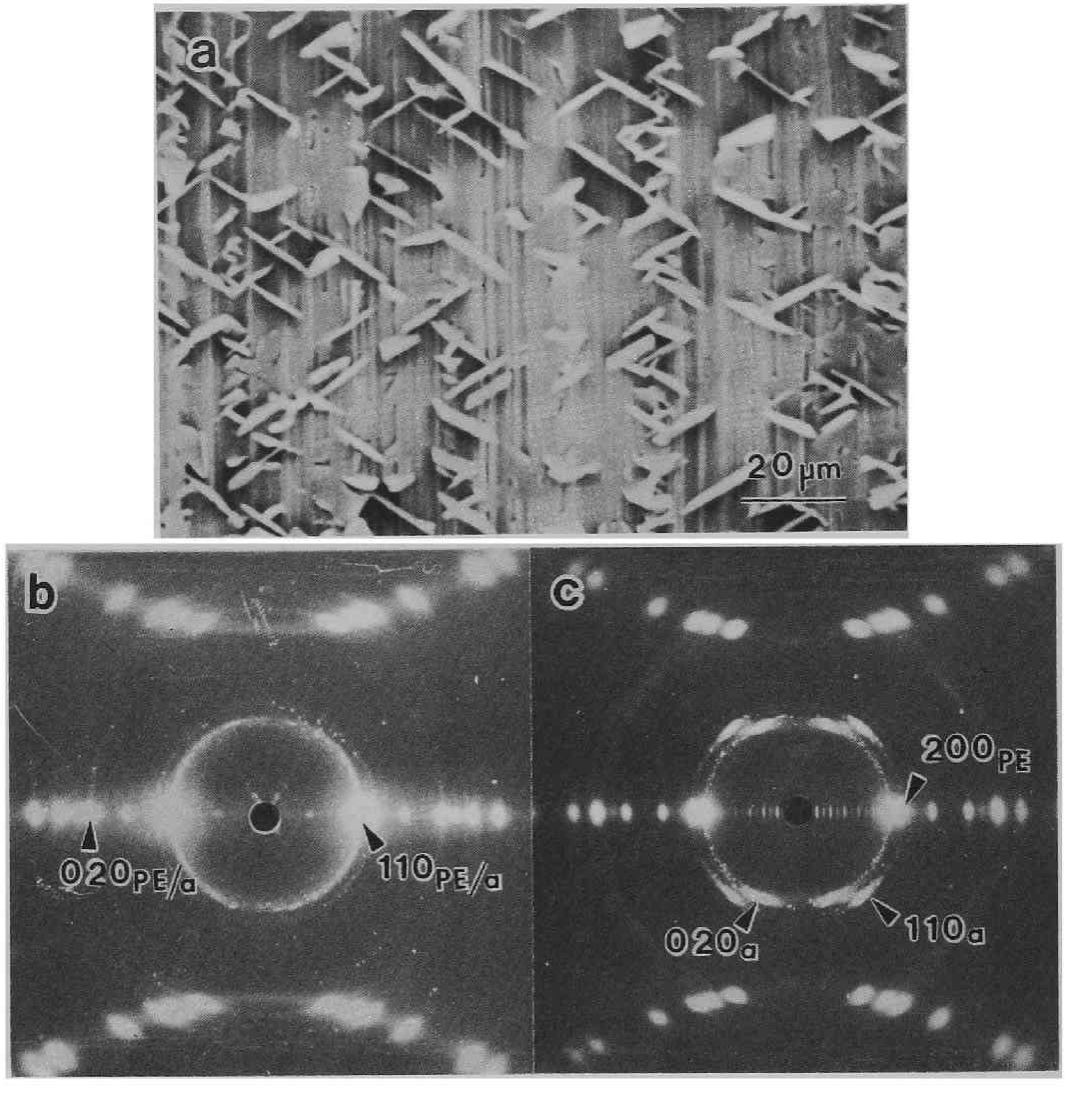

Fig. 3-8. (a) Scanning electron micrograph of n-C_{24}OH crystals grown on an UD-UHMWPE film, and the corresponding (b) *through* and (c) *edge* WAXDPs. In all figures, the PE chain axis is vertical.

the meridian parallel to the PE chain axis. The long spacing is 6.2 nm, corresponding to the β-form [13]. From these observations, we determined the following epitaxy, analogous to the mode B_2 of n-paraffin/PE systems:

$(100)_a // (100)_{PE}$, $[001]_a // [001]_{PE}$,

where a denotes n-alcohols.

The *edge* WAXDP of Fig. 3-7c shows the 00*l* reflections along the equator. This means that the n-C_{23}OH crystallites are grown flat-on in the same modification with the molecular chain stems being normal to the PE substrate. In Fig. 3-7b, the 200 reflection of the n-C_{23}OH crystals is strong on the meridian, and the 110 ones are split into four. Concordantly, on the meridian in Fig. 3-7c, the 200 reflection is stronger than the 110 spot. From this, it is concluded that there is another molecular orientation with the following lattice coincidence;

$(001)_a // (100)_{PE}$, $[010]_a // [010]_{PE}$.

This orientation is analogous to the A_3 epitaxial mode observed in the C_{26}/PE system.

Figure 3-8a shows that n-C_{24}OH platelets are arranged edge-on with their long sides tilting at an angle of $\pm 122.5°$ with respect to the PE chain direction, as seen before in the overgrowth of monoclinic, even-numbered n-paraffins. As demonstrated in Fig Sharp 3-8b, 00*l* reflections corresponding to a long spacing of 6.28 nm, are oriented in an X-shape with azimuthal angles of $\pm 32.5°$ off from the meridian. This means that the n-C_{24}OH platelets are grown in the monoclinic α-

form[13] with the following lattice coincidence;

$(010)_a // (100)_{PE}$, $[001]_a // [001]_{PE}$.

This mode of epitaxy is analogous to the B'_2 mode (see Fig. 3-3). The *edge* WAXDP of Fig. 3-8c shows that the 00*l* reflections are observed only on the equator with a long spacing of 5.41 nm, which is different from the value in Fig. 3-8b. The n-C_{24}OH crystallites of the monoclinic γ_1-form[13-15] are stacked with their surface parallel to the substrate surface. This form is designated the β-form in ref. [16]. The *edge* X-ray pattern indicates a lattice coincidence between the n-alcohol crystals and the PE substrate as follows:

$(001)_a // (100)_{PE}$, $[100]_a // [010]_{PE}$.

This corresponds to the A_3 mode of epitaxy, which is not due to tumbling of edge-on platelets of the α-form, because their crystalline form is different. Obviously, the γ_1-crystallites were over-grown in a different manner.

Figure 3-9 shows another morphology of the edge-on n-C_{24}OH crystallites epitaxially grown on the UD-UHMWPE film. The crystallites of triangular shape are arranged edge-on with their basal edge parallel to the PE *b*-axis. When such crystallites grow to a large size, they tumble in flat-on appearance shown as triangles trimmed with white lines in Fig. 3-9. Since the molecular chains are not perpendicular to the basal surface of the γ_1-form of platelets, the 110 and 020 reflections are observed off from the equator as in Fig. 3-8c. The reason why the morphology differs between α- and γ_1-forms is briefly discussed

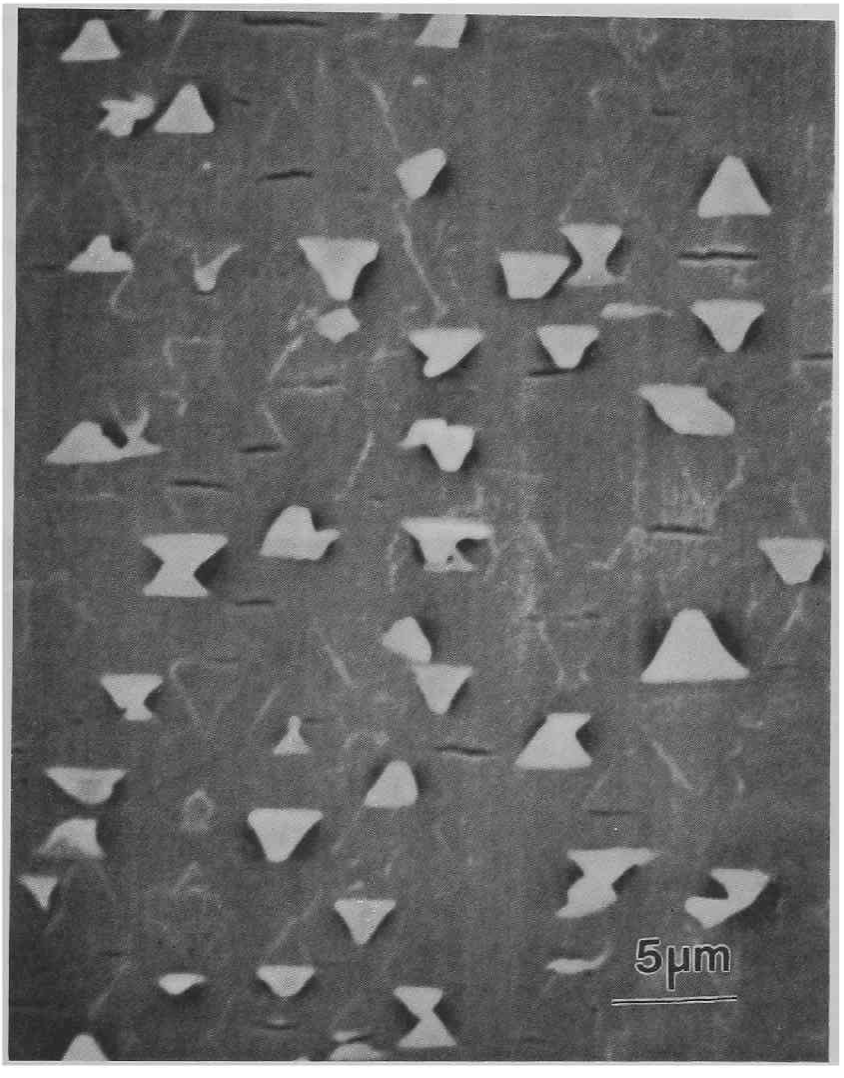

Fig. 3-9. Scanning electron micrograph of n-C_{24}OH crystals grown on the UD-UHMWPE film. Triangular platelets faceted with {110} planes grew edge-on with their root being parallel to the PE *b*-axis (horizontal). Triangles trimmed with white lines show the platelets tumbled by breaking at their roots.

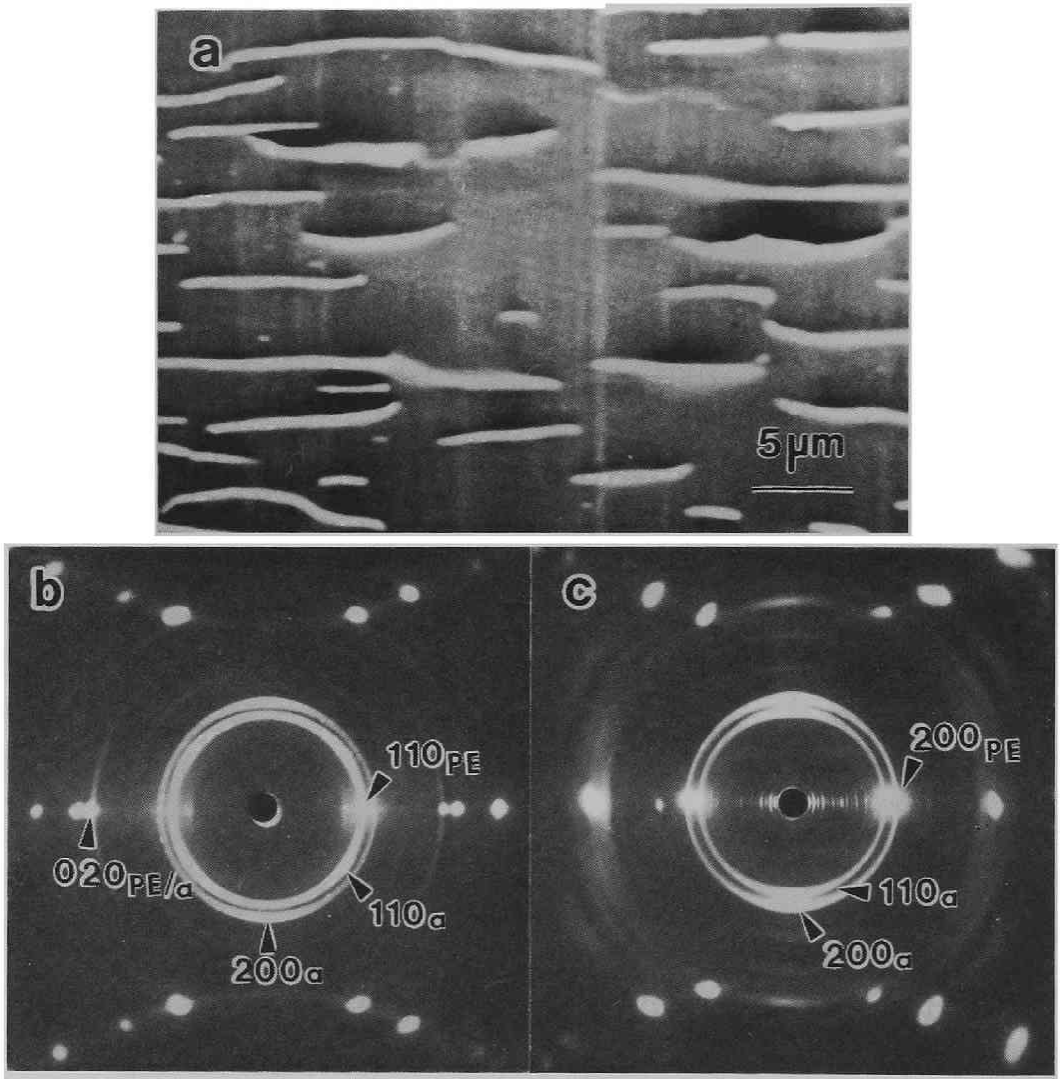

Fig. 3-10. (a) Scanning electron micrograph of n-C_{30}OH crystals grown on the UD-UHMWPE film at 50°C, and the corresponding (b) *through* and (c) *edge* WAXDPs. In these figures, the PE chain axis is vertical. Platelets grew edge-on with their long side perpendicular to the PE *c*-axis.

below.

Figures 3-10a, 3-10b and 3-10c show a scanning electron micrograph, and *through* and *edge* WAXDPs of n-C_{30}OH crystallites grown at 50°C, respectively. They are edge-on as well. In Fig. 3-10b, the 00*l* reflections on the meridian are weak, indicating the presence of the edge-on platelets. In Fig. 3-10c, the reflections are more intense on the equator. This intensity relation of the 00*l* reflections is the same as in the case of n-C_{23}OH/PE. The measured long spacing of 8.18 nm is comparable to the calculated value of the β-form(8.09)[13]. Thus, we concluded that higher homologues of the even-numbered n-alcohols also crystallized in the β-form and in the B_2 and A_3 epitaxial modes.

3.3.2.3 n-Carboxylic acids

Figures 3-11a, 3-11b and 3-11c show optical and scanning electron micrographs and *through* WAXDP of n-nonadecanoic acid (n-C_{18}COOH) crystals grown from a benzene solution at room temperature. The two photographs show that the edge-on platelets of n-C_{18}COOH are inclined in two different manners, both at oblique angles of $\pm 120^{\circ}$ with respect to the PE chain axis. The textured morphology of n-C_{18}COOH is identical to that of monoclinic n-C_{36}(Fig. 3-3). The crystallites running in the same direction revealed a beautiful parallel pattern. The 00*l* reflections are oriented in an X-shape with an azimuthal angle of 22.5° in two directions, perpendicular to the long sides of the crystallites. It is assumed that the crystals in Fig. 3-11 are of

the monoclinic B'-form, since the calculated long spacing equals the observed value of 4.58 nm [17]. The B'-modification is analogous to the monoclinic form of n-paraffins in the structural features, such as the subcell structure and the successive staggering of hydrocarbon chains along the chain axis [11]. Hence the epitaxial mode is assumed to be the B'_2 mode:

$(010)_c // (100)_{PE}$, $[001]_c // [001]_{PE}$,

where c denotes n-carboxylic acids.

As an example of even-numbered n-carboxylic acids, stearic acid ($n\text{-}C_{17}COOH$) was examined. The epitaxial growth from a benzene solution at room temperature was quite identical to that of $n\text{-}C_{18}COOH$ (Fig. 3-11) with the B'_2 mode. The crystalline form is the B-modification, as the long spacing was measured at 4.3 nm [18,19]. However, different growth was observed at elevated temperatures. Figure 3-12 shows the different morphology of $n\text{-}C_{17}COOH$ crystals grown from benzene and n-heptane solutions at 50°C. Obviously, the growth pattern is not the same as those of other compounds. Yet, the *through* and *edge* WAXDPs show that the molecular chains are well ordered. In the *through* pattern (Fig. 3-12b), no sharp 00*l* reflection is observed. In contrast, the 00*l* reflections clearly appear at an angle of ±39° off from the meridian in the *edge* pattern (Fig. 3-12c), giving rise to a long spacing of 4.07 nm. The long spacing explains that the crystals are in the C-form[20]. When the lozenge-shaped crystals of the C-form are truncated with the (100) plane and stand in edge-on wise on the plane, they lean towards the substrate surface with a

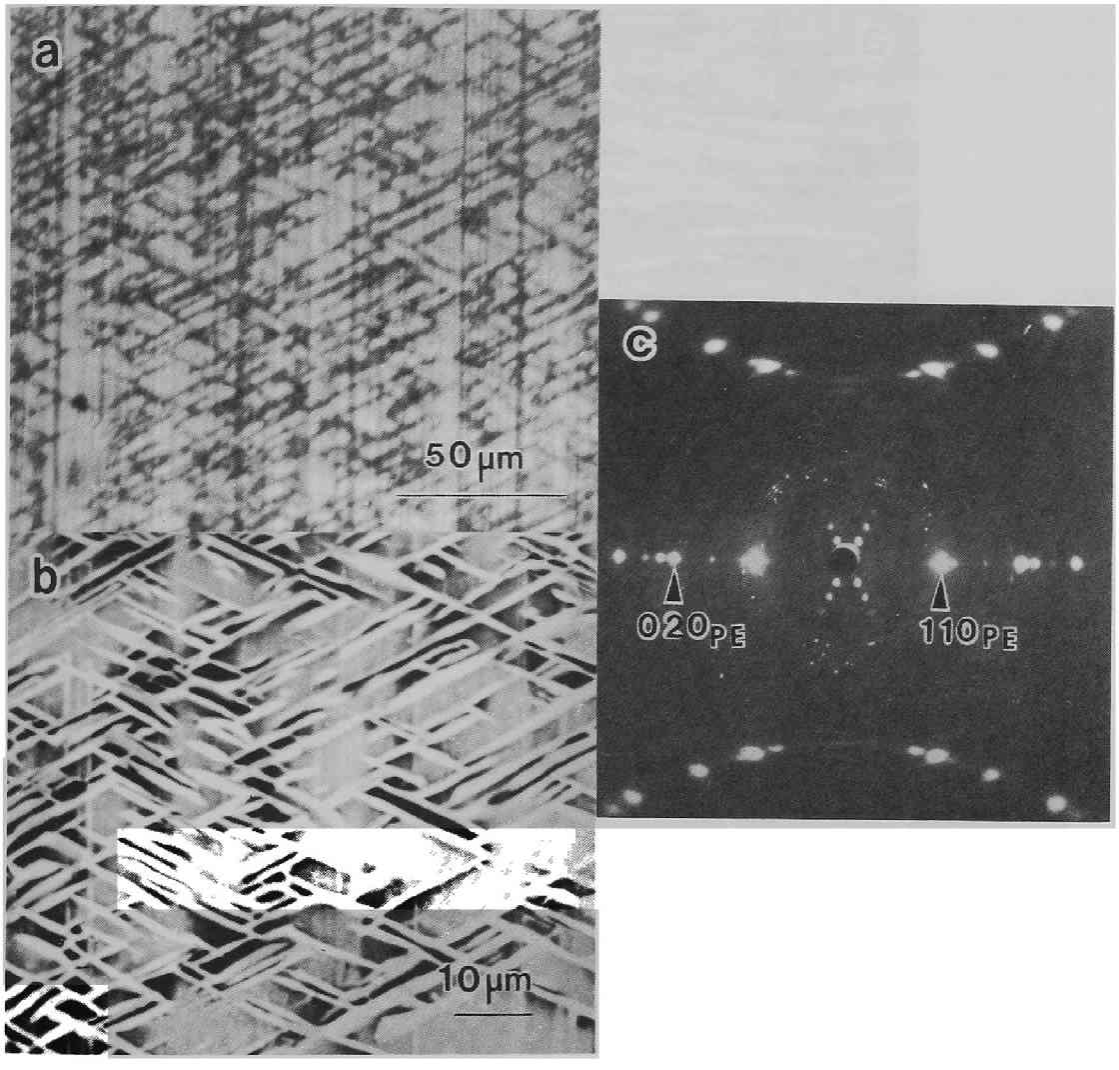

Fig. 3-11. (a) Optical and (b) scanning electron micrographs of n-C_{18}COOH crystals grown on the UD-UHMWPE film, and (c) the corresponding *through* WAXDP. In these, the PE c-axis is vertical. The optical micrograph was taken under crossed polarizers which were directed at $\pm 45°$ from the vertical direction, respectively. Dark striations in (a) denote the epitaxially grown edge-on platelets as revealed in contrast in (b).

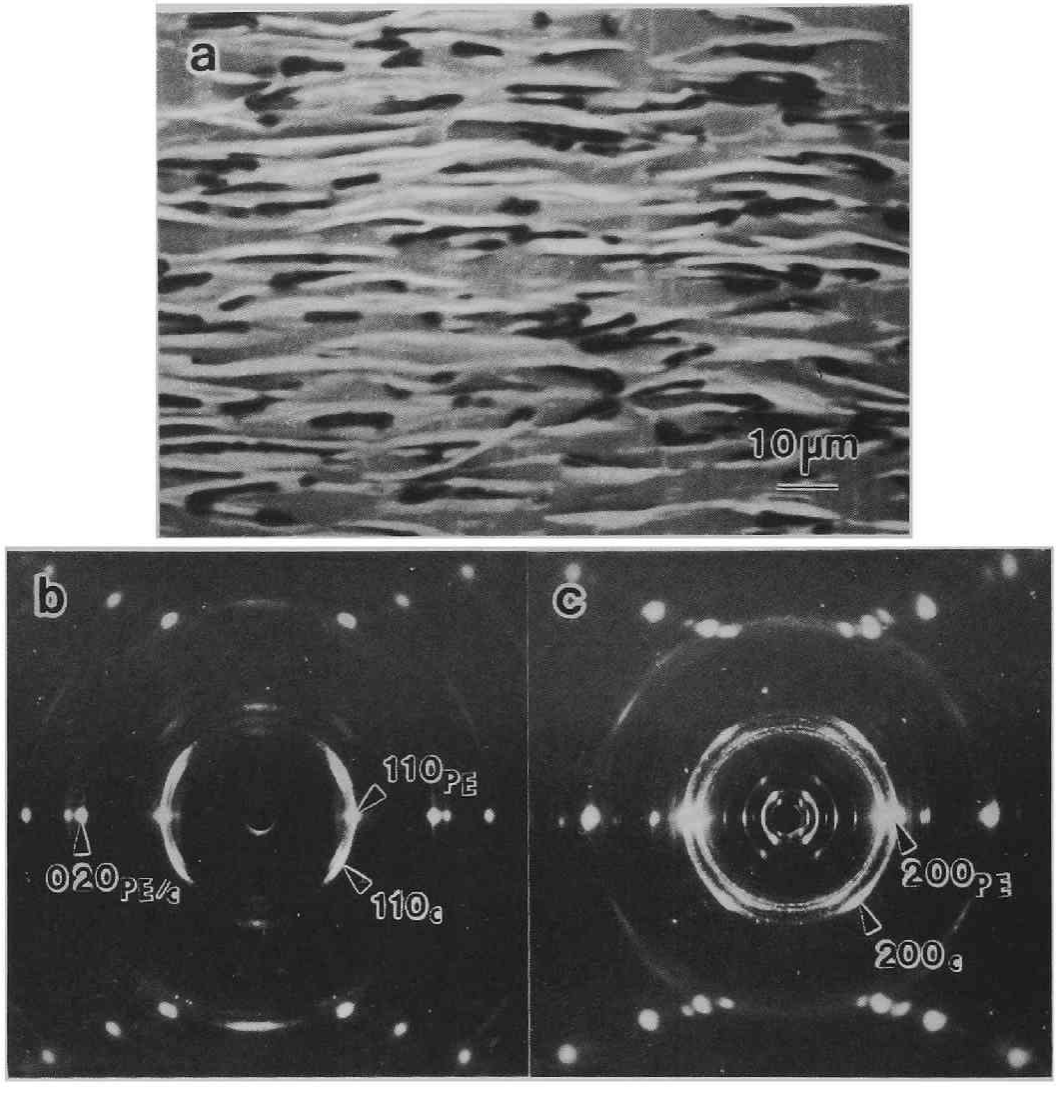

Fig. 3-12. (a) Scanning electron micrograph of the C-form of n-C_{17}COOH crystals grown on the UD-UHMWPE film from a benzene solution at 50℃, and the corresponding (b) *through* and (c) *edge* WAXDPs. In these figures, the PE *c*-axis is vertical. In (a), the long axis of epitaxially grown crystallites is perpendicular to the PE *c*-axis.

supplementary angle (equal to 39°) of the unique angle β of the unit cell. Figure 3-13 shows the habit of such leaning crystals. Consequently, the 00*l* reflections are observed in the directions off from the meridian in the *edge* pattern only. The epitaxial mode is defined as follows;

$(100)_c // (100)_{PE}$, $[001]_c // [001]_{PE}$.

This description is the B_2 mode.

Other even-numbered carboxylic acids(n-tetracosanoic acid, n-hexacosanoic acid and n-triacontanoic acid), which crystallized in the B'-modification, also exhibited the B'_2 mode at room and elevated temperatures. Although some lower members also have the analogous crystal structure of the B-form, they do not show such remarkable epitaxial crystallization behavior as the longer chain compounds.

3.4. Discussion

In this experiment, we found that different epitaxial growths of long-chain compounds with various crystalline modifications occur on the (100) surface of PE, depending on the kind of compound itself and the respective crystalline forms of each compound. In addition, the morphology and crystallite orientation varied according to the epitaxial mode. It is worth noting that the molecular chains lay on the substrate to align their hydrocarbon chains parallel to the PE chains in the all epitaxial modes, except for A_3. Irrespective of the nature of compounds, the epitaxial modes of various compounds are

classified into three types in terms of the orientation of the crystallites and the molecular orientation with respect to the PE axis and the substrate surface. They are summarized as I, II and III in Fig. 3-14 as the projection onto the (100) plane of PE. Stereoscopic views of the corresponding morphologies of the platelet of the compounds are depicted in Fig. 3-15. In the inclined case II, two differently oriented crystals are produced, but both are essentially the same in the lateral packing at the interface between them and PE. The angle θ is comparable to the unique angle β of the monoclinic unit cell, which displays the inclined morphology, but not strictly equal to it, because the molecular chain axis in the unit cell is not always parallel to the c-axis of the unit cell.

The relation of morphologies I, II and III to the epitaxial modes and crystalline forms of various compounds is summarized in Table 3-1. The crystallographic data for crystalline forms observed in the present various compounds are listed in Table 3-2. Examining the data in this table carefully, we have deduced the following remarks. The normal long-chain compounds examined here have a variety of unit cells; the orthorhombic and monoclinic forms and even the triclinic one in n-carboxylic acids. However, all the crystals which revealed the characteristic epitaxial growth on the UD-UHMWPE film have an identical orthorhombic subcell that corresponds to the PE unit cell[21].

In Table 3-2, the a and b subcell dimensions are

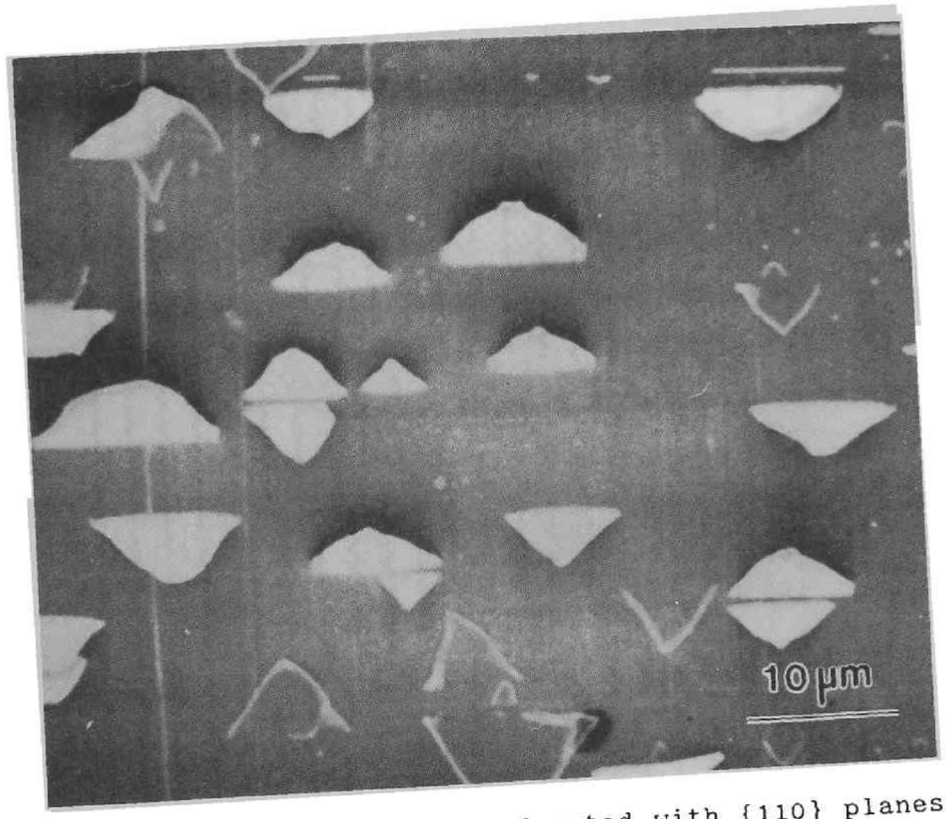

Fig. 3-13. Triangular platelets, faceted with {110} planes, grew edge-on with their (100) plane in contact with the (100) plane of PE. The direction of their roots is perpendicular to the PE c-axis (vertical). Triangles trimmed with white lines denote the tumbled platelets at their roots.

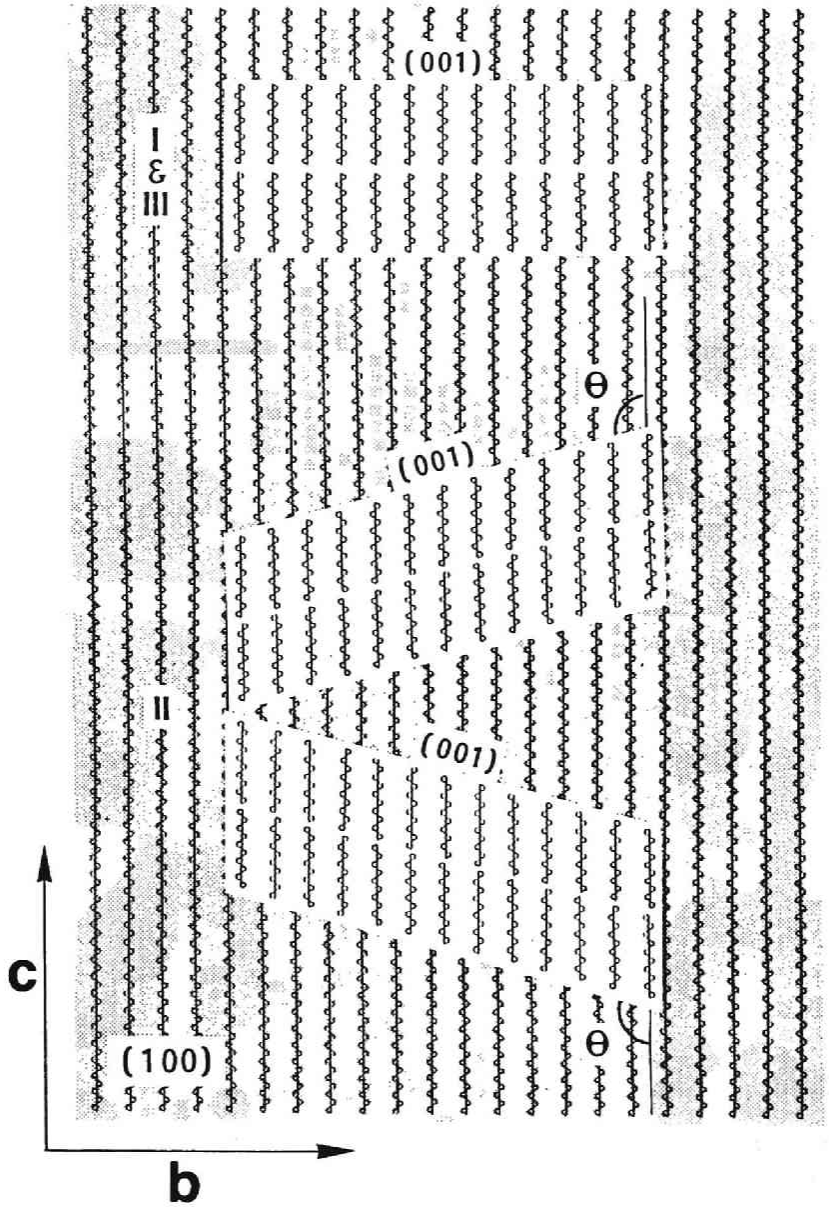

Fig. 3-14. Orientational relation of normal long-chain compound molecules to PE chains, given as the projection onto the (100) plane of Pe, and the related crystallite orientations. The (001) plane denotes the projected (001) basal plane of the crystallite. The angle θ refers to the inclination angle of crystallites with respect to the PE chain axis.

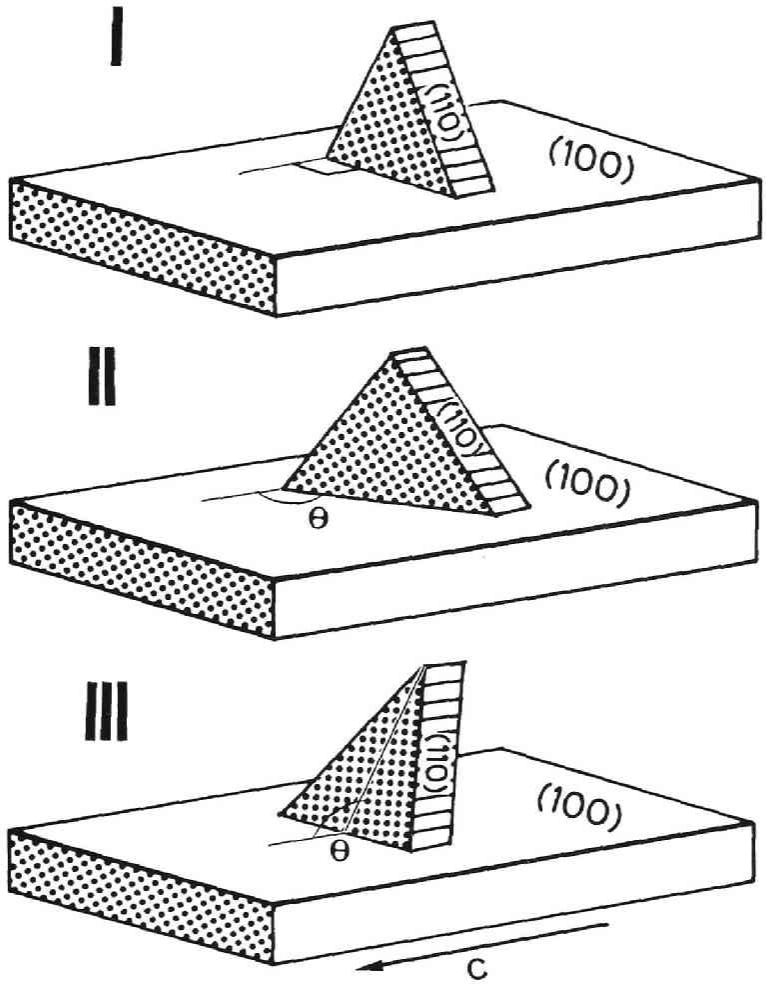

Fig. 3-15. Stereoscopic models of the morphology and orientation of crystallites, grown epitaxially edge-on-wise with their (100) plane in contact with the (100) plane of PE. Model I is for the orthorhombic unit cell and model II and III are for the M_{011} and M_{201} types of monoclinic unit cells, respectively. Details are discussed in the text. The arrowed *c*-direction shows the PE *c*-axis.

Table 3-1 Morphological types, unit cell forms and epitaxial modes of various long chain compounds.

Morphology	Compound	Unit cell	Epitaxial mode	Figures
I	n-Pentacosane	Orthorhombic	B_2	2
	n-Hexatriacontane	Orthorhombic		5a
	n-Tricosanol	Orthorhombic		7
II	n-Hexatriacontane	Monoclinic	B_2'	3, 4
	n-Tetracosanol	Monoclinic α		8
	n-Nonadecanoic acid	Monoclinic B′		11
III	n-Tetracosanol	Monoclinic γ_1	B_2	9
	Stearic acid	Monoclinic C		12a, 13

Table 3-2 Crystallographic data of various long-chain compounds.

Compound	Modification	a (nm)	b (nm)	c (nm)	α (deg)	β (deg)	γ (deg)	Type	Ref.
$n\text{-}C_{36}H_{74}$	Orthorhombic	0.742	0.496	9.514	90	90	90		[12]
	Monoclinic	0.557	0.742	4.835	90	119.6	90	M_{011}	[11]
		(0.4945)	(0.742)	(0.2546)					
$n\text{-}C_{24}H_{49}OH$	Monoclinic (α)	–	0.744	6.278	90	122.5	90	M_{011}	
$n\text{-}C_{23}H_{47}OH$	Monoclinic (β)	0.496	0.737	9.45	90	91.20	90		[13]
	(or orthorhombic)								
$n\text{-}C_{16}H_{33}OH$	Monoclinic (γ_1)	0.895	0.493	8.81	90	122.23	90	M_{201}	[14]
		(0.742)	(0.493)	(0.253)					
$n\text{-}C_{17}H_{35}COOH$	Monoclinic	0.5587	0.7386	4.933	90	117.24	90	M_{011}	[18]
	(B form)	(0.496)	(0.739)	(0.250)					
	Monoclinic	0.936	0.495	5.07	90	128.15	90	M_{201}	[20]
	(C form)	(0.740)	(0.495)	(0.250)					
$n\text{-}C_{14}H_{29}COOH$	Triclinic	0.5543	0.8061	4.258	114.18	114.15	80.37	M_{011}	[17]
	(B′ form)	(0.507)	(0.735)			(90.23)			
$n\text{-}C_{10}H_{21}COOH$	Monoclinic	0.9622	0.4915	3.418	90	131.17	90	M_{201}	[22]
	(C′ form)								

interchanged in the monoclinic n-C_{36}, the α-form of n-C_{24}OH and the B- and B'-forms of n-carboxylic acids in comparison with the subcell of orthorhombic n-paraffins. We usually designated the monoclinic phases of these normal long-chain compounds by defining their (001) plane in terms of the Miller indices of the subcell. These are listed in Table 3-2. For example, the M_{011} of n-C_{36} means that the (001) plane corresponds to the (011) subcell plane, since this form is obtained from the orthorhombic unit cell by translating each $-CH_2-$ unit, in the adjacent molecules along the *b*-axis, by two $-CH_2-$ units parallel to the *c*-axis. The M_{201} form is also obtained from the orthorhombic unit cell by translating each $-CH_2-$ unit, in the adjacent molecules along the *a*-axis, by four $-CH_2-$ units parallel to the *c*-axis. Hence the (001) plane of the unit cell corresponds to the (201) subcell plane. As a result, the molecules are inclined toward the *b*-axis of the orthorhombic cell in case of M_{011}, and toward the *a*-axis in case of M_{201}. According to the notation rule of the crystallographic parameters, the unique axis and the corresponding angle of the monoclinic system are assigned to *b* and β, respectively. Therefore, the subcell axes *a* and *b* are interchanged in the M_{011} type of monoclinic crystals. However, the packing manner of hydrocarbon chains and related symmetry of the subcell of these compounds are in complete agreement with that of PE. Hence, there is no basic change in these crystal structures, even if the M_{011} subcell is re-defined by interchanging *a* and *b* to be in line with the notation of other

forms. In order to simplify further systematic discussion on the basis of the subcell, we temporarily change the assignment of the *a* and *b* subcell axes of the M_{011} type of monoclinic crystals.

When the B_2 and B'_2 epitaxial modes are re-examined on the basis of this unified subcell, they can all be explained in terms of a unique relation between the subcell and the PE unit cell, irrespective of different crystalline modification and the related morphologies. This is depicted in Fig. 3-16. In the epitaxy, the (010) subcell plane coincides with the (010) plane of PE. Although there is a small difference between the cell dimensions of the PE unit cell and the orthorhombic subcell of the compounds, the packing continuity of the methylene sequences across the interface between the crystallites and the substrate can be maintained with no serious destruction. It is this subcell lattice matching that drives various long-chain compounds to crystallize epitaxially on the (100) plane of PE.

The unique lattice coincidence holds in both inclined crystallite orientations of case II in Fig. 3-13. The two orientations are in a twin relation with respect to the (010) subcell plane, which is parallel to the PE chain axis and perpendicular to the substrate surface. It is easily understood from Fig. 3-15 that no serious packing disorder of hydrocarbon chains arised at the (010) twin boundary, because their planar zigzag planes in the subcell are inclined making an angle of 42° with the a_0-axis [11,12]. Therefore, even when crystallites inclined in two different ways meet with and intersected each

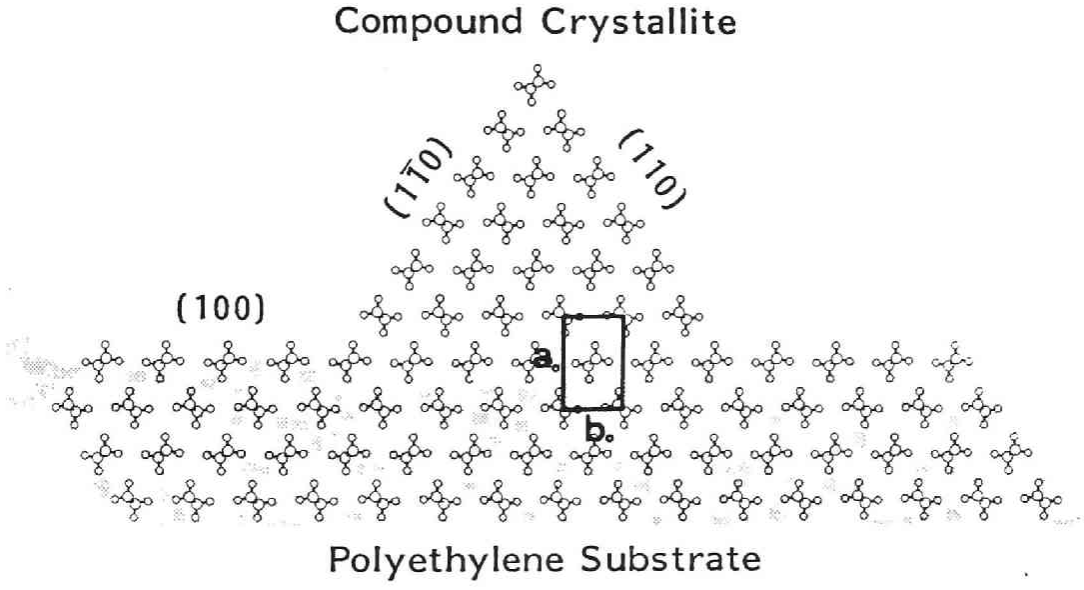

Fig. 3-16. Side-by-side packing of methylene sequences of the PE substrate and a normal long-chain compound crystallite epitaxially grown on it, depicted on the cross-section perpendicular to their chain axes. The shaded part is the PE substrate. a_0 and b_0 denote the cell dimensions of the unfied subcell. Large and small open circle stand for carbon and hydrogen atoms, respectively. Structural motifs made of two large circles and four small ones denote methylene units projected onto the cross-section.

other, the side-by-side packing of the long chains is easily retained, keeping the identical molecular orientation at the (010) plane boundary. In this way, the intersected morphology of edge-on n-C_{36} platelets in Fig. 3-4 is understood. Although not in a twin relation, a coherent lattice continuity is also possible to occur at the boundary between the orthorhombic (I) and monoclinic (II) crystals. This may explain how the network textures in Figs. 3-3, 3-5 and 3-11 are constructed.

The B_1 mode described in Chapter 2 and the present B mode are basically identical in the sense that the long chains lie on the PE substrate, laying their chain axes parallel to the PE chain axis. The single difference is that the crystallographic plane, at which the epitaxial crystallization occurs, is the {110} planes for the B_1 mode, and the (100) plane for the B mode. The shorter n-paraffins and n-alcohols and the A and A' crystalline modifications of n-carboxylic acids with the triclinic unit cell [16], whose subcell is also triclinic, did not exhibit the definite epitaxial crystallization. It is not surprising that oriented overgrowth was not easily achieved, since there is no lattice compatibility between the triclinic subcell and the orthorhombic PE unit cell.

The lozenge-shaped crystallites of the long-chain compounds bounded by {110} planes are often grown from solution [22,23]. When platelets of this shape are grown in the above epitaxial mode on the substrate, a truncated lozenge, standing edge-on with its (100) plane in contact with the substrate, is expected to

form. Polymorphism of a certain long-chain compound and different forms of various long-chain compounds originate from the difference of staggering manner between neighboring hydrocarbon chains, as mentioned above. At the interface of normal long chain compounds and the PE surface, they crystallize to fit their (010) plane of "unified subcell" to the (010) plane of PE. Hence, the inclination angle and direction of the (001) basal plane of the growing crystallite are determined by the staggering manner. From this point of view, three types of morphologies depicted in Fig. 3-15 are expected for the various crystalline forms. Lozenge-shaped platelets of monoclinic n-C_{36}, faceted with the {110} planes and truncated with the (100) plane at one side in the *a*-axis direction, stand perpendicular to the substrate so as to fit their (100) plane in contact with the (100) surface plane of PE. Their roots are inclined with respect to the PE chain at an angle that corresponds to the unique angle β of the unit cell. The morphology in Fig. 3-4 typifies the growth behavior. In the form of n-C_{24}OH and the C-form of stearic acid, the molecular chains are inclined in the basal plane of unit cell towards the *a*-axis, and hence the (100) plane is inclined identically. When the platelets truncated with the (100) plane are arranged on the (100) plane, while maintaining the lattice coincidence of Fig. 3-16, the the triangular shape of platelets leaning toward the PE axis is expected to be of type III in Fig. 3-15. This morphology is seen in Figs. 3-9 and 3-13. As shown in these examples, the actual morphologies are in complete agreement with the predicted

formulation of the epitaxial growth. This accord also shows that the surface of the present UD-UHMWPE film indeed is the (100) plane, although X-ray diffraction did not reveal the structure except that the (100) plane was preferentially oriented parallel to the film surface.

The *edge* WAXDPs of Figs. 3-1, 3-7 and 3-10 suggest the existence of the A_3 epitaxial mode:

$(001)_{uc}//(100)_{PE}$, $[010]_{uc}//[010]_{PE}$.

Here uc refers to the unit cell of normal long-chain compound crystals. We must note the following disorder of crystallites in a thick specimen employed for X-ray investigation. When the platelets continue to grow upwards, edge-on and normal to the substrate surface, they bend, flex and even tumble onto the substrate, keeping the direction of their long side parallel to the [010] direction of PE. When edge-on platelets tumble by breaking at their roots and are stacked onto one another, the a-axis of the unit cell of the compounds, which is directed upwards from the substrate surface in their edge-on orientation, is on the substrate surface. Consequently, such *edge* WAXDPs in Figs. 3-1 and 3-10 as show the strong, meridional 200 reflection (off-meridional 020 one in Fig. 3-7c) might be given rise to. Some scanning electron micrographs, as a matter of fact, reveal signs of breaking of platelets in this manner (see Figs. 3-2 and 3-7). Anyhow, this mode of epitaxy needs further studies.

It is found in Chapter 2 and 3 that the normal long-chain compounds with the orthorhombic subcell can be arranged in the

ordered molecular orientation on a PE film with a well-defined crystallographical surface. In fact, we succeeded in epitaxially crystallizing a number of other long- chain compounds such as the methyl- and ethyl-esters of carboxylic acids. Figure 3-17 shows the morphologies of crystals of methyl- and ethyl-esters of tetracosanoic acid grown on the UD-UHMWPE film from the solution. Nowadays, many efforts have been attempted to make thin, ordered films of these compounds, using the Langumuir-Blodgett technique. The present study proves that the epitaxial procedure is a promising method to prepare thin, well oriented organic films.

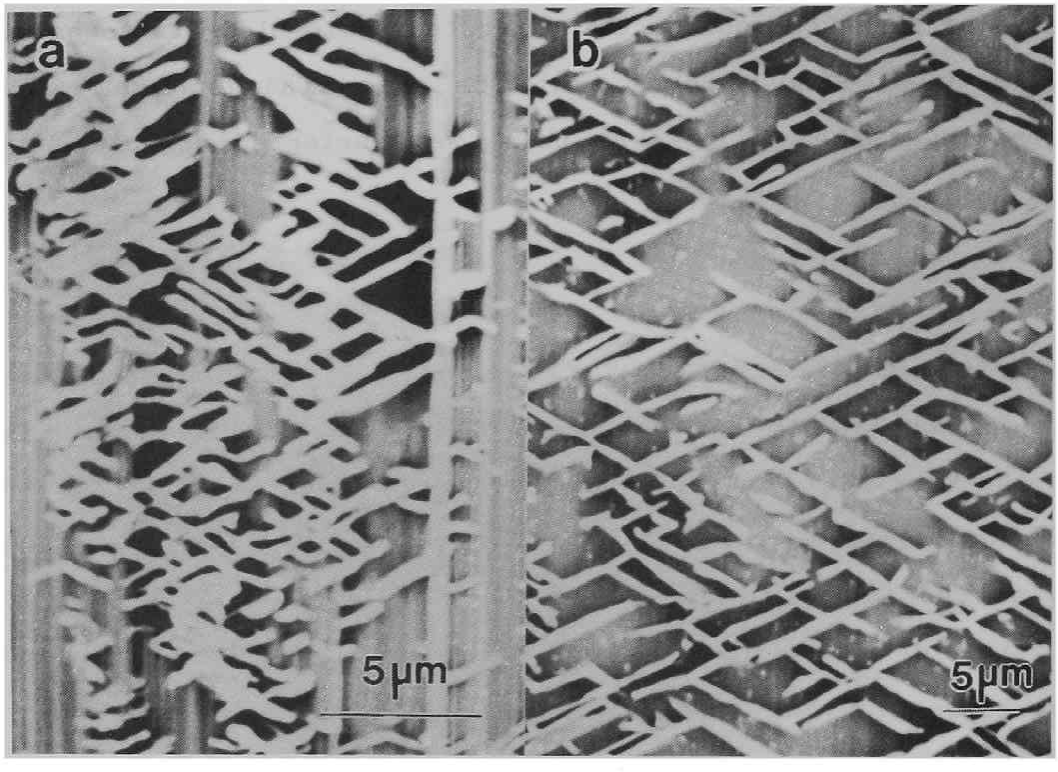

Fig. 3-17. Scanning electron micrographs of crystals of ester of tetracosanoic acid grown epitaxially on the UD-UHMWPE film. (a) crystals of methyl tetracosanate and (b) crystals of ethyl tetracosanate.

References

[1] T. Okihara, A. Kawaguchi, M. Ohara and K. Katayama, J. Crystal Growth 106(1990)318.

[2] P.H. Geil, in: Polymer Single Crystals (Interscience, New York, 1963).

[3] P. Smith, P.J. Lemstra, J.P.L. Pijpers and A.M. Kiel, Colloid Polymer Sci. 259(1981)1070.

[4] K. Furuhata, T. Yokokawa, C. Seoul and M. Miyasaka, J. Polymer Sci. Polymer Phys. 24(1986)59.

[5] C. Seoul and S.Y. Kim, J. Polymer Sci. Polymer Phys. 26(1988)1965.

[6] F.C. Frank, A. Keller and A. O'Connor, Phil. Mag. 3(1958)64.

[7] R.B.Richard, J. Polymer Sci. 6(1951)397.

[8] K. Kobayashi, in: Polymer Single Crystals (Interscience, New York, 1963).

[9] M.G. Broadhurst, J. Res. Natl. Bur. Std.(US)66A(1962)241.

[10] A. Kawaguchi, T. Okihara, M. Ohara, M. Tsuji, K. Katayama and J. Petermann, J. Crystal Growth 94(1989)857.

[11] H.M.M. Shearer and V. Vand, Acta Cryst. 9(1956)379.

[12] P.W. Teare, Acta Cryst. 12(1959)294.

[13] K. Tanaka, T. Seto, A. Watanabe and T. Hayashi, Bull. Inst. Chem. Res. Kyoto Univ. 37(1959)281.

[14] S. Abrahamsson, G. Lasson and E. von Sydow, Acta Cryst. 13(1969)770.

[15] K. Fujimoto, T. Yamamoto and T. Hara, Polymer Preprints, Japan 34(1987)805.

[16] S. Amelinckx, Acta Cryst. 8(1955)530.

[17] E. von Sydow, Acta Cryst. 7(1954)823.

[18] M. Goto and E. Asada, Bull. Chem. Soc. Japan 51(1978)2456.

[19] R.F. Holland and J.R. Nielsen, J. Mol. Spectrosc. 9(1962)482.

[20] V.Malta, O. Gelotti, R. Zannetti and A.F. Martelli, J. Chem. Soc. 13(1971)548.

[21] C.W. Bunn, Trans. Faraday Soc. 35(1939)482.

[22] E. von Sydow, Acta Cryst. 8(1955)810.

[23] S. Amelinckx, Acta Cryst. 9(1956)217.

Chapter 4. Growth of Crystal of Long-Chain Compound on Drawn Films of Isotactic Polypropylene

4.1. Introduction

Epitaxial growth of long-chain compounds on the polyethylene (PE) substrate was detailed in Chapters 2 and 3. In the case of the polyethylene substrate, similarity of its crystal structure to the subcell of long-chain compound crystals has a decisive effect on epitaxial growth of the crystals. On the other hand, PE itself crystallizes on isotactic polypropylene (iPP) epitaxially[1,2]. From these facts, it is expected that iPP could be a substrate for long-chain compound crystals to grow epitaxially on it. Really, epitaxial growth of n-paraffins on a uniaxially drawn iPP film took place[3]. There were observed three types of epitaxial orientations where the molecular axes of n-paraffins were perpendicular to the substrate surface. The orientational relations were described in chapter 1; type A_1 has the orientational relation of $(001)_p // (010)_{iPP}$ and

$[110]_p // [001]_{iPP}$, type A_2 $(001)_p // (010)_{iPP}$ and $[010]_p // [001]_{iPP}$, type A_3 $(001)_p // (010)_{iPP}$ and $[110]_p // [001]_{iPP}$. In addition, there is another epitaxial mode that molecular chains of n-paraffins lie parallel to the iPP substrate surface;

$(100)_p // (010)_{iPP}$ and $[010]_p \lesssim 46^\circ [001]_{iPP}$.

This orientational relation is the same as that in the epitaxy of PE/iPP system. This epitaxial mode was observed in n-paraffins with carbon number longer than 40. In this chapter, epitaxial growth of other long-chain compounds such as n-alcohols and n-carboxylic acids was studied. These compounds usually crystallize in a monoclinic or triclinic crystalline form and not crystallize in an orthorhombic form. Odd-numbered carboxylic acids crystallize in one or two of triclinic A'-, B'- and monoclinic C'-forms depending on the chain length and crystallization condition[4-8]. Even-numbered carboxylic acids crystallize in one or two of A-, B- and C-forms[9,10]. n-Alcohols also crystallize in one or two crystalline forms of α-, β- and γ_1-forms[11,12]. These long-chain compounds are similar to n-paraffins in the chemical structure in that they have a long normal hydrocarbon chain and in the crystal structure in that their crystals have a similar orthorhombic subcell to that of n-paraffins; the subcell is the same as the unit cell of PE[13].

2. Experimental

Thin iPP substrate films for transmission electron microscopy were prepared by the method reported by Petermann and

Gohil[14]. iPP was supplied by Tokuyama Soda Co., Ltd. The experimental procedure to make specimens was as follows: a few drops of dilute solution of a long-chain compound were spread on the iPP film and the solvent was evaporated. Then, the film was heated above the melting point of the compound and cooled down to room temperature. The vapor-deposition crystallization was also applied. A thin iPP film and a long-chain compound were put in an evacuated chamber, and the compound was vapor-deposited onto the iPP substrate. Samples thus prepared were observed by a transmission electron microscope JEOL JEM-200CS. Long-chain compounds used in this study are n-paraffins with the carbon number 31 to 50, n-alcohols with the carbon number 17 to 30, n-carboxylic acids with the carbon number 17 to 30 and methyl and ethyl esters of some acids. They were purchased from Tokyo Kasei Kogyo Co.,Ltd.

4.3.Results

4.3.1. Crystallization from melt

When various kinds of n-alcohols were crystallized from the melt on the iPP drawn film, their crystals showed three different types of preferential orientations which are characterized by electron diffraction patterns shown in Figs. 4-1a, b and c. The patterns show *hk*0 net patterns of n-alcohol crystals which superimposed on the iPP fiber pattern with a definite orientational relation to it. The presence of *hk*0 net pattern indicates that molecular chains in n-alcohol crystals stand

perpendicular to the iPP substrate in all three cases. In these cases, n-alcohols crystallized in the monoclinic β-form whose lattice parameter β (the unique angle of the unit cell) is 89° . Here, the molecular chains orient almost perpendicular to the substrate surface when the (001) plane is parallel to it. Odd-numbered alcohols crystallize in the β-form in a normal crystallization condition. Even-numbered alcohols are crystallized normally in γ_1-form. However, they crystallized in β-form on the iPP substrate. The above three orientations are distinguished in that the crystallographic *b*-axis of an n-alcohol make different angles with the c-axis of the substrate. They are named A_1, A_2 and A_3 according to the notation in Chapter 1, because the respective orientational relations of *hk*0 net patterns are quite similar to those of corresponding epitaxial types for n-paraffins.

(1) Figure 4-1a shows the first type, A_3, which is observed most frequently. This type is identified by the feature that the 110 reflection from n-alcohol crystal coincides with the 111 reflection from the iPP fiber pattern. This mode of epitaxy has the same orientation as the mode expressed as A_3 in Chapter 1 for n-paraffins on iPP.

(2) The second type A_2 is characterized by Fig. 4-1b. In this figure, the 200 reflection from an n-alcohol crystal is on the equator of the iPP fiber pattern as described in Chapter 1, and in other words, the 020 reflection appears on the meridian of iPP.

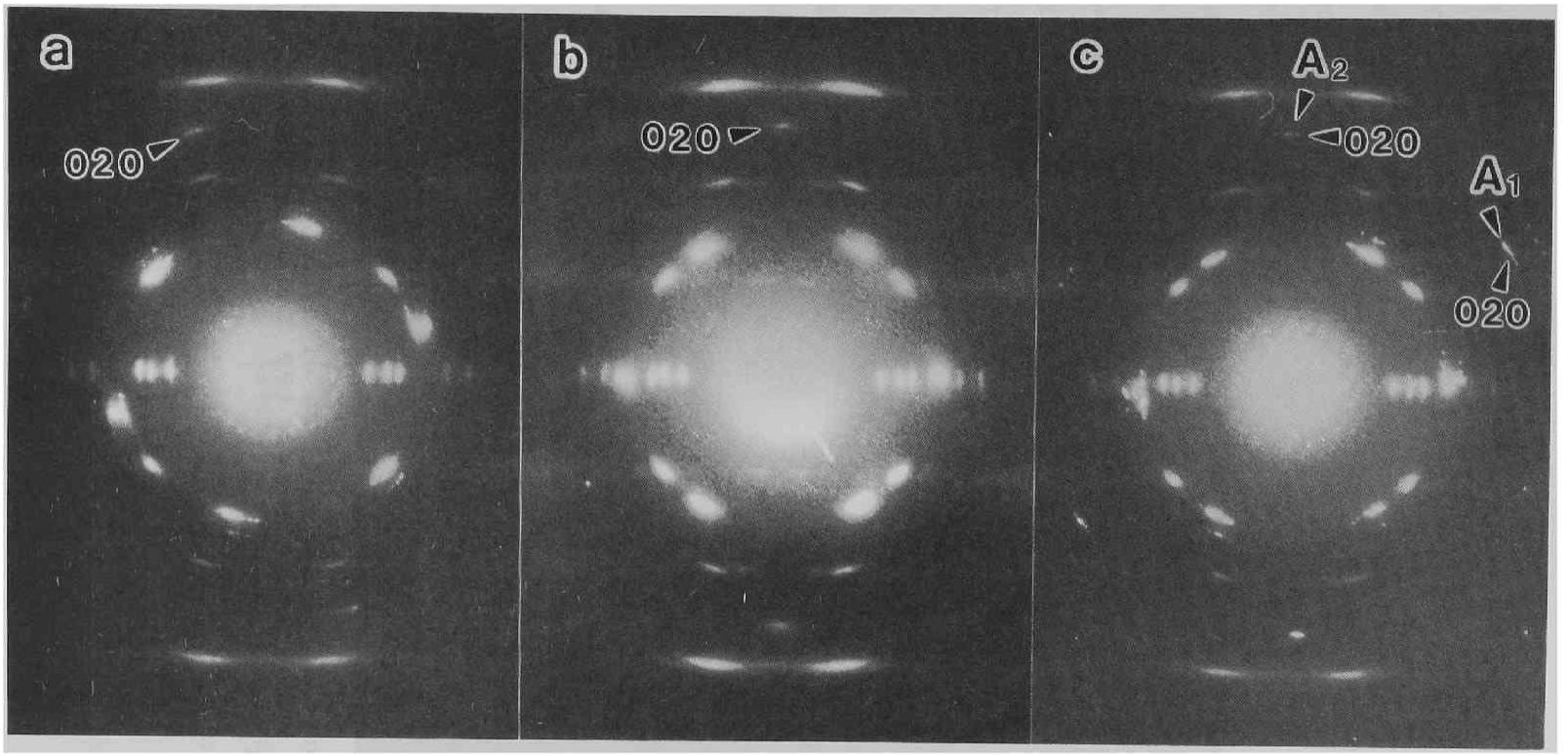

Fig.4-1 Electron diffraction patterns of n-alcohol crystals grown on the uniaxially drawn iPP film. (a) 1-tetracosanol crystallized with mode A_3. (b) 1-triacontanol crystallized with mode A_2. (c) 1-tetracosanol crystallized with modes A_1 and A_2.

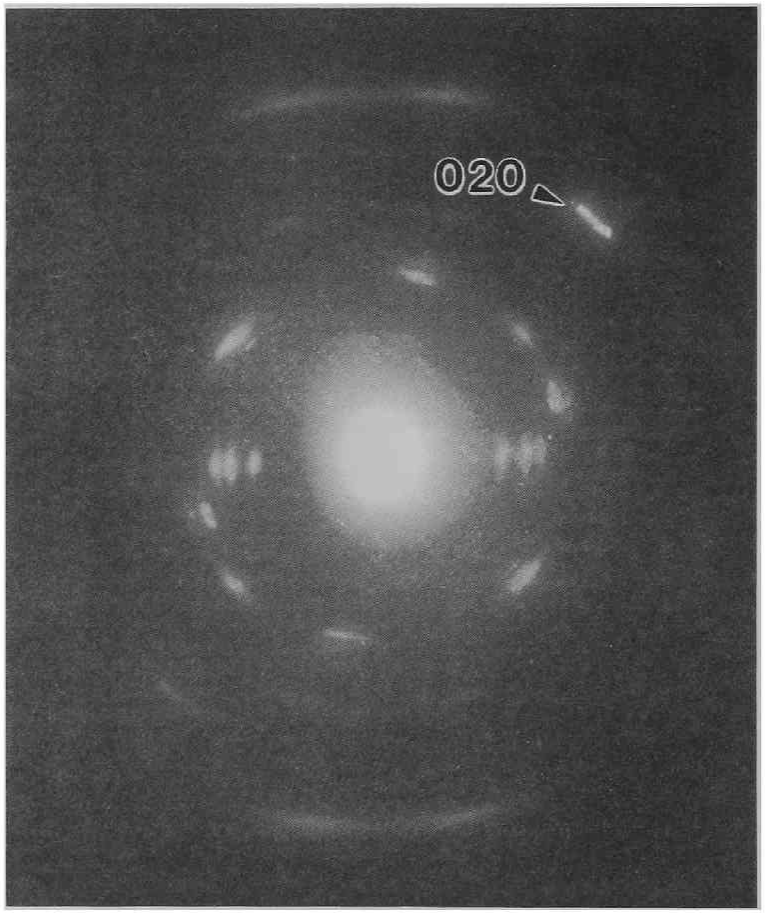

Fig.4-2 Electron diffraction pattern of stearyl alcohol crystals grown on the uniaxially drawn iPP film. Stearyl alcohol crystallized in γ_1-form.

(3) Figure 4-1c shows the third type A_1. This is less often observed. In this figure, the 110 reflection of an n-alcohol is on the equator of the iPP fiber pattern. This type of orientation was the same as type A_1 of n-paraffins in Chapter 1.

Figure 4-2 shows an electron diffraction pattern of stearyl alcohol crystallized on a drawn iPP film. By measuring the lattice spacings, it is found that stearyl alcohol crystallized in the monoclinic γ_1-form. Since the molecular axis is oblique toward the *a*-axis, the dimension of *a* of the unit cell is larger than that of PE unit cell. The subcell of the γ_1-form is, however, orthorhombic and almost identical to the PE unit cell. In Fig. 4-2, the 020 spot of the n-alcohol is observed in the same direction with respect to the iPP fiber axis as in the case of the B mode of epitaxy of n-paraffins (see Chapter 1). In both cases, thus, the b-axis is in the same direction as regards the iPP fiber axis. The a-axis of the n-alcohol also lies parallel to the substrate surface, that is to say, the (001) plane is in contact with the iPP substrate surface.

Figure 4-3 shows typical electron diffraction patterns of various carboxylic acids crystallized on an iPP substrate. When most of carboxylic acids examined here, except for heptadecanoic acid, were crystallized on the iPP substrate from the melt or on the substrate kept at high temperatures by vapor-deposition, they showed one or more types of differently oriented overgrowth. The strong spots indicated with thick arrows are all indexed as 020. Lattice spacings of weak spots indicated with a thin arrows range

from 0.420nm to 0.440nm. These are indexed as 11*l* (*l* is dependent on the chain length, i.e. the kind of carboxylic acid). All diffraction patterns are interpreted on the basis of the Ewald construction for diffraction as shown in Fig. 4-4. The c^*-axis of the reciprocal lattice of an n-carboxylic acid is parallel the incident electron beams. In this orientation, the 020 and 11*l* reciprocal points are placed on the sphere of reflection at the same time. That means the (001) plane of the acid crystal is in contact with the iPP substrate. Even-numbered carboxylic acids crystallize in monoclinic C-form and odd-numbered carboxylic acid in C'-form. The molecular arrangement and inclination toward the *a*-axis in the C-form unit cells of the carboxylic acids is similar to that of n-alcohols with the γ_1-form, except for the magnitude of inclination angle β of molecules against the basal plane. In both kinds of crystals, their subcells are orthorhombic and the molecular packing in them is quite similar. Thus, these carboxylic acids and n-alcohols exhibit one or more types of oriented overgrowth characterized by electron diffraction patterns in Fig. 4-3. On the basis of the difference in the orientation of the 020 spot with respect to the fiber axis of iPP, the orientational modes distinguished by diffraction patterns in Figs. 4-3a, b, c and d are here denoted as A_{1m}, A_{2m}, A_{3m} and A_{4m}, respectively. According to the same notation as in the case of n-paraffins, A means that molecular chains stand on the substrate surface (not always perpendicular), the subscript i (i=1,2,3 and 4) denotes the same orientation of the b-axis as the

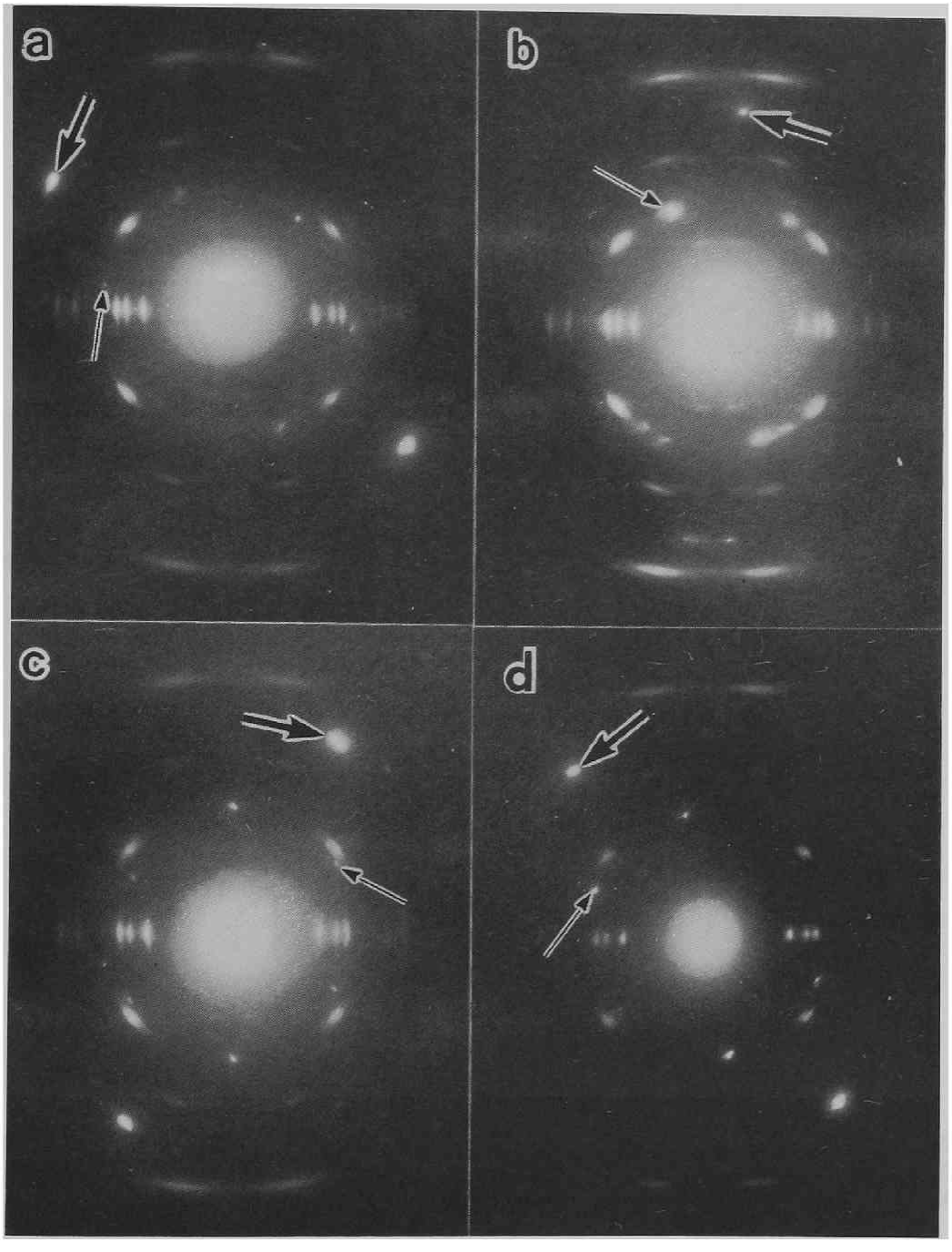

Fig. 4-3 Electron diffraction patterns of various n-carboxylic acid crystals grown from the melt on the uniaxially drawn iPP film. (a) n-nonadecanoic acid crystallized with mode A_{1m}. (b) n-tetracosanoic acid crystallized with mode A_{2m}. (c) n-nonadecanoic acid crystallized with mode A_{3m}. (d) stearic acid crystallized with mode A_{4m}.

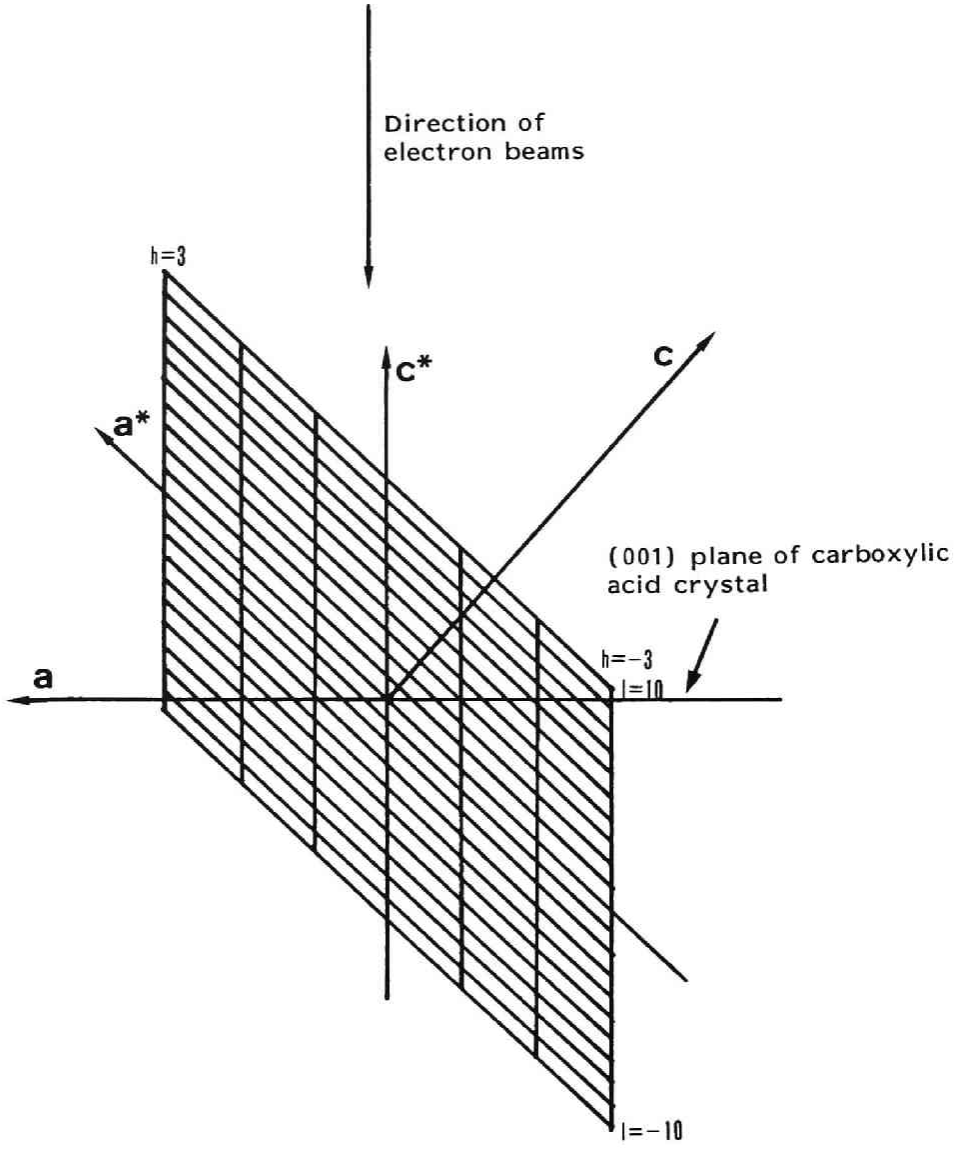

Fig. 4-4 Illustration for relation between the reciprocal lattice of an n-carboxylic acid crystal and incident electron beams. b and b^* axes are normal to the figure.

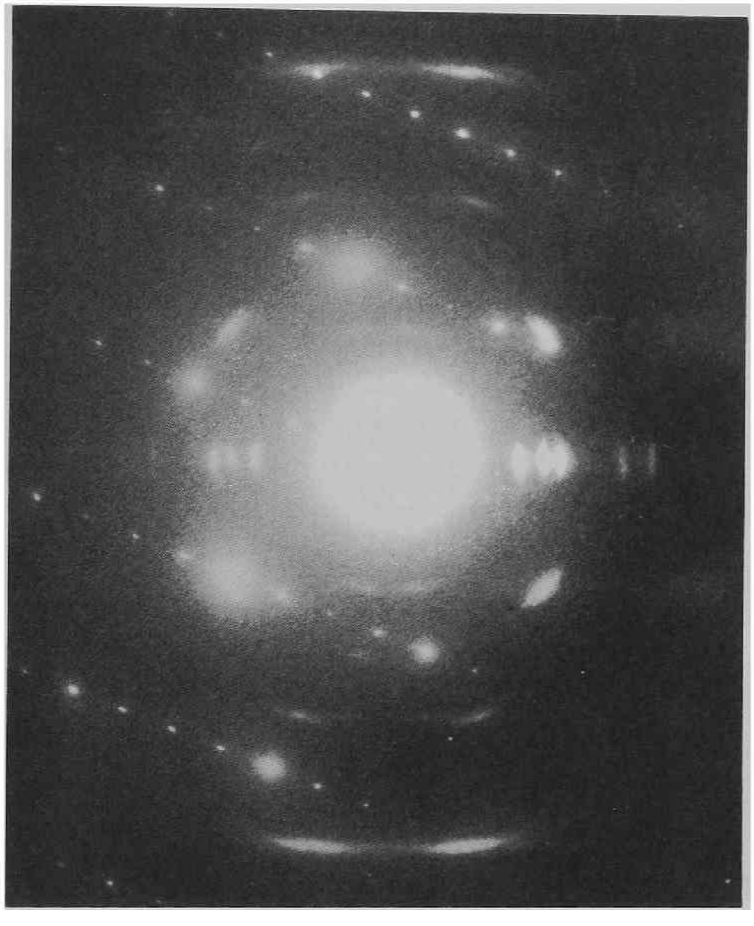

Fig. 4-5 Electron diffraction pattern of heptadecanoic acid crystallized from the melt on the uniaxially drawn iPP film.

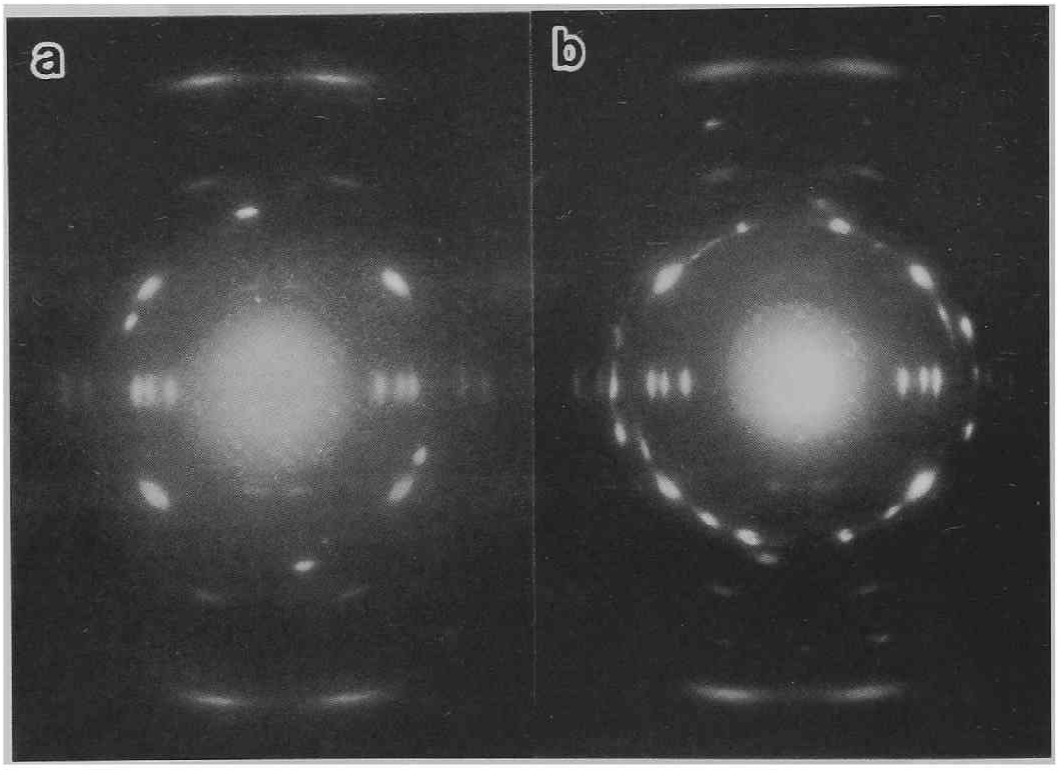

Fig. 4-6 Electron diffraction pattern of tetracosanoic acid ester crystal grown on the uniaxially drawn iPP film. (a) methyl ester and (b) ethyl ester.

corresponding subscript in n-paraffins do and m denotes that the crystalline form of carboxylic acids is monoclinic. Type A_{4m} shows the same orientation as described in the case of stearyl alcohol crystallized in γ_1-form (see Fig. 4-2).

Heptadecanoic acid crystallized in a different orientation from that of longer homologues. Its electron diffraction pattern is shown in Fig.4-5. From the observed lattice spacings, it is found that all spot-like diffractions from the acid are indexed as $0kl$, i.e. the $0kl$ net pattern superimposes on the fiber pattern of iPP. The figure is understood on the reflection condition that the electron beams are incident onto the acid crystals in the direction almost parallel to the a-axis, so that the $0kl$ net pattern can be observed; the electron beams are incident horizontally (parallel to the *a*-axis) in Fig. 4-4. It is concluded that the (100) plane to which molecular chains align parallel is in contact with the substrate surface. Since the orientation of the $0kl$ net pattern with respect to the iPP fiber axis differs from photograph to photograph, it seems that heptadecanoic acid does not crystallize epitaxially on the iPP substrate because of the shortness of molecular chain.

Other long-chain compounds showed epitaxial growth on the iPP substrate. Figure 4-6 shows electron diffraction patterns of methyl and ethyl tetracosanates crystallized on the iPP substrate from the melt. The crystal structures of these compounds are not reported, but the crystal structure of methyl stearate which has a subcell similar to that of n-paraffins is reported by

Aleby[15]. The crystallization behavior of methyl triacontanate on the (001) plane of KCl was reported by Ueda[16]. Though the crystal structure of this ester is also not analysed yet, he has concluded that molecular chains of the methyl ester are perpendicular to the substrate, because his electron diffraction experiment showed the *hk*0 net pattern of the subcell similar to that of n-paraffins and methyl stearate. In the present cases, the analogous *hk*0 net patterns were observed, and hence, it is concluded that molecular chains stand perpendicular to the substrate. Further, since the *hk*0 net pattern is oriented with respect to the fiber pattern in the same way as in the case of n-paraffins, epitaxial crystallization occurs.

3.2 Crystallization from the vapor phase

Figure 4-7 shows the morphology of vapor-deposited tetracosanoic acid on iPP kept at room temperature. Both edge-on and flat-on lamellae were observed and their orientation was random. It is likely that this vapor-deposition condition was not favorable for the carboxylic acid to crystallize epitaxially on the iPP substrate. In contrast to carboxylic acids, when n-alcohols were vapor-deposition on the iPP substrate at room temperature, they crystallized epitaxially. Figure 4-8 shows the morphology of n-triacontanol vapor-deposited on the iPP film at 25℃ and the corresponding electron diffraction pattern. The pattern indicates that three types of epitaxial growth occurred on iPP. The presence of 00*l* reflections along the meridian of the

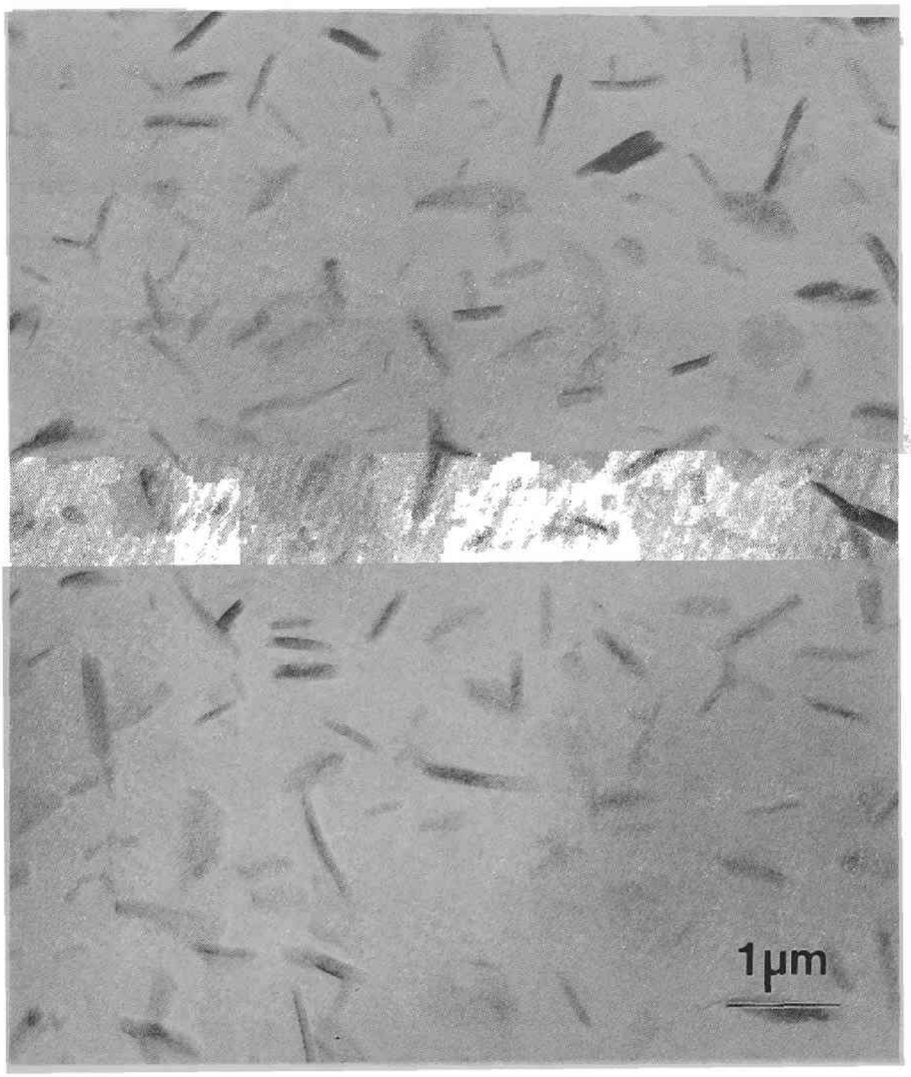

Fig.4-7 Transmission electron micrograph of tetracosanoic acid crystals grown by vapor-deposition on a uniaxially drawn iPP film.

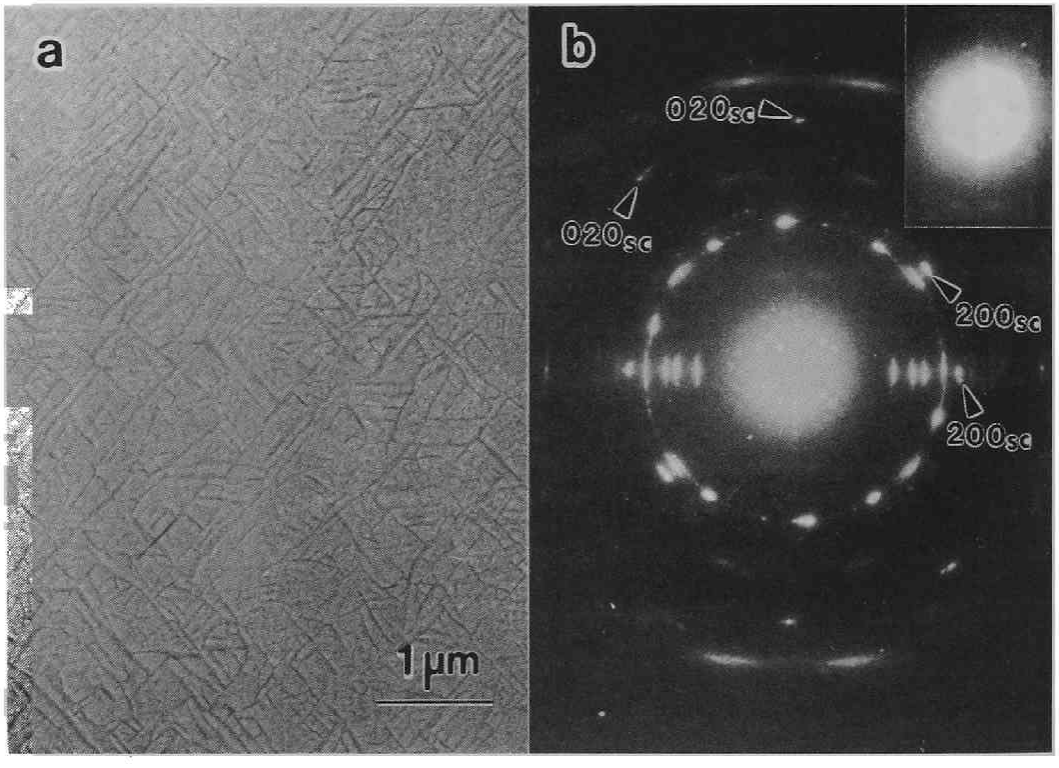

Fig. 4-8 (a) Transmission electron micrograph of n-triacontanol crystals grown on a uniaxially drawn iPP film and (b) the corresponding diffraction pattern. The inset is the enlarged pattern of the central part.

iPP pattern indicates that molecular chains of the n-alcohol are parallel to the *c*-axis of the substrate. The others are flat-on lamellae grown epitaxially on the substrate. They are identified with two types of *hk*0 net patterns of n-alcohol crystals which are definitely oriented with respect to the iPP fiber pattern. In them, the (001) plane of n-alcohol lamellae is in contact with the surface of the iPP substrate. Further, there is another orientation, though it is not recognized in Fig. 4-8b, in which orientation n-alcohol molecular chains take the same parallel orientation as those of PE chain do when PE crystallized epitaxially on iPP from the melt. All the types of epitaxy are distinguished by the difference of lamellar orientation on the substrate surface, as described in the case of crystallization from the melt. The epitaxial crystallization behaviors of n-alcohols are quite similar to those of n-paraffins.

4.Discussion

In Chapter 1, we discussed the lattice matching in epitaxial growth of n-paraffins on iPP. In that case, the (010) plane of the iPP substrate plays an important role on epitaxy.

Figure 4-9a shows a model of the molecular orientation of the β-form of an n-alcohol crystallized epitaxially on the iPP substrate. The molecular chains are almost perpendicular to the substrate surface. In the case of crystallization of n-alcohols from the melt, they crystallized in β-form, but stearyl alcohol

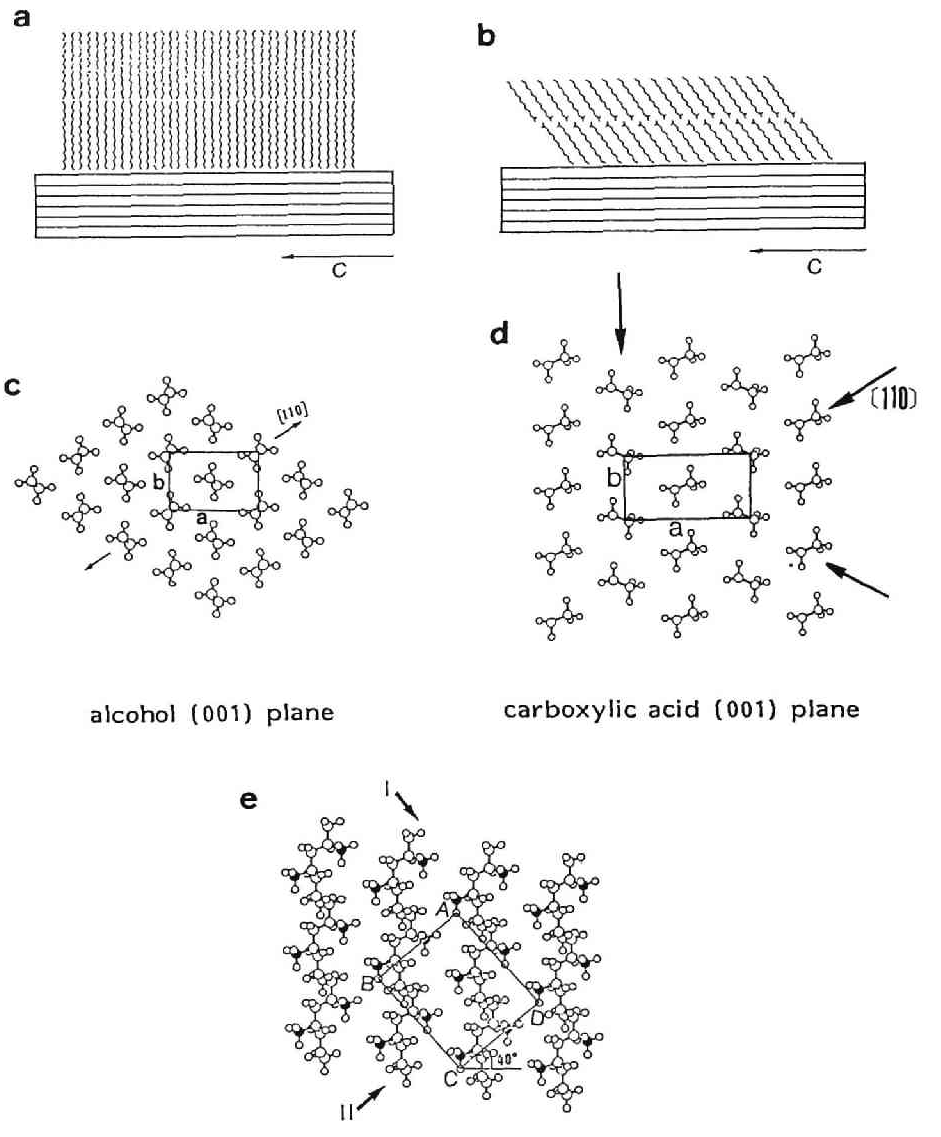

Fig. 4-9 (a) illustration of flat-on lamellar crystal of n-alcohol with -form, (b) illustration of flat-on lamellar crystal of n-carboxylic acid, (c) molecular arrangement of (001) plane of n-alcohol crystal with β-form, (d) end methyl group arrangement of carboxylic acid crystal with C'-form and (e) molecular arrangement of polypropylene (010) surface In (c), (d) and (e) large and small circles mean carbon atoms and hydrogen atoms, respectively. In (e), there is a rectangle ABCD which is a two-dimensional lattice of iPP (010) plane. The spacings of this lattice are as follows; AB=0.846nm and AD=1.005nm.

has another modification, that is, β-form. This result indicates that the β-form is favorable for the epitaxial growth of n-alcohols on iPP. Because the unique angle β of the unit cell is 89°, the crystal structure of the β-form is nearly orthorhombic and close to that of orthorhombic n-paraffins. Thus, the lattice matching similar to that of n-paraffin/iPP can be easily formed between n-alcohols with a β-form and iPP. n-Alcohol molecules are dimerized in the crystal lattice by forming hydrogen bonds between -OH groups. It is supposed that the coupled n-alcohol molecules behave in epitaxial crystallization as n-paraffins, because the end methyl groups are arranged in the same manner on the (001) plane as in the n-paraffin crystals. From the epitaxial crystallization behavior analogous to that of n-paraffins, it is considered that the contact plane with the iPP substrate is the (001) plane in which the end methyl groups are arranged as shown in Fig. 4-9c. It is stressed that the iPP (010) plane plays an important role on the A_3 mode of epitaxy of n-paraffins. Here, it is most likely that the iPP (010) plane is in contact with the (001) plane of n-alcohols, realizing the following lattice coincidence. Figure 4-9e represents the molecular arrangement in the iPP (010) plane (see Chapter 1). Rows of end methyl groups shown by the arrows in Fig. 4-9c are parallel to the [110] direction. The interval between the rows is close to half of distance AB in Fig. 4-9e. Thus, the A_3 epitaxial mode is achieved by fitting the end methyl rows of n-alcohols in the valleys between the side methyl rows on the iPP (010) plane,

as described in Chapter 1.

From the electron diffraction, it is found that in the (001) plane of the carboxylic acids was in contact with the iPP substrate and consequently, molecular chains are tilted on the substrate surface as modeled in Fig. 4-9b. Figure 4-9d shows the arrangement of end methyl groups on the (001) basal plane of carboxylic acid crystals of the C-form. In Fig. 4-9d, thin arrows indicate the direction in which end methyl groups align most densely. For examples, the interval between the rows of end methyl groups in the [110] direction is 0.436nm which is nearly equal to the (110) spacing of the orthorhombic n-paraffin cell (0.411nm) (see Chapter 1). This spacing is in good agreement with half of the lattice spacing AB (0.846nm) shown in Fig. 4-9e. Thus, the row of end methyl groups in the (001) face of carboxylic acids fits in between two neighboring rows of side methyl groups in the iPP surface, as shown by the arrow I in Fig. 4-9e. Accordingly, the epitaxy mode A_{3m} is $(001)_c//(010)_{iPP}$, and $[110]_c//[101]_{iPP}$ where c denotes a carboxylic acid. The distance AD in Fig. 4-9e is nearly equal to the dimension of *a* (twice of the interval between rows of end methyl groups aligned along the *b*-axis, as shown in Fig. 4-9d). The A_{1m} mode of epitaxy is caused as follows: the rows of end methyl groups fit in the valleys between the rows of side methyl groups in the (010) iPP surface oriented in the direction of the arrow II in Fig. 4-9e. The observed electron diffraction pattern of this epitaxy is explained on the basis of this orientation of carboxylic acids

(see Fig. 4-3a). In the case of A_{4m}, the *b*-axis of carboxylic acids is in the direction AD. Since the orientation with respect to the iPP fiber axis is the same as that in the B mode epitaxy (see Chapter 1), this epitaxy occurs in when carboxylic acid molecules lie down to fit in the channels running in the direction II. We should examine by energy calculation whether the epitaxy is energetically favorable or not. However, it is very difficult because too many atoms must be taken into consideration for the calculation. Analysis of A_{2m} is also difficult because there is no suitable lattice matching between the (001) plane of carboxylic acids and the (010) iPP plane for this mode of epitaxy, and again we must rely on the energy calculation to know this mode in detail. There are two problems in this epitaxy; one is whether this epitaxy is stable from the view point of interaction energy between carboxylic acids and the iPP substrate and the other is which surface of the iPP substrate is assigned to this epitaxy, the (010) plane or any of others. So good explanation is not yet provided for A_{2m} mode epitaxy.

Table 4-1 shows the grouping of epitaxial mode for long-chain compounds observed in melt crystallization.

In crystallization by vapor-deposition, carboxylic acid crystals did not show epitaxy on the substrate kept at room temperature (see Fig. 4-7). From this result, the epitaxial temperature of n-carboxylic acids seems to be higher than room temperature. In vapor-deposition crystallization of n-paraffins and n-alcohols, epitaxially oriented edge-on lamellae were

Table 4-1. Classification of epitaxial mode of long-chain compounds on the iPP substrate.

compound	epitaxial mode
$C_{17}OH$	A_1, A_3
$C_{18}OH$ (β-form) (γ_1-form)	A_2, A_3 A_{4m}
$C_{23}OH$	A_1, A_2, A_3
$C_{24}OH$	A_1, A_2, A_3
$C_{26}OH$	A_1, A_2, A_3
$C_{30}OH$	A_2, A_3
$C_{17}COOH$	A_{2m}, A_{4m}
$C_{18}COOH$	A_{1m}, A_{2m}, A_{3m}, A_{4m}
$C_{23}COOH$	A_{1m}, A_{2m}, A_{3m}, A_{4m}
$C_{25}COOH$	A_{1m}, A_{3m}, A_{4m}
$C_{29}COOH$	A_{1m}, A_{2m}, A_{3m}
$C_{23}COOCH_3$	A_3
$C_{23}COOC_2H_5$	A_2, A_3

observed on the iPP substrate at room temperature. Edge-on lamellae were not observed in the crystallization from the melt except for longer homologues. They take two orientations; one is explained by the B-mode epitaxy of n-paraffins on iPP[3], and the other is that molecular chains of long-chain compounds are parallel to the c-axis of iPP. In the latter, however, there is no lattice matching of a small misfit. Further accumulation of experimental data gives an explanation of this epitaxy.

Since the subcell of long chain compounds is the same as PE unit cell, the epitaxy on PE is performed to adjust the crystallographic plane of the subcell to the corresponding one of the PE unit cell. In the present long chain compound/iPP systems, the subcell also plays an important role. However, no subcell plane matches to "any of the lattice spacing on the (010) iPP surface" justly as in the long-chain compound/PE system. Consequently, a small misfit is inevitable. Because of this misfit, atoms or molecules placed near the interface can not occupy the stable position to form the stable crystal lattice of their own. As crystals grow, a lattice spacing gradually varies from the interface toward inside the crystal of the compound and reaches the value of the stable crystal lattice. Otherwise, to avoid this unstableness, the misfit dislocation is introduced at the interface. Though the epitaxially grown crystals remain unstable at the interface, their instability is eliminated by introducing the dislocation, and then they grow to be a stable form, maintaining the epitaxial orientation with the substrate.

The long-chain compound crystals which grew on the iPP substrate are in contact with the substrate surface in a wide range. However, the lattice fitting between the crystal and the substrate could not be maintained over the entire interface. At the stage of nucleation, the orientational relation of the epitaxial growth is determined, i.e. this epitaxy is nucleation-controlled. A small contact area has an important role for epitaxial growth.

References

[1] G.Broza, U.Rieck, A.Kawaguchi and J.Petermann, J. Polymer Sci. Polymer Phys. Ed., 23(1985)2623.

[2] J.Petermann, G.Broza, U.Rieck and A.Kawaguchi, J. Mater. Sci., 22(1987)1477.

[3] A.Kawaguchi, T.Okihara, M.Ohara, M.Tsuji, K.Katayama and J.Petermann, J.Crystal Growth, 94(1989)857.

[4] E.von Sydow, Acta Cryst., 7(1954)529.

[5] E.von Sydow, Acta Cryst., 7(1954)823.

[6] E.von Sydow, Acta Cryst., 8(1955)810.

[7] E.von Sydow, Acta Cryst., 8(1955)845.

[8] E.von Sydow, Acta Chem. Scand., 9(1955)1685.

[9] E.von Sydow, Acta Cryst., 8(1955)557.

[10] V.Vand, W.M.Morley and T.R.Lomer, Acta Cryst., 4(1951)324.

[11] K.Tanaka, T.Seto, A.Watanabe and T.Hayashida, Bull. Inst. Chem. Res. Kyoto Univ.,37(1959)281.

[12] S.Abrahamsson, G.Larsson and E.von Sydow, Acta Cryst., 13(1960)770.

[13] C.W.Bunn, Trans. Faraday Soc., 35(1939)482.

[14] J.Petermann and R.M.Gohil, J. Mater. Sci., 14(1979)2260.

[15] S.Aleby, Acta Cryst. 15(1962)1248.

[16] Y.Ueda, Bull. Chem. Soc. Jpn., 59(1986)3775.

Summary

Chapter 1: Epitaxial Growth of Normal Paraffins From the Melt on Uniaxially Drawn Films of Polyolefins

n-Paraffins of n-$C_{20}H_{42}$ to n-$C_{50}H_{102}$ were epitaxially crystallized on oriented polyolefins; polyethylene(PE), isotactic polypropylene(iPP), poly-1-butene(PB) and poly-4-methyl-1-pentene(P4MP). In most cases, n-paraffin crystals were epitaxially grown on the substrate surface with the (001) basal plane parallel to it, maintaining a two-dimensional lattice coincidence with the polymer substrate. The epitaxial modes with this orientation were classified into the following three types irrespective of polymers:

(1) $(001)_p$ // SS, $\langle 110\rangle_p$ // FA,

(2) $(001)_p$ // SS, $[010]_p$ // FA,

(3) $(001)_p$ // SS, $\langle 110\rangle_p \measuredangle \alpha$ FA,

where p, SS and FA denote n-paraffin crystals, substrate surface and fiber axis of the polymers, respectively. The angle α depends on the kind of polymer substrate. n-Paraffins longer than n-$C_{40}H_{82}$ were laid down in parallel on the polypropylene substrate with their axes at an angle of 46° with respect to the substrate fiber axis.

Chapter 2:Crystallization Behavior of Long-Chain Compounds on the (110) Plane of Polyethylene

PE films with surfaces bounded by (110) planes were

prepared. On the film surface, various normal long-chain compounds, such as normal paraffins (n-C_nH_{2n+2}) with n of 23 through 50, n-alcohols (n-$C_nH_{2n+1}OH$) and carboxylic acids (n-$C_{n-1}H_{2n-1}COOH$) were epitaxially crystallized from solution, melt and vapor phase. The molecular chains lie down parallel to the chain axis of PE when crystallized at low temperatures, exhibiting different crystalline modifications. Irrespective of the nature of the compounds, the epitaxy was explained in terms of a common lattice coincidence between orthorhombic subcells of the compounds and the unit cell of PE:

$(110)_{sc} // (110)_{PE}, [001]_{sc} // [001]_{PE}$,

where sc and PE denote the subcells of the compounds and the unit cell of PE, respectively. By contrast, when crystallized at high temperatures from vapor phase and melt, the molecules stood normal on or tilted to the substrate, keeping the relations that the (001) basal plane of the unit cell of the compounds is parallel to $(110)_{PE}$ and the [110] direction parallel to the [001] direction of PE.

Chapter 3: Crystallization Behavior of Long-Chain Compounds on the (100) Plane of Polyethylene

PE films with surfaces bounded by the (100) plane were prepared by high drawing of ultra-high molecular weight PE mats made of solution-grown crystals. Normal long-chain compounds, the same as used in Chapter 2, were crystallized from solution by solvent evaporation and from the melt on the PE films. Epitaxial

crystallization was observed for these compounds which have the same orthorhombic subcell as the PE unit cell. In the epitaxial overgrowth, the normal long-chain compounds are arrayed with their axis parallel to the chain axis of PE on the (100) plane of PE, realizing the lattice coincidence of the (010) plane of PE with their corresponding subcell plane, irrespective of the chemical and crystal structures of the crystallized materials.

Chapter 4: Growth of Crystals of Long-Chain Compound on Drawn Film of Isotactic Polypropylene

The epitaxial modes of the long-chain compounds on a uniaxially drawn iPP substrate were studied. They crystallized from the melt and by vapor-deposition onto iPP. In the case of crystallization from the melt, the n-alcohol crystals grew with their (001) basal plane parallel to the substrate surface. The molecules were arranged with their chain axes normal or oblique to the surface, as observed in n-paraffins/iPP in Chapter 1. Carboxylic acids crystallized in monoclinic C- and C'-forms showed the epitaxial modes with the orientation analogous to that of the n-paraffin /iPP system. In crystallization by vapor-deposition, carboxylic acids did not show epitaxial growth, but n-alcohols exhibit several modes of epitaxial growth which are classified by the molecular orientation with respect to the iPP chain axis. Two modes of them are similar in that molecular chains of n-alcohols are parallel to the substrate surface; one has the same orientation as that in PE/iPP epitaxy, and in the

other molecular chains of n-alcohols are oriented parallel to the c-axis of the iPP substrate. The other modes have the same normal or oblique orientation as observed in the crystallization from the melt; flat-on lamellae grew.

Conclusion

Crystals of long-chain compounds such as n-paraffins, n-alcohols and carboxylic acids were epitaxially grown on the polyolefin substrate. In most cases of crystallization from the melt, their (001) basal planes were in contact with the substrate surface. However, they also grew edge-on with the (100) subcell plane in contact on the PE (100) plane, and longer n-paraffins and PE crystallized aligning parallel to the iPP substrate surface. In crystallization from solution and by vapor-deposition at low temperatures, edge-on lamellae of most of long-chain compounds were grown on the substrate surface, their molecular axes being arranged parallel to it. In these types of epitaxy, the subcells of long-chain compound play a very important role. Which orientational mode occurs depends on the crystallization temperature and the kind of the substrate. On the PE (110) plane, long-chain compounds crystallized with their molecular chains stood or inclined at high temperatures and they crystallized with their molecular chains parallel to the PE c-axis at low temperatures. On the PE (100) plane, long-chain compounds crystallized with their molecular chains parallel to the substrate PE c-axis irrespective of temperature.

The epitaxy of longer n-paraffins on iPP has a close relation to the PE/iPP epitaxy. Longer-chain n-paraffin crystals are grown epitaxially on the iPP substrate to which molecular chains are arranged parallel. Their subcell, the same as the unit cell of PE, matched with the two-dimensional rectanglar unit cell in the iPP (010) plane. PE crystallized epitaxially with their molecular chains oriented in the same way as longer paraffins do.

On the other hand, short-chain n-paraffins crystallized with their molecular chains stood on the substrate surface. The difference in the epitaxial behavior between short n-paraffins and longer homologues including PE is due to the difference in the chain length between them. Thus, the fact that PE consists of a long methylene sequence is the driving force of the epitaxial orientation.

When normal long-chain compounds were vapor-deposited onto the iPP substrate, two epitaxial modes occur. One is the same as in the PE/iPP case. The other has the orientation with the molecular chains of long-chain compounds parallel to the substrate c-axis. This orientation was not observed in melt-crystallization. The reason why this orientation does not take place in melt-crystallization is left for further study.

The compounds with a normal long alkyl chain whose crystalline form has the same subcell as the unit cell of PE crystallize epitaxially on the polyolefin films, and the orientation of long-chain compound crystals can be controlled by crystallization temperature, the kind of the substrate and the

crystallographic nature of its surface. As the long alkyl chain plays an important role on the epitaxy, various compounds with a long alkyl chain have a potential for the epitaxial crystallization on polyolefins. Thus, this epitaxy on polymer substrates seems to be utilized for preparing thin films of compounds with functional groups.

List of publication

(1) "Epitaxial Growth of Paraffins on the Substrates of olefinic polymers [II]"
Polymer Preprints, Japan, 36(1987)2372.

(2) "Epitaxial Growth of Long Normal Chain Compounds on the Substrates of Oriented Polyolefins. [I] Classification of Epitaxial Mode."
Polymer Preprints, Japan, 37(1988)1170.

(3) "Epitaxial Growth of Functional Molecules with Long Alkyl Group on Drawn Polyolefins"
Prepr. of the IUPAC Int'l Symposium on Macromol. (1988)854.

(4) "Epitaxial Growth of Normal Long Chain Compounds on the Substrates of Oriented Polyolefins [III] Mechanism of Epitaxy."
Polymer Preprints, Japan, 37(1988)2507.

(5) "Crystallization Behavior of Normal Long Chain Compounds on Polyolefin Thin Film."
Polymer Preprints, Japan, 38(1989)857.

(6) "Substrate-induced Crystallization of n-Paraffins on Oriented Polyolefins"
J. Crystal Growth, 94(1989)857.

(7) "Crystallization Behavior of Normal Long Chain Compounds on Polyolefin Thin Film II."
Ploymer Preprints, Japan,38(1989)3329.

(8) "Orientational Control of Normal Long Chain Compounds on Polyolefin Thin Film by Epitaxial Growth."
Sen-i Gakkai Preprints (1989)F-164.

(9) "Oriented Crystallization of Normal Long Chain Compounds on Polyolefins"
J. Crystal Growth, 99(1990)1028.

(10) "Subcell-matched Epitaxy of Normal Long Chain Compounds on Polyethylene I. On the (110) plane."
J. Crystal Growth, 106(1990)318.

(11) "Subcell-matched Epitaxy of Normal Long Chain Compounds on Polyethylene II. On the (100) plane."
J. Crystal Growth, 106(1990)333.

Acknowledgments

The present study has been carried out from 1986 to 1991 at the Laboratory of Polymer Crystals, the Institute for Chemical Research, Kyoto University.

The author is deeply indebted to Professor Ken-ichi Katayama for his guidance, many helpful discussions and continuous interest in this work.

The author is grateful to Associate Professor Akiyoshi Kawaguchi for his helpful and instructive discussions and collaborations on this work.

The author thanks Dr. Masaki Tsuji for his teaching of technical expertise and his helpful discussions.

The author thanks Professor Jürgen Petermann of Technische Universität Hamburg-Harburg for his collaborations and helpful discussions on this work.

The technical assistance of Messrs. Masayoshi Ohara, Shozo Murakami and Sakumi Moriguchi is greatly acknowledged.

The author thanks Associate Professor Seiji Isoda for his valuable comments on this work.

The author is also grateful to Professor Paul Smith of the University of California at Santa Barbara, USA, for his constructive criticism of the manuscript in Chapters 2 and 3.

February, 1991 Takumi Okihara